

AD-A286 006



Final Report



FULL-WAVE ANALYSIS AND COMPUTATION OF MICROWAVE
INTEGRATED CIRCUITS

January 1, 1988 - June 30, 1990

by

Roger F. Harrington

Department of Electrical and Computer Engineering
Syracuse University
Syracuse, New York 13244-1240

Contract No. N00014-88-K-0027

This document has been approved
for public release and sale; its
distribution is unlimited.

with

Office of Naval Research
800 North Quincy Street
Arlington, VA 22217-5000

Date: June 30, 1990

Submitted by: Roger F. Harrington

94-34536



1180

94 3 28 024

CONTENTS

	Page
Final Report-----	1
First Year's Annual Report-----	3
Second Year's Annual Report-----	8
Quasi-Static Analysis of a Microstrip Via Through a Hole in a Ground Plane (reprint)-----	16
The Inductance Matrix of a Multiconductor Transmission Line in Multiple Magnetic Media (reprint)-----	22
Boundary Integral Formulations for Homogeneous Material Bodies (reprint)-----	25
The Excess Capacity of a Microstrip Via in a Dielectric Substrate (reprint)-----	40
A Stable Integral Equation for Electromagnetic Scattering from Homogeneous Dielectric Bodies (reprint)-----	49
On the Location of Leaky Wave Poles for a Grounded Dielectric Slab (manuscript)-----	51
Fundamental Mode Dispersion of a Microstrip Transmission Line (manuscript)-----	66
On the Dynamic Model for Passive Microwave Printed Circuits (dissertation proposal)-----	92

Accession For	
NTIS CRA&I	<input checked="" type="checkbox"/>
DTIC TAB	<input type="checkbox"/>
Unannounced	<input type="checkbox"/>
Justification	
By	
Date	
A-1	

I. OBJECTIVES

The objectives of this project were to investigate the full-wave (Maxwellian) analysis for solving and computing the electromagnetic behavior of microwave integrated circuits.

II. SUMMARY OF WORK DONE

The majority of the work was done in the first two years of this project. Summary reports for the first year's work and the second year's work are included to give details. The final six month's period was used primarily to prepare final manuscripts for submission to journals, and to give a preliminary organization for Mr. Hsu's Ph.D. dissertation. All publications to date and the preliminary version of Mr. Hsu's dissertation are appended to this report. The following is a list of these appendices:

1. Annual Report for the period January 1, 1988 to December 31, 1988.
2. Annual Report for the period January 1, 1989 to December 31, 1989.
3. "Quasi-Static Analysis of a Microstrip Via Through a Hole in a Ground Plane," by Taoyun Wang, R. F. Harrington, and J. R. Mautz, IEEE Trans. on MTT, Vol. 36, No. 6, pp. 1008-1013, June 1988.
4. "The Inductance Matrix of a Multiconductor Transmission Line in Multiple Magnetic Media," J. R. Mautz, R. F. Harrington, and C-I G. Hsu, IEEE Trans. on MTT, Vol. 36, No. 8, pp. 1293-1295, August 1988.
5. "Boundary Integral Formulations for Homogeneous Material Bodies," R. F. Harrington, Journ. of EM Waves and Appl, Vol. 3, No. 1, pp. 1-5, 1989.
6. The Excess Capacitance of a Microstrip Via in a Dielectric Substrate," IEEE Trans. on CAD, Vol. 9, No. 1, pp. 48-56, January 1990.
7. "A Stable Integral Equation for Electromagnetic Scattering from

Homogeneous Dielectric Bodies," J. R. Mautz, IEEE Trans. on AP, Vol. 37, No. 8, pp. 1070-1071, August 1989.

8. "On the Location of Leaky Wave Poles for a Grounded Dielectric Slab," C-I G. Hsu, R. F. Harrington, J. R. Mautz, and T. K. Sarkar, submitted to IEEE Trans. on MTT.

9. "Fundamental Mode Dispersion of a Microstrip Transmission Line," G-I G. Hsu, R. F. Harrington, J. R. Mautz, and C Jan, submitted to IEEE Trans. on MTT.

10. "On the Dynamic Model for Passive Microwave Printed Circuits," C-I G. Hsu, dissertation proposal, June 1990.

III. PERSONNEL

The following persons have worked on this project:

Roger F. Harrington, Principal Investigator, Professor of Electrical Engineering, Syracuse University.

Joseph R. Mautz, Research Engineer, Department of Electrical and Computer Engineering, Syracuse University.

Chung-I Gavin Hsu, Research Assistant, Graduate Student, Department of Electrical and Computer Engineering, Syracuse University.

Ing-Chieh Jan, Research Assistant, Graduate Student, Department of Electrical and Computer Engineering, Syracuse University.

Annual Report
FULL-WAVE ANALYSIS AND COMPUTATION OF MICROWAVE
INTEGRATED CIRCUITS

for the period
January 1, 1988 - December 31, 1988

by

Roger F. Harrington

Department of Electrical and Computer Engineering
Syracuse University
Syracuse, NY 13244-1240

Contract No. N00014-88-K-0027

with

Office of Naval Research
800 North Quincy Street
Arlington, VA 22217-5000

Date: December 10, 1988

Submitted by:

Roger F. Harrington

I. OBJECTIVES

The objectives of this project are to obtain full-wave (Maxwellian) analyses suitable for computing the electromagnetic behavior of micro-wave integrated circuits. Initial work has been on (a) attempting to extend the quasi-static analyses to include correction terms to allow application at higher frequencies, and (b) full-wave analyses to two-dimensional problems such as multiconductor transmission lines in multiple dielectric media.

II. SUMMARY OF FIRST YEAR'S WORK

A) Preliminary to extending the analyses to higher frequencies, we completed some quasi-static solutions. The following topics have led to papers published or pending, as listed in Section IV.

(1) Quasi-static analysis of a microstrip via through a hole in a ground plane and in a dielectric substrate. Abstract of [1]: The equivalent circuit of a via which connects two semi-infinitely long transmission lines through a circular hole in a ground plane is considered. The π -type equivalent circuit consists of two excess capacitances and an excess inductance. They are quasi-static quantities and thus are computed statically by the method of moments from the integral equations. The integral equations are established by introducing a sheet of magnetic current in the electrostatic case and a layer of magnetic charge in the magnetostatic case. Parametric plots of the excess capacitances, the excess inductance, and the characteristic admittance of the via are given for reference.

Abstract of [4]: The equivalent circuit of a via which connects two semi-infinitely long microstrip transmission lines imbedded in a dielectric medium above a ground plane is considered. The Γ -type equivalent circuit consists of an excess capacitance and an excess inductance. The excess inductance of the via is the same as the one computed in the case of free space (without a substrate). The excess capacitance of the via is computed quasi-statically by the method of moments and the image method from the integral equations. It converges rapidly as the number of image terms is increased. Parametric plots of the excess capacitance of the via are given for reference.

(2) The equivalent circuit of a microstrip crossover with and without a dielectric substrate. Abstract of [4]: The equivalent circuit of a microstrip crossover is found. Integral equations are obtained for the densities of excess charge, and these equations are solved by the method of moments. Introduction of a specified transverse distribution of charge, which satisfies the edge condition, reduces the computing time dramatically while the accuracy remains excellent. Several plots of the excess charge densities are provided along with numerical values of lumped excess capacitances.

Abstract of [5]: A quasi-static analysis is carried out to examine the capacitive coupling between two nonintersecting microstrip lines above a ground plane and in a dielectric substrate. The charge density along

the width of each strip is described using a prescribed charge distribution. A pair of coupled integral equations is derived and solved via the method of moments to obtain the excess charge densities. The lumped excess capacitances are computed and compared to the ones obtained using wire lines with radii equal to the equivalent radii of the strips.

(3) The inductance matrix of a multiconductor transmission line in multiple magnetic media. Abstract of [2]: Consider a multiconductor transmission line consisting of N_c conducting cylinders in inhomogeneous media consisting of N_d homogeneous regions with permeabilities μ_i and permittivities ϵ_i . The inductance matrix $[L]$ for the line is obtained by solving the magnetostatic problem of N_c conductors in N_d regions with permeabilities μ_i . The capacitance matrix $[C]$ for the line is obtained by solving the electrostatic problem of N_c conductors in N_d regions with permittivities ϵ_i . It is shown that $[L] = \mu_0 \epsilon_0 [C']^{-1}$, where $[C']$ is the capacitance matrix of an auxiliary electrostatic problem of N_c conductors in N_d regions with relative permittivities set equal to the reciprocals of the relative permeabilities of the magnetostatic problem, i.e., $\epsilon_i' / \epsilon_0 = \mu_0 / \mu_i$.

B) Work has been done on the following full-wave solutions:

(1) The full-wave solution for the microstrip transmission line has been investigated using the volume integral formulation. This gives an integral equation formulation where the unknowns are the conduction current and charge on conducting boundaries, the bound charge of the dielectric boundaries, and the polarization current in the dielectric volume. For waves, the propagation constant is obtained from the solution of a nonlinear eigenvalue equation. A numerical solution to this equation has been obtained to allow computation of the propagation constant, or, equivalently, the effective dielectric constant. The solution is complicated, and the computations are time consuming. We are presently looking for ways to simplify this solution.

(2) The full-wave solution for the microstrip transmission line has been investigated using a surface integral formulation. This gives an integral equation where the unknowns are the conduction current on the conducting boundaries and the equivalent electric and magnetic surface currents on the dielectric boundaries. Again the propagation constant is obtained from the solution to a nonlinear eigenvalue equation. The numerical solution to this equation has not yet been successfully obtained. Work is continuing on this solution.

There are many different surface integral formulations for any particular problem. These are summarized in the paper on boundary integral formulations for homogeneous material bodies ([3] of Section IV). The following is an abstract of [3]: There are many boundary integral formulations for the problem of electromagnetic scattering from the transmission into a homogeneous material body. The only formulations which give a unique solution at all frequencies are those which involve both electric and magnetic equivalent currents, and satisfy boundary conditions on both tangential \vec{E} and tangential \vec{H} . Formulations which involve only electric (or magnetic) equivalent currents, and those which involve boundary condi-

tions on only tangential \vec{E} (or tangential \vec{H}) are singular at frequencies corresponding to the resonant frequencies of a resonator formed by a perfect conductor covering the surface of the body and filled with the material exterior to the body in the original problem.

III. PLANS FOR THE SECOND YEAR'S WORK

A) Study of the volume integral formulation for the full-wave solution of 2-D problems will continue. Methods of reducing the complexity of the solution will be considered. In particular, a perturbation approach, starting from the quasi-TEM solution and adding correction terms will be studied and compared to the direct solution.

B) Study of the surface integral formulation for the full-wave solution of 2-D problems will continue. Again methods of reducing the complexity of the solution will be considered. However, this formulation does not appear to be as well suited to the perturbation approach as does the volume integral formulation of A above.

C) Study of the integral formulations for the full-wave solution of 3-D problems will be started. The particular approach to be taken will depend on the results of A and B above. It is hoped that a 3-D solution will lead to a formulation useful for actual printed circuits.

IV. PUBLICATIONS

- [1] T. Wang, R. F. Harrington, and J. R. Mautz, "Quasi-Static Analysis of a Microstrip Via through a Hole in a Ground Plane," IEEE Trans., vol. MTT-36, No. 6, June 1988.
- [2] J. R. Mautz, R. F. Harrington, and C-I G. Hsu, "The Inductance Matrix of a Multiconductor Transmission Line in Multiple Magnetic Media," IEEE Trans., vol. MTT-36, No. 8, pp. 1293-1295, Aug. 1988.

Accepted for publication:

- [3] R. F. Harrington, "Boundary Integral Equations for Homogeneous Material Bodies," Journ. Electromagnetic Waves and Applications, in press, to appear 1988.

Submitted for publication:

- [4] T. Wang, J. R. Mautz, and R. F. Harrington, "The Excess Capacitance of a Microstrip Via in a Dielectric Substrate," submitted to IEEE Transactions on Integrated Circuits and Systems.
- [5] S. Papatheodorou, R. F. Harrington, and J. R. Mautz, "The Equivalent Circuit of a Microstrip Crossover," submitted to Transactions of the Society for Computer Simulation.

- [6] S. Papatheodorou, R. F. Harrington, and J. R. Mautz, "The Equivalent Circuit of a Microstrip Crossover in a Dielectric Substrate," submitted to IEEE Transactions on Microwave Theory and Techniques.

Report:

- [7] S. Papatheodorou, J. R. Mautz, and R. F. Harrington, "The Equivalent Circuit of a Microstrip Crossover in a Dielectric Substrate," Report TR-88-11, Department of Electrical and Computer Engineering, Syracuse University, August 1988.

V. PERSONNEL

The following is the project staff for the first year:

Principal Investigator: Dr. Roger F. Harrington,
Professor of Electrical Engineering.

Research Engineer: Dr. Joseph R. Mautz,
Department of Electrical and Computer Engineering.

Research Assistant: Mr. Chung-I Gavin Hsu, Graduate Student,
Department of Electrical and Computer Engineering.

Annual Report
FULL-WAVE ANALYSIS AND COMPUTATION OF MICROWAVE
INTEGRATED CIRCUITS

for the period
January 1, 1989 - December 31, 1989

by

Roger F. Harrington

Department of Electrical and Computer Engineering
Syracuse University
Syracuse, NY 13244-1240

Contract No. N00014-88-K-0027

with

Office of Naval Research
800 North Quincy Street
Arlington, VA 22217-5000

Date: January 3, 1990

Submitted by:

R F Harrington

1. OBJECTIVES

The objectives of this project are to obtain full-wave (Maxwellian) analyses suitable for computing the electromagnetic behavior of microwave integrated circuits. Initial work has been on (a) attempting to extend the quasi-static analyses to include correction terms to allow application at higher frequencies, and (b) full-wave analyses to two-dimensional problems such as multiconductor transmission lines in multiple dielectric media. More recent work has been on (c) the solution of three-dimensional problems.

II. SUMMARY OF THE SECOND YEAR'S WORK

A) Publication of the first year's work as journal articles: The following papers have been published during the second year:

1. Roger F. Harrington, "Boundary Integral Formulations for Homogeneous Material Bodies," Journal of Electromagnetic Waves and Applications, vol. 3, No. 1, pp. 1-15, 1989.

Abstract - There are many boundary integral formulations for the problem of electromagnetic scattering from and transmission into a homogeneous material body. The only formulations which give a unique solution at all frequencies are those which involve both electric and magnetic equivalent currents, and satisfy boundary conditions on both tangential \bar{E} and tangential \bar{H} . Formulations which involve only electric (or magnetic) equivalent currents, and those which involve boundary conditions on only tangential \bar{E} (or tangential \bar{H}) are singular at frequencies corresponding to the resonant frequencies of a resonator formed by a perfect conductor covering the surface of the body and filled with the material exterior to the body in the original problem.

2. Joseph R. Mautz, "A Stable Integral Equation for Scattering from Homogeneous Dielectric Bodies," IEEE Transactions on Antennas and Propagation, vol. 37, No. 8, pp. 1070-1071, August 1989.

Abstract - It is shown that a previously derived integral equation for electromagnetic scattering from a homogeneous dielectric body does not have a unique solution at resonant frequencies of the cavity formed by making the surface S of the body perfectly conducting and filling the region internal to S with the external medium. This integral equation was formulated so that an equivalent electric current radiates in the presence of the homogeneous external medium to produce the scattered field external to the body. A combination of equivalent electric and magnetic currents is used to formulate an integral equation whose solution is always unique.

3. Taoyun Wang, J. R. Mautz, and R. F. Harrington, "The Excess Capacitance of a Microstrip Via in a Dielectric Substrate," IEEE Transactions on Computer-Aided Design, vol. 9, No. 1, pp. 48-56, January 1989.

Abstract - The equivalent circuit of a via which connects two semi-infinitely long microstrip transmission lines imbedded in a dielectric medium above a ground plane is considered. The Γ -type equivalent circuit consists of an excess capacitance and an excess inductance. The excess inductance of the via is the same as the one computed in the case of free space (without a substrate). The excess capacitance of the via is computed quasi-statically by the method of moments and the image method from the integral equations. It converges rapidly as the number of image terms is increased. Parametric plots of the excess capacitance of the via are given for reference.

B) Two-dimensional full-wave solutions of printed circuits: The surface integral formulation was found to be more suitable for computation than was the volume integral formulation. Hence, this solution was used for the final computations. A Technical Report was written: "Fundamental Mode Dispersion of a Microstrip Transmission Line," by Chung-I G. Hsu, R. F. Harrington, J. R. Mautz, and I-C Jan, Report TR-89-6, November 1989. A paper by the same name and authors has been submitted to the IEEE Transactions on Microwave Theory and Techniques.

Abstract - A spectral domain type solution with nonuniform subdomain basis functions is implemented to investigate the dispersion characteristics of the fundamental mode of a microstrip transmission line. Agreement with the data available in the literature is demonstrated in several plots, where only the longitudinal current is used in numerical computation. This numerical scheme proves to be an alternative, or rather a supplement, to various well-developed methods in this area.

C) Integral formulations and solutions for the three-dimensional printed circuit problem. We have obtained a formulation for the 3-D circuit as an extension of the arbitrarily-shaped wire formulation for the homogeneous dielectric case. (For example, see Chapter 4 of FIELD COMPUTATION BY MOMENT METHODS, R. F. Harrington, Krieger Publishing Co., 1982). The solution for the printed circuit problem is much more difficult than that for the homogeneous dielectric problem, because now the Green's function contains a Sommerfeld integral. Some approximate and numerical methods for evaluating the integral have been obtained in the literature, but the solution is still complicated. We intend to use an "equivalent radius" simplification to obtain a wire-type solution for

arbitrary printed circuits. The equivalent radius will be obtained from the simpler 2-D problem of a printed circuit transmission line.

D) Software packages for printed circuit multiconductor transmission lines: Three menu-driven, user-friendly software packages have been published by Artech House. These are:

(1) "Matrix Parameters of Multiconductor Transmission Lines," by A. R. Djordjevic, R. F. Harrington, T. K. Sarkar, and M. B. Bazdar. This program calculates the quasistatic matrix parameters of multiconductor transmission lines, i.e., matrices of inductance, capacitance, resistance, and conductance. The program can treat multiple dielectric layers as well as multiple conductors of arbitrary shape. A complete user's manual accompanies the computer program.

(2) "Time-Domain Response of Multiconductor Transmission Lines," by A. R. Djordjevic, R. F. Harrington, T. K. Sarkar, and M. B. Bazdar. This program uses the output of the previous program as input. It computes the response of a lossless multiconductor transmission line with linear or nonlinear loads. It uses the modal time-domain solution, which is the most accurate and fastest one. The terminating networks may contain generators, resistors, short circuits, open circuits, interconnectors, inductors, capacitors, and nonlinear resistors. The output consists of voltage waveforms on all lines at specified points along the line.

3) "Scattering Parameters of Microwave Networks with Multiconductor Transmission Lines," by A. R. Djordjevic, M. B. Bazdar, G. M. Vitosevic, R. F. Harrington, and T. K. Sarkar. This program uses the output of the first program as input. It analyzes networks consisting of multiconductor transmission lines and discrete elements. The output is the scattering matrix, the impedance matrix, and the admittance matrix of the

network. The transmission lines are treated by modal analysis in the time domain, including losses. The output is in a format similar to that obtained from network analyzers used for experimental measurements.

III. PLANS FOR FUTURE WORK

A) The work on mode dispersion on a microstrip transmission line, item IIB above, will be published.

B) Study of the solution to three-dimensional printed circuits, item IIC above, will continue. It is planned to develop a user-friendly computer program to handle three-dimensional integrated circuits of arbitrary shape.

C) If time permits, the full-wave solution of a microstrip transmission line, item IIB above, will be generalized to a multiconductor line with conductors of arbitrary shape.

IV. PUBLICATIONS

- [1] Roger F. Harrington, "Boundary Integral Formulations for Homogeneous Material Bodies," Journal of Electromagnetic Waves and Applications, vol. 3, No. 1, pp. 1-15, 1989.
- [2] Joseph R. Mautz, "A Stable Integral Equation for Scattering by Homogeneous Dielectric Bodies," IEEE Transactions on Antennas and Propagation, vol. 37, No. 8, pp. 1070-1071, August 1989.
- [3] T. Wang, J. R. Mautz, and R. F. Harrington, "The Excess Capacitance of a Microstrip Via in a Dielectric Substrate," IEEE Transactions on Computer-Aided Design, vol. 9, No. 1, pp. 48-56, January 1989.
- [4] C-I G. Hsu, R. F. Harrington, J. R. Mautz, and I-C Jan, "Fundamental Mode Dispersion of a Microstrip Transmission Line," Submitted to

IEEE Transactions on Microwave Theory and Techniques.

V. PERSONNEL

The following is the project staff for the second year:

Principal Investigator: Dr. Roger F. Harrington, Professor of
Electrical Engineering.

Research Associate: Dr. Joseph R. Mautz, Department of Electrical and
Computer Engineering

Research Assistant: Mr. Chung-I Gavin Hsu, Graduate Student, Department
of Electrical and Computer Engineering

Research Assistant: Mr. Ing-Chieh Jan, Graduate Student, Department of
Electrical and Computer Engineering.

**Quasi-Static Analysis of a Microstrip Via Through a Hole
in a Ground Plane**

**Taoyun Wang
Roger F. Harrington
Joseph R. Mautz**

**Reprinted from
IEEE TRANSACTIONS ON MICROWAVE THEORY AND TECHNIQUES
Vol. 36, No. 6, June 1988**

Quasi-Static Analysis of a Microstrip Via Through a Hole in a Ground Plane

TAOYUN WANG, STUDENT MEMBER, IEEE, ROGER F. HARRINGTON, FELLOW, IEEE,
AND JOSEPH R. MAUTZ, SENIOR MEMBER, IEEE

Abstract—The equivalent circuit of a via which connects two semi-ininitely long transmission lines through a circular hole in a ground plane is considered. The π -type equivalent circuit consists of two excess capacitances and an excess inductance. They are quasi-static quantities and thus are computed statically by the method of moments from the integral equations. The integral equations are established by introducing a sheet of magnetic current in the electrostatic case and a layer of magnetic charge in the magnetostatic case. Parametric plots of the excess capacitances, the excess inductance, and the characteristic admittance of the via are given for reference.

I. INTRODUCTION

THE GEOMETRY of the problem to be considered in this paper is shown in Fig. 1. Two semi-ininitely long transmission lines, wire 1 and wire 2, are connected by a via through a hole in a conducting ground plane. The via consists of wire 3 and wire 4. The radii of wires 1, 2, 3, 4, and the hole, denoted a_1 , a_2 , a_3 , a_3 , and a_3 , respectively, are very small compared to the heights, h_1 and h_2 , of wire 1 and wire 2 with respect to ground. The media in the upper region (region a) and the lower region (region b) may be different. Let us assume that (ϵ_1, μ_1) and (ϵ_2, μ_2) are the constitutive constants for region a and region b, respectively. Also, the media and all the conductors are perfect (lossless). For simplicity, the equivalent circuit of the via is assumed to be π -type, as is shown in Fig. 2. In Fig. 2, Y_{01} is the characteristic admittance of wire 1 above the ground plane and Y_{02} is the characteristic admittance of wire 2 below the ground plane. The circuit of Fig. 2 is valid when only a small portion of the line voltage is dropped across L_e and when only a small portion of the line current is shunted through C_{e1} and C_{e2} . We desire to determine the capacitances C_{e1} and C_{e2} and the inductance L_e . The problem described here is of practical interest. For example, printed circuits on different sides of a ground plane inside computers are often connected by a via through a hole in the ground plane. The related problems of the connection of two perpendicular strips above a ground plane [1], the connection of two parallel wires

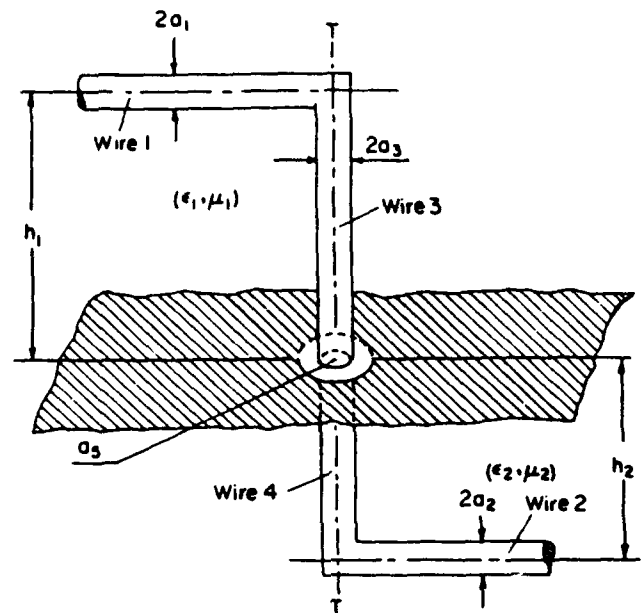


Fig. 1. The geometrical structure of the problem.

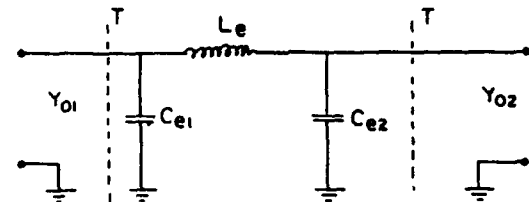


Fig. 2. The equivalent circuit for the problem.

above a ground plane [2], and the connection of two parallel strips above a ground plane [3], [4] were previously considered.

The equivalent capacitance C_{e1} of the portion of the via above the ground plane is a quasi-electrostatic quantity and is defined as [2], [3]

$$C_{e1} = \lim_{l_1 \rightarrow \infty} \frac{Q_1 + Q_3 - l_1 q_{01}}{V} \quad (1)$$

Here Q_1 is the total electric charge on the portion of wire 1 of length l_1 , Q_3 is the total charge on wire 3, V is the constant voltage maintained at the surface of the wires with respect to ground, and q_{01} is the uniform charge density on wire 1 far away from the via, or equivalently, the charge density required to raise the potential of wire 1

Manuscript received August 21, 1987; revised January 4, 1988. This work was supported by the Office of Naval Research, Arlington, VA 22217, under Contract N00014-88-K-0027 and by the New York State Center for Advanced Technology in Computer Applications and Software Engineering, Syracuse University.

The authors are with the Department of Electrical and Computer Engineering, Syracuse University, Syracuse, NY 13244-1240.
IEEE Log Number 8820438.

to V volts if the hole were closed, wire 3 were removed, and wire 1 were extended to infinity. Henceforth in the electrostatic case, charge density means charge per unit length. However, since the numerator of the right-hand side of (1) approaches a constant that is very small compared to Q_1 and $l_1 q_{01}$, as l_1 becomes large, numerical calculation of C_{e1} from (1) would result in significant error. To avoid this, we subtract the uniform charge density from the total charge density so that the difference, called the excess charge density, is the unknown in the boundary integral equations. The equivalent capacitance C_{e1} is then the sum of the total excess charge on wire 1 and wire 3 if the voltage V is set to one volt. Hence C_{e1} is also called the excess capacitance of the upper part of the via (wire 3). In a similar manner, the equivalent capacitance C_{e2} is defined and is called the excess capacitance of the lower part of the via (wire 4).

The equivalent inductance L_e is a quasi-magnetostatic quantity defined by [2], [4]

$$L_e = \frac{1}{I} \left\{ \int_{\text{wire 1}} (A_1 - A_{10}) \cdot dl + \int_{\text{wire 3}} A_3 \cdot dl \right\} + \frac{1}{I} \left\{ \int_{\text{wire 2}} (A_2 - A_{20}) \cdot dl + \int_{\text{wire 4}} A_4 \cdot dl \right\} \quad (2)$$

where A_i is the total magnetic vector potential on wire i , $i=1,2,3,4$, due to the steady electric current of filamentary strength I flowing from wire 1 through the via to wire 2. A_{10} is the uniform magnetic vector potential on wire 1 far away from the via or, equivalently, the magnetic vector potential that would be produced by an I ampere current on wire 1 if the hole were closed, wire 3 were removed, and wire 1 were extended to infinity. A_{20} is similarly defined. The sum of the four integrals in (2) is a line integral from a point far to the left on the surface of wire 1 to a point far to the right on the surface of wire 2. Equation (2) is derivable from [4, eq. (1)]. L_e is also called the excess inductance of the via. For convenience, we call the first bracketed term the excess inductance of the upper via (wire 3) and the second bracketed term the excess inductance of the lower via (wire 4).

II. FORMULATION

The excess capacitances C_{e1} and C_{e2} are quasi-electrostatic quantities and thus computed in the electrostatic case. As shown in Fig. 3, we first close the hole by a conductor and place a sheet of magnetic current M just above the hole and $-M$ just below it. Steady in that it has no surface divergence, this magnetic current is related to the electric field E_A over the hole by

$$M = E_A \times n \quad (3)$$

where n is the unit vector normal to the ground plane and pointing upwards (from region b to region a). By the uniqueness theorem [5, sec. 3-3] and the equivalence principle [5, sec. 3-5], the field remains the same in region a

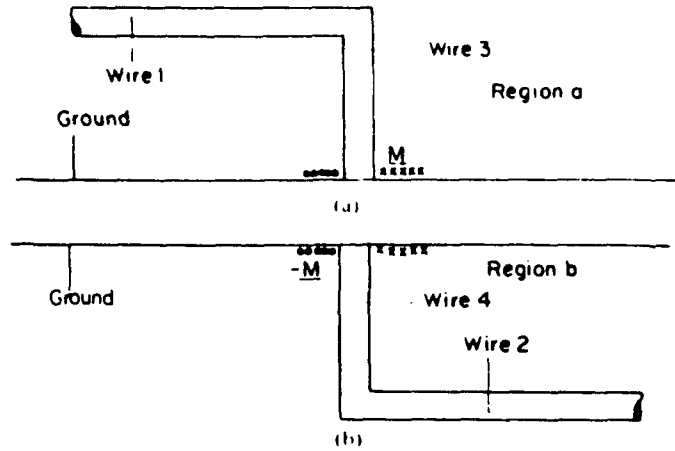


Fig. 3. The electrostatic problem divided into two parts. (a) The electric field remains unchanged in region a if the hole is closed and M is placed above the hole. (b) The electric field remains unchanged in region b if the hole is closed and $-M$ is placed just below the hole.

and region b if

$$\epsilon_1 \frac{\partial \phi^a}{\partial n} = \epsilon_2 \frac{\partial \phi^b}{\partial n} \quad \text{in the hole} \quad (4)$$

where ϕ^i is the electric potential in region i , $i=a,b$. In addition to (4) the following boundary conditions must also be satisfied:

$$\begin{aligned} \phi^a &= V & \text{on wires 1 and 3} \\ \phi^b &= V & \text{on wires 2 and 4.} \end{aligned} \quad (5)$$

Neither wire 3 nor wire 4 is connected to the ground plane in Fig. 3.

The total charge density may be recognized as the sum of the excess charge density and uniform charge density, i.e.,

$$q = \begin{cases} q_{e1} + q_{01} & \text{on wire 1} \\ q_{e3} & \text{on wire 3} \\ q_{e4} & \text{on wire 4} \\ q_{e2} + q_{02} & \text{on wire 2} \end{cases} \quad (6)$$

where the subscript e on q denotes excess charge density. q_{01} and q_{02} are known and are given by

$$\begin{aligned} q_{01} &= \frac{2\pi\epsilon_1 V}{\ln(2h_1/a_1)}, & h_1 \gg a_1 \\ q_{02} &= \frac{2\pi\epsilon_2 V}{\ln(2h_2/a_2)}, & h_2 \gg a_2. \end{aligned} \quad (7)$$

If the potential V is set to one volt, the total excess charge will give rise to the desired excess capacitance, i.e.,

$$\begin{aligned} C_{e1} &= \int_{\text{wire 1}} q_{e1} dl + \int_{\text{wire 3}} q_{e3} dl \\ C_{e2} &= \int_{\text{wire 2}} q_{e2} dl + \int_{\text{wire 4}} q_{e4} dl. \end{aligned} \quad (8)$$

Let $\phi(q_{ei})$ denote the potential due to q_{ei} in the presence of the completed ground plane (hole closed). $\phi^a(M)$ the potential in region a due to M residing on the region a

side of the completed ground plane, and $\phi(M)$ the potential in region b due to M residing on the region b side. Then,

$$\begin{aligned}\phi^a &= \phi(q_{01}) + \phi(q_{e1}) + \phi(q_{e3}) + \phi^+(M) \\ \phi^b &= \phi(q_{02}) + \phi(q_{e2}) + \phi(q_{e4}) - \phi^-(M).\end{aligned}\quad (9)$$

Note that the electric potential due to a sheet of steady magnetic current is analogous to the magnetic scalar potential due to a sheet of steady electric current. The latter is studied in many fundamental electromagnetic field theory books, for example, [6]. Substitution of (9) into (4) and (5), with V being set to one volt, yields integral equations for the excess charge densities:

$$\begin{aligned}\phi(q_{e1}) + \phi(q_{e3}) + \phi^+(M) &= 1 - \phi(q_{01}) \quad \text{on wires 1 and 3} \\ \phi(q_{e2}) + \phi(q_{e4}) - \phi^-(M) &= 1 - \phi(q_{02}) \quad \text{on wires 2 and 4} \\ \epsilon_1 \frac{\partial \phi(q_{e1})}{\partial n} + \epsilon_1 \frac{\partial \phi(q_{e3})}{\partial n} + \epsilon_1 \frac{\partial \phi^+(M)}{\partial n} &- \epsilon_2 \frac{\partial \phi(q_{e2})}{\partial n} - \epsilon_2 \frac{\partial \phi(q_{e4})}{\partial n} + \epsilon_2 \frac{\partial \phi^-(M)}{\partial n} \\ &= -\epsilon_1 \frac{\partial \phi(q_{01})}{\partial n} + \epsilon_2 \frac{\partial \phi(q_{02})}{\partial n} \quad \text{in the hole.}\end{aligned}\quad (10)$$

Although q_{e1} and q_{e2} exist on the semi-infinitely long wires 1 and 2, they decay to zero rapidly as one moves away from the via. We may truncate q_{e1} and q_{e2} and the boundary equations on wire 1 and wire 2 at some distances, say $3h_1$ and $3h_2$, from the via. By doing so, we neglect the contribution to the excess capacitances from the excess charge beyond the lengths $3h_1$ on wire 1 and $3h_2$ on wire 2. Now, the method of moments may be used to solve for q_{e1} , q_{e2} , q_{e3} , q_{e4} , and M numerically. We divide wire 1 and wire 2 (truncated) and wire 3 and wire 4 into subsections, assume uniform charge distribution on each subsection, and enforce the first two of equations (10) at the center of each subsection. Furthermore, we divide the hole into annuluses, assume uniform circulating current distribution on each annulus, and enforce the third of equations (10), which is averaged over the interval from 0 to 2π for the azimuthal variation, at the midpoint between the edges of each annulus. A detailed discussion of the moment method as applied to this problem is presented in [7].

Now, we turn to the magnetostatic case to compute the excess inductance. Similar to the electrostatic case, we close the hole by a conductor and place a layer of magnetic charge density m just above the hole and $-m$ just below it, as is shown in Fig. 4. This m is equal to the normal magnetic field over the hole. Again by the uniqueness theorem and the equivalence principle, the magnetic field remains unchanged in region a and region b if

$$H_{tan}^a = H_{tan}^b \quad (11)$$

is enforced, where H_{tan}^i is the tangential magnetic intensity

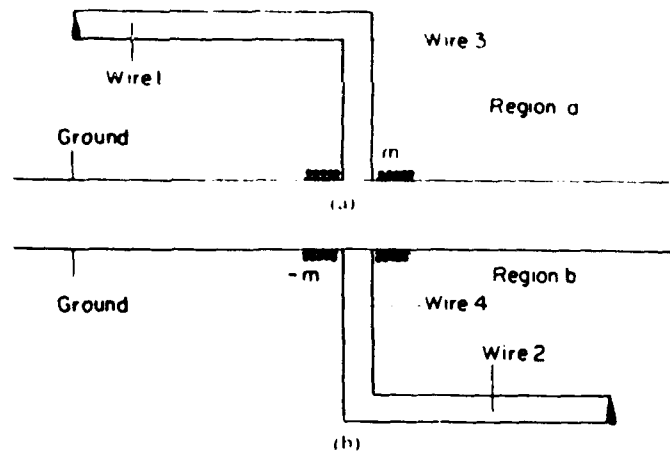


Fig. 4. The magnetostatic problem divided into two parts. (a) The magnetic field remains unchanged in region a if the hole is closed and m is placed just above the hole. (b) The magnetic field remains unchanged in region b if the hole is closed and $-m$ is placed just below the hole.

over the hole in region i , $i = a, b$. Let H (wire i) denote the magnetic intensity due to the electric current on wire i in the presence of the completed ground plane for $i = 1, 2, 3, 4$, $H^+(m)$ the magnetic intensity due to m above the completed ground plane, and $H^-(m)$ the magnetic intensity due to m below the completed ground plane. We can write

$$\begin{aligned}H^a &= H(\text{wire 1}) + H(\text{wire 3}) + H^+(m) \\ H^b &= H(\text{wire 2}) + H(\text{wire 4}) - H^-(m).\end{aligned}\quad (12)$$

Note that the magnetic intensity due to a layer of magnetic charge is analogous to the electric field due to a layer of electric charge, as discussed in [6]. Therefore, $H^+(m)$ and $H^-(m)$ may be represented by the gradients of some scalar functions $\Psi^+(m)$ and $\Psi^-(m)$. That is,

$$\begin{aligned}H^+(m) &= -\nabla \Psi^+(m) \\ H^-(m) &= -\nabla \Psi^-(m).\end{aligned}\quad (13)$$

Substitution of (12) and (13) into (11) gives

$$\begin{aligned}\nabla \Psi^+(m) + \nabla \Psi^-(m) \Big|_{tan} \\ = H(\text{wire 1}) - H(\text{wire 2}) + H(\text{wire 3}) - H(\text{wire 4}) \Big|_{tan}.\end{aligned}\quad (14)$$

Equation (14), an integral equation for m , implies that $\Psi^+(m) + \Psi^-(m)$ equals Ψ^{inc} , where Ψ^{inc} is a potential whose gradient is the right-hand side of (14). To compensate for the fact that Ψ^{inc} is only known to within an additive constant, we require that the total magnetic charge associated with m vanish. The moment method may be applied now to solve the scalar equation derived from (14) subject to the above constraint on m .

Since there is no coupling between wire 1 and wire 3 and between wire 2 and wire 4, we have

$$\begin{aligned}A_1 &= A_1(\text{wire 1}) + A_1^+(m) \\ A_2 &= A_2(\text{wire 2}) - A_2^-(m) \\ A_3 &= A_3(\text{wire 3}) + A_3^+(m) \\ A_4 &= A_4(\text{wire 4}) - A_4^-(m)\end{aligned}\quad (15)$$

where A_i (wire i) is the magnetic vector potential on the surface of wire i due to the current I on wire i in the presence of the completed ground plane, $i=1,2,3,4$. Moreover, $A_i^+(m)$ is the vector potential on the surface of wire i , $i=1,3$, due to m residing on the region a side of the completed ground plane, and $A_i^-(m)$ is the vector potential on the surface of wire i , $i=2,4$, due to m residing on the region b side. Note that (15) is valid only for the vector potential component tangent to each wire and that the other component is not of interest. Letting I be one ampere and putting (15) into (2), we get the excess inductance of wire 3:

$$L_{e1} = \int_{\text{wire 1}} (A_1(\text{wire 1}) - A_{10}) \cdot dl + \int_{\text{wire 3}} A_3(\text{wire 3}) \cdot dl + \int_{\text{wire 1}} A_1^+(m) \cdot dl + \int_{\text{wire 3}} A_3^+(m) \cdot dl. \quad (16)$$

The excess inductance of wire 4 is obtained from the above expression by replacing all the 1's by 2's, 3's by 4's, m 's by $-m$'s, and superscripts $+$ by $-$, that is,

$$L_{e2} = \int_{\text{wire 2}} (A_2(\text{wire 2}) - A_{20}) \cdot dl + \int_{\text{wire 4}} A_4(\text{wire 4}) \cdot dl - \int_{\text{wire 2}} A_2^-(m) \cdot dl - \int_{\text{wire 4}} A_4^-(m) \cdot dl. \quad (17)$$

Because of the small radii of the wires, the current on the surface of each wire may be approximated by a filamentary current I on the axis of the wire. Thus the first two integrals in (16) can be evaluated analytically [2]. The last two integrals may be expressed in terms of magnetic intensities according to Stokes's theorem. The result is

$$L_{e1} = \frac{\mu_1}{4\pi} \left[2h_1 \ln \left(\frac{4h_1}{a_3} \right) - 4h_1 + a_1 + a_3 \right] + \mu_1 \int_{S_1} H_n^+(m) ds \quad (18)$$

where in the last integral, S_1 is the planar surface bounded by the axes of wire 1 and wire 3 and the ground. The subscript n on $H^+(m)$ denotes the component normal to S_1 and pointing into the paper. The expression for L_{e2} is similar to (18) in form. The excess inductance of the via is then the sum of L_{e1} and L_{e2} .

III. NUMERICAL RESULTS AND DISCUSSION

In order to implement the computer program on a PC/AT, we simplify the computation by choosing only one expansion function for the magnetic current and none for the magnetic charge. This is justified as follows. Since the radius of the hole is very small compared to the heights h_1 and h_2 , the couplings (electric and magnetic) through the hole between wire 1 and wire 2 are negligible to the first-order approximation. In other words, the fields in the hole are primarily from the via (wire 3 and wire 4). In the electrostatic case, the tangential electric field in the hole is

in the radial direction with the variation being of the form

$$E_A = \frac{K}{\rho \sqrt{1 - (\rho/a_s)^2}} \quad (19)$$

where ρ is the radial distance from the center of the hole and K is a constant determined by

$$\int E_A \cdot dl = 1. \quad (20)$$

The integration path is chosen in the radial direction from the surface of wire 3 to the edge of the hole. Substitution of (19) into (20) gives

$$K = \frac{1}{\ln(a_s/a_3 + \sqrt{(a_s/a_3)^2 - 1})}. \quad (21)$$

Thus the magnetic current is circulating and its amplitude is given by

$$M = \frac{1}{\ln(a_s/a_3 + \sqrt{(a_s/a_3)^2 - 1})} \cdot \frac{1}{\rho \sqrt{1 - (\rho/a_s)^2}}. \quad (22)$$

In the magnetostatic case, the normal magnetic field in the hole is negligible. Hence the magnetic charge may be neglected and a closed form for the excess inductance of the via is obtained. That is,

$$L_e = \frac{\mu_1}{2\pi} h_1 \ln \left(\kappa_1 \frac{h_1}{a_3} \right) + \frac{\mu_2}{2\pi} h_2 \ln \left(\kappa_2 \frac{h_2}{a_3} \right) \quad (23)$$

where κ_1 and κ_2 are constants. Approximately, $\kappa_1 = \kappa_2 = 0.5413$.

In Figs. 5-7, the normalized excess capacitance of the upper via (wire 3) $C_{e1}/(\epsilon_1 a_3)$ is plotted. The curves are also applicable to the normalized excess capacitance $C_{e2}/(\epsilon_2 a_3)$ of the lower via (wire 4) if all the subscripts 1 are replaced by 2. In Figs. 8 and 9¹ the normalized excess inductance $L_e/(2\mu_1 a_3)$ of a symmetric via is plotted. A via is symmetric if $(h_1, a_1, \epsilon_1, \mu_1) = (h_2, a_2, \epsilon_2, \mu_2)$. These plots can also be viewed as plots for the normalized excess inductance $L_{e1}/(\mu_1 a_1)$ of the upper via. If the subscripts 1 are replaced by 2, they become plots of $L_{e2}/(\mu_2 a_1)$, the normalized inductance of the lower via. In Figs. 10 and 11 the characteristic admittance $\eta_1 Y_e$ of a symmetric via is plotted. Here η_1 is the intrinsic impedance of the medium. The characteristic admittance of the via is defined as

$$Y_e = \sqrt{(C_{e1} + C_{e2})/L_e}. \quad (24)$$

If a TEM wave approaches the via along wire 1 and if wire 2 is terminated with a matched load (Y_{02}), then it can be shown that the least reflection will occur when

$$Y_e = \sqrt{Y_{01} Y_{02}}. \quad (25)$$

¹Note that the curves in Figs. 8 and 9 are plotted under the assumption that the hole is small in relation to the heights h_1 and h_2 . To emphasize this and to be consistent with other plots, we add the restriction $a_s < 2a_1$.

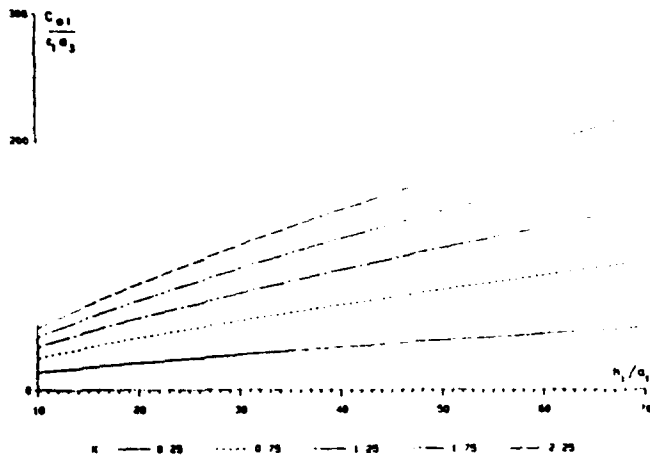


Fig. 5. Normalized excess capacitance of the upper via ($a_5 = 2a_3$, $k = a_1/a_3$).

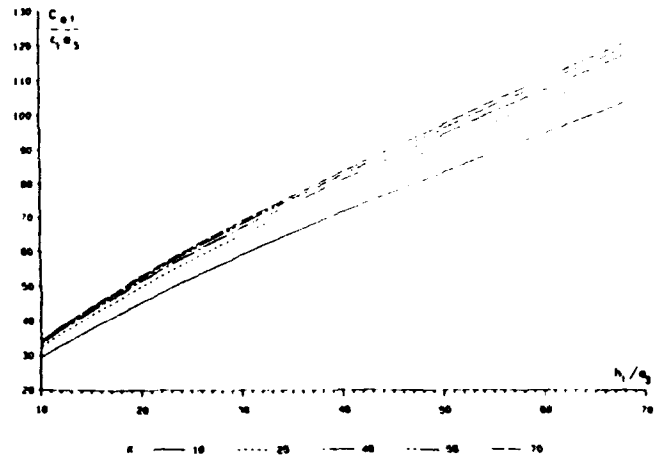


Fig. 7. Normalized excess capacitance of the upper via ($a_5 = 2a_3$, $k = h_1/a_3$).

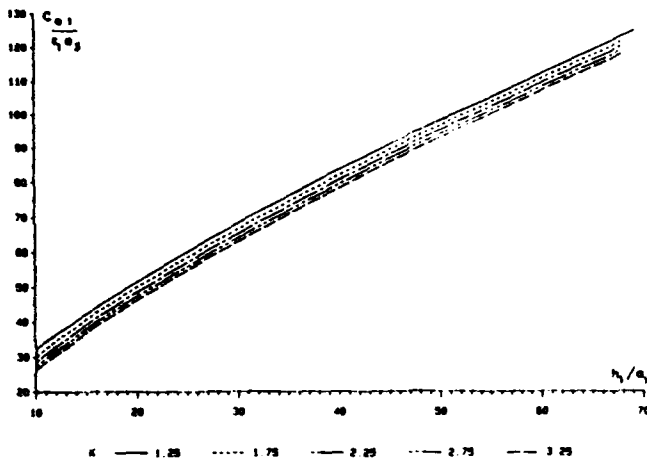


Fig. 6. Normalized excess capacitance of the upper via ($a_1 = a_3$, $k = a_5/a_3$).

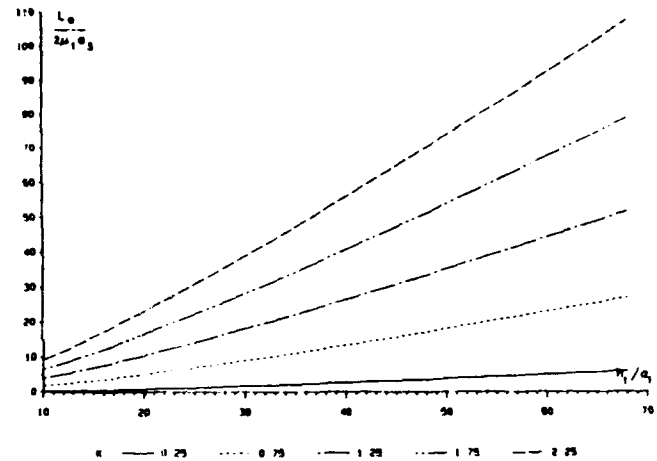


Fig. 8. Normalized excess inductance of a symmetric via ($a_5 = 2a_3$, $k = a_1/a_3$).

To see this, we notice that the voltage reflection coefficient at the T plane on wire 1 in Fig. 2 is given by

$$\Gamma = \frac{\frac{Y_{01}(1 - \omega^2 L_e C_{e2}) - Y_{02}(1 - \omega^2 L_e C_{e1})}{j\omega L_e} + Y_{01}Y_{02} - \frac{1}{L_e} \left[C_{e1} \left(1 - \frac{\omega^2 L_e C_{e2}}{2} \right) + C_{e2} \left(1 - \frac{\omega^2 L_e C_{e1}}{2} \right) \right]}{\frac{Y_{01}(1 - \omega^2 L_e C_{e2}) + Y_{02}(1 - \omega^2 L_e C_{e1})}{j\omega L_e} + Y_{01}Y_{02} + \frac{1}{L_e} \left[C_{e1} \left(1 - \frac{\omega^2 L_e C_{e2}}{2} \right) + C_{e2} \left(1 - \frac{\omega^2 L_e C_{e1}}{2} \right) \right]} \quad (26)$$

where ω is the angular frequency. Usually, $\omega^2 L_e (C_{e1} + C_{e2}) \ll 1$. The above expression then reduces to

$$\Gamma = \frac{Y_{01} - Y_{02} + j\omega L_e Y_{01} Y_{02} - j\omega (C_{e1} + C_{e2})}{Y_{01} + Y_{02} + j\omega L_e Y_{01} Y_{02} + j\omega (C_{e1} + C_{e2})} \quad (27)$$

When (25) is satisfied, the magnitude of the numerator of (27) assumes its minimum, the magnitude of the denominator is roughly $Y_{01} + Y_{02}$, and thus $|\Gamma|$ is minimized. The reflection from the via is minimized. Furthermore, if (25) is satisfied and if the system is symmetric ($Y_{01} = Y_{02}$), there is no reflection from the via. That is, all of the power from the incident wave will be transmitted through the via to the matched load. In this case, the via is called reflectionless.

To design a reflectionless via, consider the following numerical example. Suppose that

$$\begin{aligned} h_1 &= h_2 = 1.00 \text{ cm} \\ a_1 &= a_2 = 0.10 \text{ cm} \\ a_5 &= 2a_3 \end{aligned} \quad (28)$$

and that we wish minimize reflection from the via. Since

$$Y_{01} = Y_{02} = \frac{2\pi}{\eta \ln(2h_1/a_1)} = \frac{2.10}{\eta} \quad (29)$$

the reflectionless condition becomes

$$\eta Y_e = 2.10. \quad (30)$$

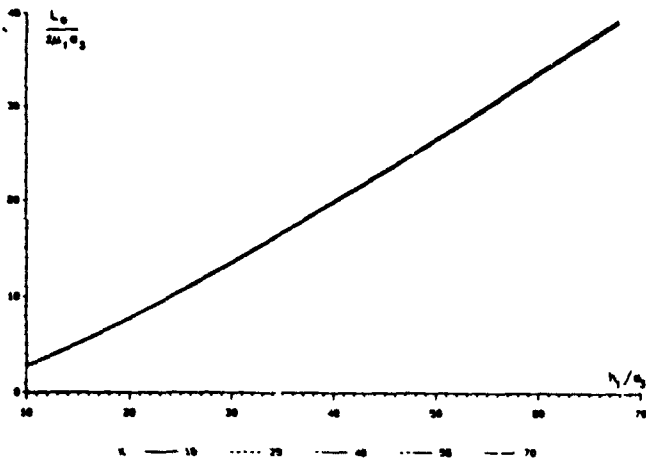


Fig. 9. Normalized excess inductance of a symmetric via ($a_2 = 2a_1$, $k = h_1/a_1$).

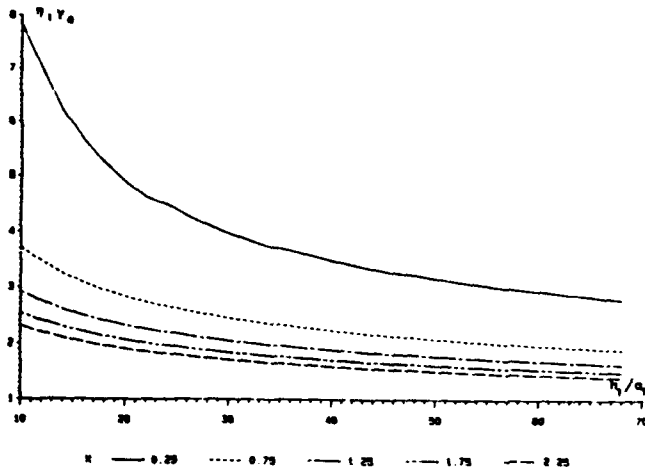


Fig. 10. Normalized characteristic admittance of a symmetric via ($a_2 = 2a_1$, $k = a_1/a_3$).

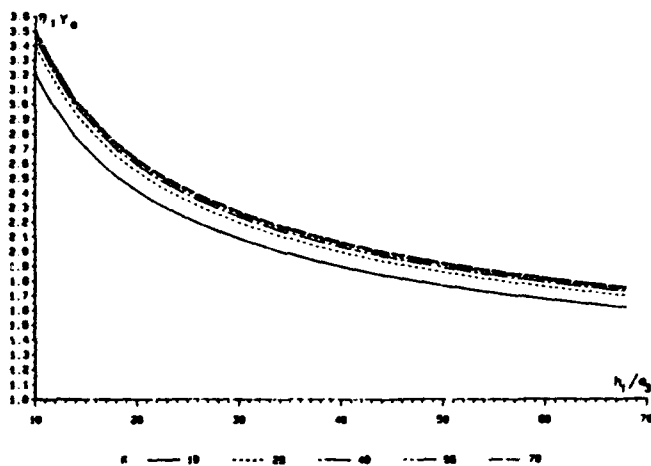


Fig. 11. Normalized characteristic admittance of a symmetric via ($a_2 = 2a_1$, $k = h_1/a_1$).

Using the $k = 10$ curve in Fig. 11, we find that the above condition is satisfied when $a_3 = 0.034$ cm. Hence, given (28), the via will be reflectionless when the radius of the via is 0.034 cm.

REFERENCES

- [1] A. E. Ruelhi and P. A. Brennan, "Capacitance models for integrated circuit metallization wires," *IEEE J. Solid-State Circuits*, vol. SC-10, pp. 530-536, Dec. 1975.
- [2] T. Wang, R. F. Harrington, and J. R. Mautz, "The equivalent circuit of a via," *Trans. Soc. Comput. Simulation*, vol. 4, in press, 1987.
- [3] J. R. Mautz and R. F. Harrington, "Calculation of the excess capacitance of a microstrip discontinuity," Tech. Rep. TR-84-2, Department of Electrical and Computer Engineering, Syracuse University, Syracuse, NY, Jan. 1984.
- [4] J. R. Mautz and R. F. Harrington, "Calculation of the excess inductance of a microstrip discontinuity," Tech. Rep. SYRU/DECE/TR-84/5, Department of Electrical and Computer Engineering, Syracuse University, Syracuse, NY, May 1984.
- [5] R. F. Harrington, *Time-Harmonic Electromagnetic Fields*. New York: McGraw-Hill, 1961.
- [6] J. R. Reitz, F. J. Millford, and R. W. Christy, *Foundations of Electromagnetic Theory*, 3rd ed. Reading, MA: Addison-Wesley, 1980.
- [7] T. Wang, "The excess capacitance of a microstrip via," master's thesis, Graduate School, Syracuse University, Syracuse, NY, Dec. 1984.



and transmission, microstrip circuits, and numerical methods.



Dr. Harrington is a member of Tau Beta Pi, Sigma Xi, and the American Association of University Professors.



solving field problems.

Taoyun Wang (S'84) was born in 1963. He received the B.S. degree in 1982 from Xian Jiaotong University, China, and the M.S. degree in 1984 from Syracuse University, Syracuse, NY, both in electrical engineering. He is currently working toward the Ph.D. degree in electrical engineering and the M.S. degree in mathematics at Syracuse University. Since September 1983, he has been actively involved with the electromagnetic research group at Syracuse University. His research areas include electromagnetic scattering

Roger F. Harrington (S'48-A'53-M'57-SM'62-F'68) was born in Buffalo, NY, on December 24, 1925. He received the B.E.E. and M.E.E. degrees from Syracuse University, Syracuse, NY, in 1948 and 1950, respectively, and the Ph.D. degree from Ohio State University, Columbus, OH, in 1952.

From 1945 to 1946, he served as an Instructor at the U.S. Naval Radio Materiel School, Dearborn, MI, and from 1948 to 1950, he was employed as an Instructor and Research Assistant at Syracuse University. While studying at Ohio State University, he served as a Research Fellow in the Antenna Laboratory. Since 1952, he has been on the faculty of Syracuse University, where he is presently Professor of Electrical Engineering. During 1959-1960, he was visiting Associate Professor at the University of Illinois, Urbana; in 1964 he was Visiting Professor at the University of California, Berkeley; and in 1969 he was Guest Professor at the Technical University of Denmark, Lyngby, Denmark.

Joseph R. Mautz (S'66-M'67-SM'75) was born in Syracuse, NY, on April 29, 1939. He received the B.S., M.S., and Ph.D. degrees in electrical engineering from Syracuse University, Syracuse, NY, in 1961, 1965, and 1969, respectively.

He is a Research Engineer in the Department of Electrical Engineering, Syracuse University, working on radiation and scattering problems. His primary fields of interest are electromagnetic theory and applied mathematics. He is currently working in the area of numerical methods for

The Inductance Matrix of a Multiconductor Transmission Line in Multiple Magnetic Media

JOSEPH R. MAUTZ, SENIOR MEMBER, IEEE,
 ROGER F. HARRINGTON, FELLOW, IEEE, AND
 CHUNG-I G. HSU, STUDENT MEMBER, IEEE

Abstract—Consider a multiconductor transmission line consisting of N_c conducting cylinders in inhomogeneous media consisting of N_d homogeneous regions with permeabilities μ , and permittivities ϵ . The inductance matrix $[L]$ for the line is obtained by solving the magnetostatic problem of N_c conductors in N_d regions with permeabilities μ . The capacitance matrix $[C]$ for the line is obtained by solving the electrostatic problem of N_c conductors in N_d regions with permittivities ϵ . It is shown that $[L] = \mu_0 \epsilon_0 [C']^{-1}$, where $[C']$ is the capacitance matrix of an auxiliary electrostatic problem of N_c conductors in N_d regions with relative permittivities set equal to the reciprocals of the relative permeabilities of the magnetostatic problem, i.e., $\epsilon'_i/\epsilon_0 = \mu_0/\mu_i$.

I. INTRODUCTION

Fig. 1 shows a multiconductor transmission line consisting of N_c conductors and N_d insulating materials above a perfectly conducting ground plane. The system is uniform in the z direction (direction of propagation), and the cross-sectional shapes of the conductors and insulators are arbitrary. The insulators have arbitrary permeabilities μ , and permittivities ϵ . An upper ground plane could be present and treated as an additional conductor in a manner similar to that of [1].

To the quasi-static approximation, the multiconductor transmission line is characterized by a capacitance matrix $[C]$, obtained from an electrostatic analysis, and an inductance matrix $[L]$, obtained from a magnetostatic analysis. The formulation of the problem for $[C]$ and a numerical algorithm for its computation are given in [1]. In the appendix of [1] it is shown that if the insulating matter is nonmagnetic, the inductance matrix of the line is given by

$$[L] = \mu_0 \epsilon_0 [C_0]^{-1} \quad (1)$$

Here $[C_0]$ is the capacitance matrix of the multiconductor transmission line if all dielectric constants are set equal to 1.

In this paper we shall show that when the insulators are magnetic, a modified relationship holds. In particular, it is

$$[L] = \mu_0 \epsilon_0 [C']^{-1} \quad (2)$$

where $[C']$ is the capacitance matrix of the line if all relative permittivities are set equal to the reciprocals of the relative permeabilities, i.e.,

$$\frac{\epsilon'_i}{\epsilon_0} = \frac{\mu_0}{\mu_i}, \quad i = 1, 2, \dots, N_d. \quad (3)$$

Note that the auxiliary problem for finding $[C']$ has relative permittivities less than unity if the corresponding relative permeabilities are greater than unity.

Relationship (2) is strictly true only if all conductors are perfect. It assumes that all current in the magnetostatic problem flows on the surfaces of conductors. For actual conductors,

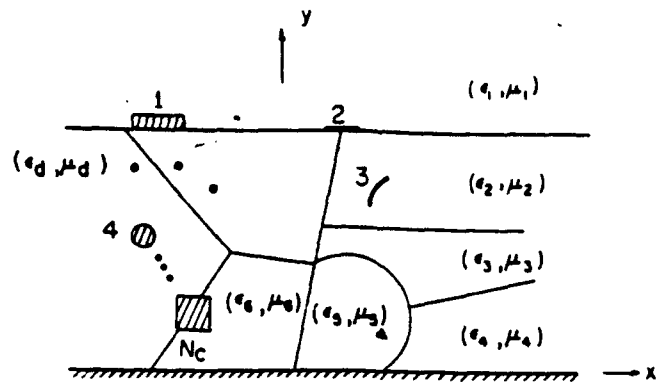


Fig. 1. A multiconductor transmission line in a multilayered dielectric and magnetic region above a ground plane.

depending on the frequency, some of the current flows internal to the conductors. Relationship (2) is then only approximate.

Although (2) can be inferred from the last two sentences in [2, sec. V], we have not seen an explicit proof in the literature. The purpose of this short paper is to give a simple proof of (2) for the multiconductor case with layered media.

II. PROOF OF (2)

The electrostatic problem from which $[C]$ is calculated is formulated in detail in [1]. We shall refer to that formulation when needed. The magnetostatic problem from which $[L]$ is calculated is an extension of the formulation for nonmagnetic media, given in the appendix of [1]. The formulation for magnetic media is given below.

The inductance matrix $[L]$ is an $N_c \times N_c$ matrix that satisfies

$$\vec{\psi} = [L] \vec{I} \quad (4)$$

where $\vec{\psi}$ and \vec{I} are $N_c \times 1$ column vectors. The j th element of \vec{I} is the z -directed conduction current on the j th conductor. The i th element of $\vec{\psi}$ is the x -directed magnetic flux passing between a unit length of the i th conductor and the lower ground plane. If

$$\vec{I} = \frac{1}{\mu_0 \epsilon_0} [C'] \vec{\psi} \quad (5)$$

and if $[C']^{-1}$ exists, then (4) will imply that the desired relationship (2) is true. In the remainder of this section, we establish (5).

We formulate the magnetostatic problem with magnetic media in terms of the total electric current $J_T n_z$ on the surfaces of the conducting cylinders and on the boundaries between different magnetic media. The total electric current on the conducting surfaces is the conduction current plus the magnetization current. The total electric current on the magnetic media boundaries is the magnetization current. The magnetic flux density B is given by

$$B = \nabla \times A = \nabla A_z \times n_z \quad (6)$$

where A_z is the only component of A due to steady current flowing in the z direction. For the two-dimensional problem, it is given by

$$A_z(\rho) = \frac{\mu_0}{2\pi} \sum_{j=1}^M \int_{l_j} J_T(\rho') \ln \left(\frac{|\rho - \hat{\rho}'|}{|\rho - \rho'|} \right) dl' \quad (7)$$

where l_j denotes the j th interface. The first N_c interfaces are the surfaces of the N_c conductors. If the upper ground plane is

Manuscript received November 28, 1987; revised March 7, 1988. This work was supported by the Office of Naval Research, Arlington, VA 22217, under Contract N00014-85-K-0082 and by the New York State Center for Advanced Technology in Computer Applications and Software Engineering, Syracuse University.

The authors are with the Department of Electrical and Computer Engineering, Syracuse University, Syracuse, NY 13244-1240.

IEEE Log Number 8822040.

present, the $(N_c + 1)$ th interface is the surface of this plane. The last N_j' interfaces are the magnetic media boundaries. Thus,

$$M = M_1 + N_j' \quad (8)$$

where M_1 is N_c if the upper ground plane is absent. If the upper ground plane is present, then M_1 is $N_c + 1$. The number N_j' of magnetic media boundaries could be greater than $N_j - 1$ because these boundaries are arbitrarily shaped, not necessarily parallel to one another or to the lower ground plane. In (7), ρ' is the position vector of dl' , and $\hat{\rho}'$ is the position vector of the image of dl' about the lower ground plane.

Substituting (7) into (6) and assuming that ρ is not on any of the interfaces $\{l_i\}$, we obtain

$$B(\rho) = -\frac{\mu_0}{2\pi} \sum_{j=1}^M \int_{l_j} J_T(\rho') \left(\frac{\rho - \rho'}{|\rho - \rho'|^2} - \frac{\rho - \hat{\rho}'}{|\rho - \hat{\rho}'|^2} \right) \times u_z dl' \quad (9)$$

The limits of (9) as ρ approaches l_i from either side are

$$B^\pm(\rho) = -\frac{\mu_0}{2\pi} \sum_{j=1}^M \int_{l_j} J_T(\rho') \left(\frac{\rho - \rho'}{|\rho - \rho'|^2} - \frac{\rho - \hat{\rho}'}{|\rho - \hat{\rho}'|^2} \right) \times u_z dl' \\ \mp \frac{\mu_0 J_T(\rho)}{2} (n \times u_z), \quad \begin{cases} \rho \text{ on } l_i \\ i=1, 2, \dots, M \end{cases} \quad (10)$$

where f_{l_i} denotes the principal value of the integral over l_i , and n is a unit vector normal to l_i at ρ . Moreover, $B^+(\rho)$ is $B(\rho)$ on the side of l_i toward which n points, and $B^-(\rho)$ is $B(\rho)$ on the other side of l_i .

On the surface of the i th conductor, A_z is constant and is the x -directed magnetic flux ψ_i passing between a unit length of the i th conductor and the lower ground plane. Hence, similar to [1, eq. (A2)],

$$A_z(\rho) = \psi_i, \quad \begin{cases} \rho \text{ on } l_i \\ i=1, 2, \dots, M_1 \end{cases} \quad (11)$$

If the upper ground plane is present, it is the $(N_c + 1)$ th conductor and, because A_z vanishes on it, $\psi_{N_c+1} = 0$. Substitution of (7) into (11) gives

$$\frac{\mu_0}{2\pi} \sum_{j=1}^M \int_{l_j} J_T(\rho') \ln \left(\frac{|\rho - \hat{\rho}'|}{|\rho - \rho'|} \right) dl' = \psi_i, \quad \begin{cases} \rho \text{ on } l_i \\ i=1, 2, \dots, M_1 \end{cases} \quad (12)$$

Continuity of the tangential component of magnetic intensity on the magnetic media boundaries requires that

$$n \times \left[\frac{B^+(\rho)}{\mu_i^+} - \frac{B^-(\rho)}{\mu_i^-} \right] = 0, \quad \begin{cases} \rho \text{ on } l_i \\ i = M_1 + 1, M_1 + 2, \dots, M \end{cases} \quad (13)$$

where n , $B^+(\rho)$, and $B^-(\rho)$ are the same as in (10). Furthermore, μ_i^+ is the permeability on the side of l_i toward which n points and μ_i^- is the permeability on the other side of l_i . Substituting (10) into (13) and then dividing (13) by $u_z [1/\mu_i^+ - 1/\mu_i^-]$, we obtain

$$\frac{\mu_0}{2} \left[\frac{1}{\mu_i^+} + \frac{1}{\mu_i^-} \right] J_T(\rho) + \frac{\mu_0}{2\pi} \sum_{j=1}^M \int_{l_j} J_T(\rho') \left(\frac{\rho - \rho'}{|\rho - \rho'|^2} - \frac{\rho - \hat{\rho}'}{|\rho - \hat{\rho}'|^2} \right) \cdot n dl' = 0, \\ \begin{cases} \rho \text{ on } l_i \\ i = M_1 + 1, M_1 + 2, \dots, M \end{cases} \quad (14)$$

If the i th conductor is of finite cross section, then l_i is a closed curve on which

$$u_i J_T(\rho) = \frac{1}{\mu_0} n \times B^+(\rho) \quad (15)$$

$$u_i J_C(\rho) = \frac{1}{\mu_i^+(\rho)} n \times B^+(\rho) \quad (16)$$

where n is the unit normal vector that points outward from the surface of the conductor. Furthermore, $B^+(\rho)$ and μ_i^+ are, respectively, the magnetic flux density and the permeability just outside the conductor. In (16), $J_C(\rho)$ is the conduction current on the conductor. Equations (15) and (16) imply that

$$J_C(\rho) = \frac{\mu_0}{\mu_i^+(\rho)} J_T(\rho) \quad (17)$$

on the surface of the i th conductor, provided this conductor is of finite cross section.

If the i th conductor is an infinitesimally thin strip, then l_i runs from one edge of the strip to the other on which

$$J_C(\rho) u_z = n \times \left[\frac{B^+(\rho)}{\mu_i^+(\rho)} - \frac{B^-(\rho)}{\mu_i^-(\rho)} \right] \quad (18)$$

Substitution of (10) for $B^\pm(\rho)$ in (18) leads to

$$J_C(\rho) = \frac{\mu_0}{2} \left[\frac{1}{\mu_i^+(\rho)} + \frac{1}{\mu_i^-(\rho)} \right] J_T(\rho) \\ + \frac{\mu_0}{2\pi} \left[\frac{1}{\mu_i^+(\rho)} - \frac{1}{\mu_i^-(\rho)} \right] \sum_{j=1}^M \int_{l_j} J_T(\rho') \\ \left(\frac{\rho - \rho'}{|\rho - \rho'|^2} - \frac{\rho - \hat{\rho}'}{|\rho - \hat{\rho}'|^2} \right) \cdot n dl' \quad (19)$$

on the surface of the i th conductor, provided this conductor is of zero thickness.

Now, consider the auxiliary electrostatic problem which has the same geometry as that of the present magnetostatic problem, but with relative permittivities ϵ_i/ϵ_0 set equal to μ_0/μ_i . The formulation presented in [1] is, in fact, valid for dielectric media of arbitrary shape. The unit vector u_z in (11) of [1] should be replaced by n when the dielectric media are arbitrarily shaped. It is clear that (12), (14), (17), and (19) have the same mathematical forms as (9), (11), (15), and (17) of [1], respectively. Therefore, the solution of the magnetostatic problem can be related to that of the auxiliary electrostatic problem by

$$J_C^{(i)}(\rho') = \frac{1}{\mu_0 \epsilon_0} \sigma_F^{(i)}(\rho'), \quad i=1, 2, \dots, N_c \quad (20)$$

where $J_C^{(i)}(\rho')$ is the conduction current of the magnetostatic problem when $\psi_i = 1$ is the only nonzero magnetic flux and $\sigma_F^{(i)}(\rho')$ is the free charge of the auxiliary electrostatic problem when the potential of the i th conductor is unity and all other conductors are grounded. Multiplying (20) by ψ_i and summing over i , we obtain

$$\sum_{i=1}^{N_c} J_C^{(i)}(\rho') \psi_i = \frac{1}{\mu_0 \epsilon_0} \sum_{i=1}^{N_c} \sigma_F^{(i)}(\rho') \psi_i \quad (21)$$

After noting that the right-hand side of (21) is $J_C(\rho')$, we integrate (21) over l_j to obtain (5) with the j th element of $[C']$ given by

$$C_j' = \int_{l_j} \sigma_F^{(i)}(\rho') dl', \quad i, j=1, 2, \dots, N_c \quad (22)$$

Premultiplication of (5) by $[C']^{-1}$ yields

$$\bar{\psi} = \mu_0 \epsilon_0 [C']^{-1} \bar{I}. \quad (23)$$

The inverse of $[C']$ exists because $[C']$ is positive definite, which can be concluded from the fact that the electrostatic energy stored in the system is always greater than zero with nontrivial free charge distribution on the conductors. Comparison of (23) with (4) gives the desired relationship (2).

III. CONCLUSION

A simple relationship between the inductance matrix and the auxiliary capacitance matrix has been given. Thanks to this

relationship, the computer code given in [1] and [3] for obtaining the capacitance matrix of the electrostatic problem can be used to obtain the inductance matrix of the magnetostatic problem.

REFERENCES

- [1] C. Wei, R. F. Harrington, J. R. Mautz, and T. K. Sarkar, "Multiconductor transmission lines in multilayered dielectric media," *IEEE Trans. Microwave Theory Tech.*, vol. MTT-32, pp. 439-450, Apr. 1984.
- [2] I. V. Lindell, "On the quasi-TEM modes in inhomogeneous multiconductor transmission lines," *IEEE Trans. Microwave Theory Tech.*, vol. MTT-29, pp. 812-817, Aug. 1981.
- [3] C. Wei and R. F. Harrington, "Extension of the multiconductor transmission line solution to zero-thickness conductors and to conductors between parallel ground planes," Department of Electrical and Computer Engineering, Syracuse Univ., Rep. TR-83-5, Mar. 1983.

Boundary Integral Formulations for Homogeneous Material Bodies

Roger F. Harrington

Department of Electrical Engineering
Syracuse University
Syracuse, NY 13244-1240, USA

Abstract— There are many boundary integral formulations for the problem of electromagnetic scattering from and transmission into a homogeneous material body. The only formulations which give a unique solution at all frequencies are those which involve both electric and magnetic equivalent currents, and satisfy boundary conditions on both tangential \vec{E} and tangential \vec{H} . Formulations which involve only electric (or magnetic) equivalent currents, and those which involve boundary conditions on only tangential \vec{E} (or tangential \vec{H}) are singular at frequencies corresponding to the resonant frequencies of a resonator formed by a perfect conductor covering the surface of the body and filled with the material exterior to the body in the original problem.

I. INTRODUCTION

In electromagnetic theory, a boundary integral equation is one which involves the integral of an unknown source times a Green's function over the surface bounding a material body. In this paper we consider boundary integral equations for determining the electromagnetic field internal and external to a homogeneous material body, when it is excited by sources external to the body. The problem when the sources are internal to the body, or when sources are both external and internal, requires a minor modification of the theory.

There are infinitely many boundary integral equations that can be formulated for calculating the electromagnetic field internal and external to a homogeneous material body. In this paper we formulate two classes of such equations, which we call *source formulations* and *field formulations*. In the source formulation the problem is formulated in terms of unknown electric and magnetic equivalent currents separately for the internal and external regions, and the boundary conditions are applied to tangential \vec{E} and tangential \vec{H} on the boundary surface S . This leads to two equations in four unknowns, and further restrictions must be made on the sources. In the field formulation, a single set of equivalent currents $\{\vec{J}, \vec{M}\}$ is used to produce the field in both the internal and external regions, and the boundary conditions are again applied to tangential \vec{E} and tangential \vec{H} on S . This leads to four equations in two unknowns, and we must make a further choice of how to satisfy the equations. Some choices of sources and field equations lead to operator equations that are singular at certain "resonant frequencies", and other choices lead to operator equations that have unique solutions at all frequencies.

A number of different boundary integral equations for homogeneous material bodies have been used for computation by various authors. For two-dimensional

problems, a formulation obtained by Müller [1] has been used by Solodukhov and Vasil'ev [2] and by Morita [3]. A formulation equivalent to our E -field method has been used by Wu and Tsai [4], and by Arvas, Rao, and Sarkar [5]. For three-dimensional problems, a formulation obtained by many investigators, called the PMCHW formulation in [6], has been used by Wu [7], by Mautz and Harrington [6] and by Umashankar, Taflov, and Rao in [8]. For references to methods not classified as boundary integral formulations, see [8].

II. DEFINITION OF OPERATORS

The problem to be considered is shown in Fig. 1. The homogeneous material body is bounded by S and has constitutive parameters μ_i, ϵ_i (i denotes *internal*). The region external to the body is also homogeneous and has constitutive parameters μ_e, ϵ_e (e denotes *external*). The impressed sources are denoted $\bar{J}^{imp}, \bar{M}^{imp}$, and the field that they produce with the body absent is denoted $\bar{E}^{imp}, \bar{H}^{imp}$. The unit normal pointing outward from S is denoted \hat{n} . The total field in the internal region is denoted \bar{E}, \bar{H} . The total field in the external region is

$$\bar{E} = \bar{E}^{imp} + \bar{E}^{scat} \quad (1)$$

$$\bar{H} = \bar{H}^{imp} + \bar{H}^{scat} \quad (2)$$

where the scattered field $\bar{E}^{scat}, \bar{H}^{scat}$ is that produced by the material body. Lossy bodies can be treated by considering ϵ_i , or μ_i , or both, to be complex.

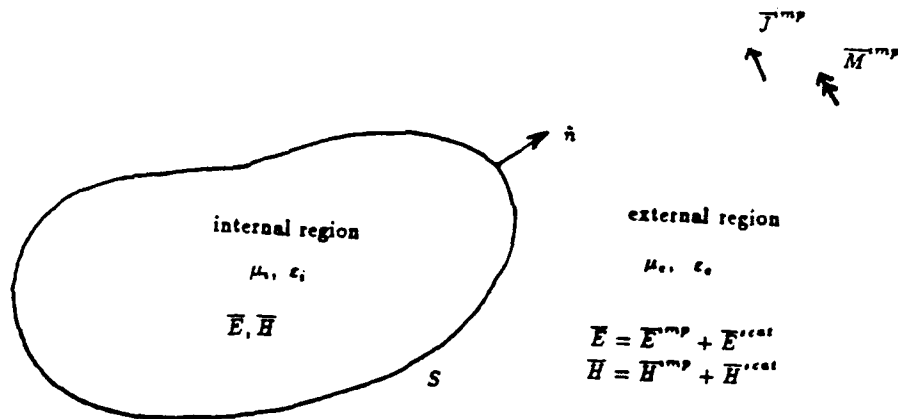


Figure 1. A material body bounded by S in the impressed field produced by $\bar{J}^{imp}, \bar{M}^{imp}$.

We use electric and magnetic surface currents radiating into homogeneous media of infinite extent as equivalent sources. The notation \bar{J}_e, \bar{M}_e denotes equivalent currents on S radiating into media having constitutive parameters μ_e, ϵ_e

everywhere, as shown in Fig. 2. The notation $\bar{E}_e(\bar{J}_e, \bar{M}_e)$, $\bar{H}_e(\bar{J}_e, \bar{M}_e)$ is used to denote the field produced by \bar{J}_e, \bar{M}_e , obtained from the usual potential integrals. In other words,

$$\bar{E}_e(\bar{J}_e, \bar{M}_e) = \bar{E}_e(\bar{J}_e, 0) + \bar{E}_e(0, \bar{M}_e) \quad (3)$$

$$\bar{H}_e(\bar{J}_e, \bar{M}_e) = \bar{H}_e(\bar{J}_e, 0) + \bar{H}_e(0, \bar{M}_e) \quad (4)$$

where

$$\bar{E}_e(\bar{J}_e, 0) = -j\omega \bar{A}_e(\bar{J}_e) - \nabla \phi_e(\bar{J}_e) \quad (5)$$

$$\bar{H}_e(\bar{J}_e, 0) = \frac{1}{\mu_e} \nabla \times \bar{A}_e(\bar{J}_e) \quad (6)$$

$$E_e(0, \bar{M}_e) = -\frac{1}{\epsilon_e} \nabla \times \bar{F}_e(\bar{M}_e) \quad (7)$$

$$H_e(0, \bar{M}_e) = -j\omega \bar{F}_e(\bar{M}_e) - \nabla \psi_e(\bar{M}_e) \quad (8)$$

Here $\bar{A}_e, \bar{F}_e, \phi_e$, and ψ_e are the usual magnetic and electric potentials

$$\bar{A}_e = \mu_e \iint_S \bar{J}_e(\bar{r}') G_e(\bar{r} - \bar{r}') ds' \quad (9)$$

$$\phi_e = \frac{1}{\epsilon_e} \iint_S q_e(\bar{r}') G_e(\bar{r} - \bar{r}') ds' \quad (10)$$

$$\bar{F}_e = \epsilon_e \iint_S \bar{M}_e(\bar{r}') G_e(\bar{r} - \bar{r}') ds' \quad (11)$$

$$\psi_e = \frac{1}{\mu_e} \iint_S m_e(\bar{r}') G_e(\bar{r} - \bar{r}') ds' \quad (12)$$

The electric charge q_e and magnetic charge m_e are related to \bar{J}_e and \bar{M}_e by the equations of continuity

$$q_e = -\frac{1}{j\omega} \nabla_s \cdot \bar{J}_e \quad (13)$$

$$m_e = -\frac{1}{j\omega} \nabla_s \cdot \bar{M}_e \quad (14)$$

where $\nabla_s \cdot$ is the surface divergence. The Green's function is that for infinite media,

$$G_e = \frac{e^{-jk_e|\bar{r}-\bar{r}'|}}{4\pi|\bar{r}-\bar{r}'|} \quad (15)$$

where $k_e = \omega \sqrt{\mu_e \epsilon_e}$.

The boundary integral equations involve the tangential components of \bar{E} and \bar{H} over S . However, the tangential component of \bar{H} is discontinuous at a surface current \bar{J} , and the tangential component of \bar{E} is discontinuous at a surface current \bar{M} . Hence, it is important to evaluate tangential components on the proper side of surface currents. For this, we define a surface $S+$ to be just outside S , and $S-$ to be just inside S (see Fig. 2). The notation

$$\hat{n} \times \bar{E}_e^+(\bar{J}_e, \bar{M}_e) \quad (16)$$

$$\hat{n} \times \bar{H}_e^+(\bar{J}_e, \bar{M}_e) \quad (17)$$

denotes tangential components evaluated on $S+$, and the notation

$$\hat{n} \times \bar{E}_e^-(\bar{J}_e, \bar{M}_e) \quad (18)$$

$$\hat{n} \times \bar{H}_e^-(\bar{J}_e, \bar{M}_e) \quad (19)$$

denotes tangential components evaluated on $S-$.

We also need equivalent surface currents (\bar{J}_i, \bar{M}_i) on S radiating into media having constitutive parameters μ_i, ϵ_i everywhere, as shown in Fig. 3. The notation $\bar{E}_i(\bar{J}_i, \bar{M}_i), \bar{H}_i(\bar{J}_i, \bar{M}_i)$ is used to denote the field produced by \bar{J}_i, \bar{M}_i , obtained from the usual potential integrals. In other words, $\bar{E}_i(\bar{J}_i, \bar{M}_i)$ and $\bar{H}_i(\bar{J}_i, \bar{M}_i)$ are given by (3)-(15) with all subscripts e changed to i . Again tangential components of \bar{E} and \bar{H} are discontinuous at surface currents \bar{J} and \bar{M} on S . Just as in the previous case, we define a surface $S+$ to be just outside S , and $S-$ to be just inside S (see Fig. 3). To denote tangential components on $S+$ we use (16) and (17) with subscripts e replaced by i . To denote tangential components on $S-$ we use (18) and (19) with subscripts e replaced by i .

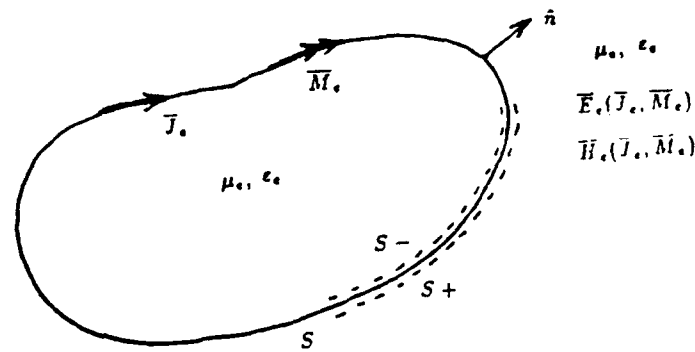


Figure 2. The surface currents \bar{J}_e, \bar{M}_e radiating into medium μ_e, ϵ_e everywhere produce fields $\bar{E}_e(\bar{J}_e, \bar{M}_e), \bar{H}_e(\bar{J}_e, \bar{M}_e)$.

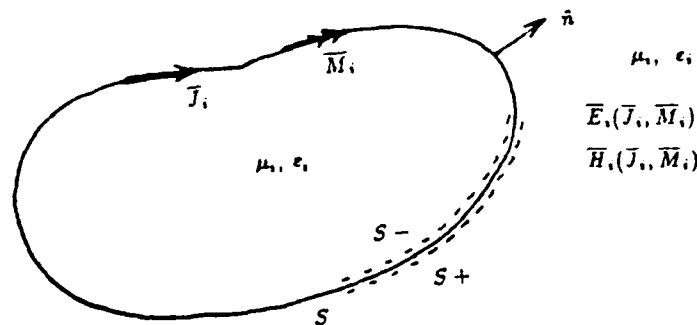


Figure 3. The surface currents \bar{J}_i, \bar{M}_i radiating into medium μ_i, ϵ_i everywhere produce fields $\bar{E}_i(\bar{J}_i, \bar{M}_i), \bar{H}_i(\bar{J}_i, \bar{M}_i)$.

III. SOURCE FORMULATIONS

To solve the original problem of Fig. 1, we have to solve the following mathematical problem: In region e , find the field (1) and (2), where \bar{E}^{imp} , \bar{H}^{imp} are a known field and \bar{E}^{scat} , \bar{H}^{scat} are an unknown solution to Maxwell's equations satisfying the radiation condition. In region i , the unknown field \bar{E} , \bar{H} is a solution to Maxwell's equations. Furthermore, the tangential components of \bar{E} and \bar{H} over $S+$ in the external region must equal the tangential components of \bar{E} and \bar{H} over $S-$ in the internal region.

By the use of equivalent currents \bar{J}_e, \bar{M}_e over S radiating into media e everywhere, Fig. 2, we can write a general expression for the field in region e as

$$\bar{E}_e = \bar{E}^{imp} + \bar{E}_e(\bar{J}_e, \bar{M}_e) \quad (20)$$

$$\bar{H}_e = \bar{H}^{imp} + \bar{H}_e(\bar{J}_e, \bar{M}_e) \quad (21)$$

By the use of equivalent currents \bar{J}_i, \bar{M}_i over S radiating into media i everywhere, we can write a general expression for the field in region i as

$$\bar{E}_i = \bar{E}_i(\bar{J}_i, \bar{M}_i) \quad (22)$$

$$\bar{H}_i = \bar{H}_i(\bar{J}_i, \bar{M}_i) \quad (23)$$

The formulas (20) and (21) give the field \bar{E}, \bar{H} outside S (and on $S+$), and the formulas (22) and (23) give the field \bar{E}, \bar{H} inside S (and on $S-$). Continuity of the tangential components of \bar{E} and \bar{H} from the external to internal regions requires that

$$\hat{n} \times [\bar{E}^{imp} + \bar{E}_e^+(\bar{J}_e, \bar{M}_e)] = \hat{n} \times \bar{E}_i^-(\bar{J}_i, \bar{M}_i) \quad (24)$$

$$\hat{n} \times [\bar{H}^{imp} + \bar{H}_e^+(\bar{J}_e, \bar{M}_e)] = \hat{n} \times \bar{H}_i^-(\bar{J}_i, \bar{M}_i) \quad (25)$$

Rearranging (24) and (25), we have

$$\hat{n} \times [\bar{E}_e^+(\bar{J}_e, \bar{M}_e) - \bar{E}_i^-(\bar{J}_i, \bar{M}_i)] = -\hat{n} \times \bar{E}^{imp} \quad (26)$$

$$\hat{n} \times [\bar{H}_e^+(\bar{J}_e, \bar{M}_e) - \bar{H}_i^-(\bar{J}_i, \bar{M}_i)] = -\hat{n} \times \bar{H}^{imp} \quad (27)$$

These are two equations to determine four unknowns ($\bar{J}_e, \bar{M}_e, \bar{J}_i, \bar{M}_i$). We must enforce two more relationships among these four unknowns before a unique solution can be obtained.

A. Electric Current Formulation

One simple way to reduce the four unknowns to two unknowns is to set

$$\bar{M}_e = \bar{M}_i = 0 \quad (28)$$

i.e., express the fields in terms of surface electric currents only. Equations (26) and (27) then reduce to

$$\hat{n} \times [\bar{E}_e^+(\bar{J}_e, 0) - \bar{E}_i^-(\bar{J}_i, 0)] = -\hat{n} \times \bar{E}^{imp} \quad (29)$$

$$\hat{n} \times [\overline{H}_e^+(\overline{J}_e, 0) - \overline{H}_i^-(\overline{J}_i, 0)] = -\hat{n} \times \overline{H}^{imp} \quad (30)$$

We will show in Section V that the operator represented by (29) and (30) becomes singular at frequencies for which S , when covered by a perfect electric conductor and filled with the external medium, forms a resonator. Hence, numerical solution of (29) and (30) must fail in the vicinity of such frequencies.

This failure can be clearly seen from Fig. 4 of [4], where, in addition to the backscattering cross section, the authors compute the condition number of the matrix of the numerical solution. The matrix becomes extremely ill-conditioned at $k_0 a = 2.405$, which is the first internal resonance of an empty conducting circular cylinder. Note that the computation went bad regardless of the losses in the material cylinder, since it is the external medium (in this case free space) which determines the frequencies of failure of the equation.

B. Magnetic Current Formulation

Another possible way to reduce the four unknowns in (26) and (27) to two unknowns is to set

$$\overline{J}_e = \overline{J}_i = 0 \quad (31)$$

i.e., express the fields in terms of surface magnetic currents only. This is the dual case to A above, and the equations are self dual. (An interchange of symbols according to duality [9, Sec. 3-2] produces equations of the same mathematical form.) Hence, the dual equations must become singular at dual frequencies, i.e., frequencies for which the surface S , covered by a perfect magnetic conductor and filled with the external medium, forms a resonator. These resonant frequencies are the same as those for the electric current case, section A above, and hence the magnetic current formulation fails at precisely the same frequencies as does the electric current formulation.

C. Combined Current Formulation

Another way to reduce the number of unknowns in (26) and (27) to two is to set

$$\overline{J}_e = -\overline{J}_i = \overline{J} \quad (32)$$

$$\overline{M}_e = -\overline{M}_i = \overline{M} \quad (33)$$

In other words, use a single unknown electric current \overline{J} to represent both \overline{J}_e and $-\overline{J}_i$, and a single unknown magnetic current \overline{M} to represent both \overline{M}_e and $-\overline{M}_i$. This we call the *combined current formulation*. The reason for choosing (32) and (33) is most easily seen from the viewpoint of the *field formation* of Section IV, where we discuss it in more detail. It is shown in Section IV-A that the combined source formulation is equivalent to the combined field formulation, which has been shown to be nonsingular at all frequencies.

D. Other Choices

Many other relationships among $\overline{J}_e, \overline{M}_e, \overline{J}_i, \overline{M}_i$ could be chosen. One choice which would lead to a formulation which has no frequencies of singularity is an

extension of the combined source formulation for conducting bodies [10]. This involves choosing

$$\overline{M}_e = \alpha_e \hat{n} \times \overline{J}_e \quad (34)$$

$$\overline{M}_i = \alpha_i \hat{n} \times \overline{J}_i \quad (35)$$

where α_e and α_i are constants to be chosen. For reasons discussed in [10], a good choice is $\alpha_e = \eta_e$ and $\alpha_i = \eta_i$, where η_e and η_i are the intrinsic impedances of region e and region i , respectively. Also, a proof similar to that used in [10] shows that the operator resulting from (34) and (35) has no singular frequencies, and no mathematical difficulties would be encountered in a numerical solution to (26) and (27).

IV. FIELD FORMULATIONS

In this formulation we use the equivalence principle [9, Sec. 3-5] to pick a given set of sources able to produce the desired field, and then satisfy sufficient boundary conditions on the field to determine the sources. This is the approach used in [6]. It might alternatively be called a *direct application of the equivalence principle*.

According to the equivalence principle, an electromagnetic field can be terminated by placing the required electric and magnetic surface currents on S . If we specify that the field and sources outside S remain the same as in the original problem, Fig. 1, then the currents

$$\overline{J} = \hat{n} \times \overline{H} = \hat{n} \times (\overline{H}^{imp} + \overline{H}^{scat}) \quad (36)$$

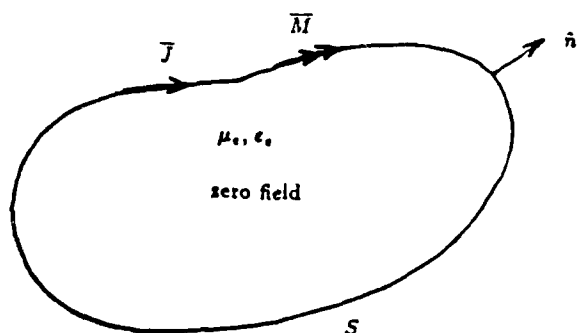
$$\overline{M} = \overline{E} \times \hat{n} = (\overline{E}^{imp} + \overline{E}^{scat}) \times \hat{n} \quad (37)$$

do not change the field outside S but produce zero field internal to S . Since the field is zero internal to S , we can change the medium to any convenient value. In particular, if we replace the internal medium by the external medium, we have \overline{J} and \overline{M} radiating into a medium with μ_e, ϵ_e everywhere. This gives us the desirable situation that the potential integrals can be used to calculate the field from \overline{J} and \overline{M} . This procedure gives us the external equivalence of Fig. 4.

A second application of the equivalence principle gives us the internal equivalence of Fig. 5. We specify that the field internal to S remain the same as in the original problem, and the field outside S be zero. This requires the *terminating currents* $\hat{n} \times (-\overline{H})$ and $(-\overline{E}) \times \hat{n}$, the minus sign resulting from the fact that \hat{n} now points into the region of zero field. Hence, the surface currents required for Fig. 5 are just the negative of those for Fig. 4, given by (36) and (37). Once again we can change the medium in the region of zero field to any desired value. In particular, we change it to be equal to the internal medium, so that we have $-\overline{J}$ and $-\overline{M}$ radiating into a medium with μ_i, ϵ_i everywhere. Hence, we can again use the potential integrals to calculate the field from $-\overline{J}$ and $-\overline{M}$.

We now use the notation of Section II to write four boundary integral equations involving the tangential components of \overline{E} and \overline{H} on S^- in Fig. 4 and S^+ in Fig. 5. Just inside S in Fig. 4, we have $\hat{n} \times \overline{E} = 0$ and $\hat{n} \times \overline{H} = 0$, or

8



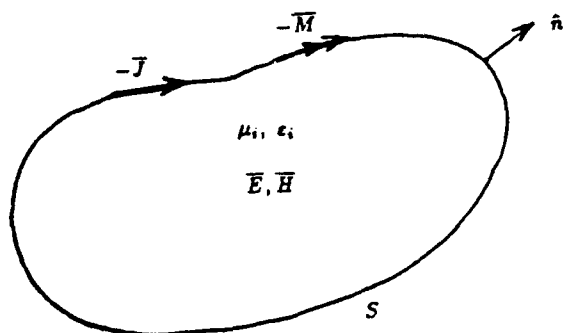
Harrington

$$\begin{array}{c} \nearrow J^{imp} \\ \nwarrow \bar{M}^{imp} \end{array}$$

 μ_e, ϵ_e

$$\begin{aligned} \bar{E} &= \bar{E}^{imp} + \bar{E}^{cat} \\ \bar{H} &= \bar{H}^{imp} + \bar{H}^{cat} \end{aligned}$$

Figure 4. The field external to S is the same as in the original problem, Fig. 1.

 μ_i, ϵ_i

zero field

Figure 5. The field internal to S is the same as in the original problem, Fig. 1.

$$\hat{n} \times [\bar{E}_e^-(\bar{J}, \bar{M}) + \bar{E}^{imp}] = 0 \quad (38)$$

$$\hat{n} \times [\bar{H}_e^-(\bar{J}, \bar{M}) + \bar{H}^{imp}] = 0 \quad (39)$$

Just outside S in Fig. 5, we have $\hat{n} \times \bar{E} = 0$ and $\hat{n} \times \bar{H} = 0$, or

$$\hat{n} \times \bar{E}_i^+(-\bar{J}, -\bar{M}) = 0 \quad (40)$$

$$\hat{n} \times \bar{H}_i^+(-\bar{J}, -\bar{M}) = 0 \quad (41)$$

Rearranging (38) and (39), and taking the minus signs out of the operator in (40) and (41), we have

$$\hat{n} \times \bar{E}_e^-(\bar{J}, \bar{M}) = -\hat{n} \times \bar{E}^{imp} \quad (42)$$

$$\hat{n} \times \bar{H}_e^-(\bar{J}, \bar{M}) = -\hat{n} \times \bar{H}^{imp} \quad (43)$$

$$\hat{n} \times \overline{E}_i^+(\overline{J}, \overline{M}) = 0 \quad (41)$$

$$\hat{n} \times \overline{H}_i^+(\overline{J}, \overline{M}) = 0 \quad (45)$$

Note that these are four equations in two unknowns $\overline{J}, \overline{M}$. Perhaps certain pairs of these equations can be used to compute $\overline{J}, \overline{M}$. More generally, linear combinations of them can be used.

A. Combined Field Formulation

The method that appears to have been used the most is to reduce the set of four equations to two by adding (42) to (44) and (43) to (45). This gives us the pair of equations

$$\hat{n} \times [\overline{E}_e^-(\overline{J}, \overline{M}) + \overline{E}_i^+(\overline{J}, \overline{M})] = -\hat{n} \times \overline{E}^{imp} \quad (46)$$

$$\hat{n} \times [\overline{H}_e^-(\overline{J}, \overline{M}) + \overline{H}_i^+(\overline{J}, \overline{M})] = -\hat{n} \times \overline{H}^{imp} \quad (47)$$

These are very similar to the equations obtained from the combined current formulation, Section III-C, except for the side of S on which the various fields are evaluated. To be explicit, if we substitute (32) and (33) into (26) and (27) we obtain

$$\hat{n} \times [\overline{E}_e^+(\overline{J}, \overline{M}) + \overline{E}_i^-(\overline{J}, \overline{M})] = -\hat{n} \times \overline{E}^{imp} \quad (48)$$

$$\hat{n} \times [\overline{H}_e^+(\overline{J}, \overline{M}) + \overline{H}_i^-(\overline{J}, \overline{M})] = -\hat{n} \times \overline{H}^{imp} \quad (49)$$

We now show that, in spite of the different positions of + and - signs, (46) and (47) are equivalent to (48) and (49).

At any current sheet we have [9, p. 34]

$$\hat{n} \times [\overline{H}^{(1)} - \overline{H}^{(2)}] = \overline{J} \quad (50)$$

$$[\overline{E}^{(1)} - \overline{E}^{(2)}] \times \hat{n} = \overline{M} \quad (51)$$

where $\overline{E}^{(1)}, \overline{H}^{(1)}$ is the field on the side of S into which \hat{n} points, and $\overline{E}^{(2)}, \overline{H}^{(2)}$ is the field on the other side of S . In terms of the notation of this paper,

$$\hat{n} \times [\overline{H}_e^+(\overline{J}, \overline{M}) - \overline{H}_e^-(\overline{J}, \overline{M})] = \overline{J} \quad (52)$$

$$\hat{n} \times [\overline{E}_e^+(\overline{J}, \overline{M}) - \overline{E}_e^-(\overline{J}, \overline{M})] = -\overline{M} \quad (53)$$

Rearranging, we have

$$\hat{n} \times \overline{H}_e^+(\overline{J}, \overline{M}) = \hat{n} \times \overline{H}_e^-(\overline{J}, \overline{M}) + \overline{J} \quad (54)$$

$$\hat{n} \times \overline{E}_e^+(\overline{J}, \overline{M}) = \hat{n} \times \overline{E}_e^-(\overline{J}, \overline{M}) - \overline{M} \quad (55)$$

The same equations are valid for subscripts e replaced by subscripts i . Substituting (55) and the same equation with subscripts e changed to i into (48), we obtain (46). Substituting (54) and the same equation with subscripts e changed to i into (49), we obtain (47). Hence, the combined field formulation of this section and the combined current formulation of Section III-C are identical.

It is shown in [6] that the combined field formulation gives a unique solution at all frequencies. Hence, the combined current formulation of Section III-C also gives a unique solution at all frequencies.

B. *E*-field Formulation

If we take only the two equations involving tangential \bar{E} , (42) and (44), we have the *E*-field formulation

$$\hat{n} \times \bar{E}_e^-(\bar{J}, \bar{M}) = -\hat{n} \times \bar{E}^{imp} \quad (56)$$

$$\hat{n} \times \bar{E}_i^+(\bar{J}, \bar{M}) = 0 \quad (57)$$

This formulation was used in [5] for the more general problem of both dielectric and conducting cylinders present. It may seem strange at first that this formulation makes no use of the boundary conditions on tangential \bar{H} . However, tangential \bar{H} is determined by tangential \bar{E} at most frequencies so that (56) and (57) are sufficient to determine \bar{J} and \bar{M} at most frequencies. However, we show in Section V that the *E*-field formulation will fail at frequencies for which *S*, when covered by a perfect electric conductor and filled with the exterior medium, forms a resonant cavity. These are precisely the same frequencies at which the electric current formulation, Section III-A, fails.

C. *H*-field Formulation

Dual to the *E*-field formulation, we can obtain an *H*-field formulation by using only (43) and (45) from the set (42)–(45). Since the *H*-field formulation is dual to the *E*-field formulation, it uniquely determines \bar{J} and \bar{M} at most frequencies. It will, however, fail at frequencies for which *S*, when covered by a perfect magnetic conductor and filled with the exterior medium, forms a resonant cavity. Since the field equations are self dual, these frequencies are precisely the same frequencies at which the *E*-field formulation fails.

D. Other Choices

Other choices of two equations from the set (42)–(45), and linear combinations of the equations, could be made. For example, instead of the simple addition of equations used in Section IV-A, we could take the more general linear combinations

$$\hat{n} \times [\bar{E}_e^-(\bar{J}, \bar{M}) + \alpha \bar{E}_i^+(\bar{J}, \bar{M})] = -\hat{n} \times \bar{E}^{imp} \quad (58)$$

$$\hat{n} \times [\bar{H}_e^-(\bar{J}, \bar{M}) + \beta \bar{H}_i^+(\bar{J}, \bar{M})] = -\hat{n} \times \bar{H}^{imp} \quad (59)$$

where α and β are constants to be chosen. It is shown in [6] that any choice of α and β for which $\alpha\beta^*$ (* denotes conjugate) is real and positive gives a formulation having a unique solution at all frequencies. In particular, the choice

$$\alpha = -\epsilon_i/\epsilon_e \quad (60)$$

$$\beta = -\mu_i/\mu_e \quad (61)$$

gives the Müller formulation [1]. This formulation has the advantage that the static electric field contribution to the left-hand side of (58) due to the electric

charge associated with \bar{J} is zero. Similarly, the static magnetic field contribution to the left-hand side of (59) due to the magnetic charge associated with \bar{M} is zero. According to the last sentence on page 300 of [1], the singularity of the kernels in (58) and (59) due to the electric and magnetic charges is no more pronounced than the reciprocal of the distance between the source point and the field point. Hence, the singularity that the kernels of the integral equations (58) and (59) exhibit as the source point passes through the field point is not as pronounced as the singularity of the kernels of (46) and (47). Computations have shown [6] that the use of Müller's formulation (this section) instead of the combined field formulation (Section IV-A) can lead to more accurate solutions for low contrast bodies.

There are infinitely many other choices of combinations of equations from the set (42)–(45) that could be made. There may be theoretical and/or computational reasons for other choices, but such reasons are not at present known. We therefore do not discuss any other choices of combinations of equations.

V. SINGULARITIES OF OPERATORS

We stated in Section III-A that the electric current formulation failed at frequencies for which S , when covered by a perfect electric conductor and filled with the external medium, formed a resonator. In Section IV-B we stated that the E -field formulation failed at these same frequencies. We now prove these statements.

For these proofs, we use the theorem that, given an equation

$$Lf = g \quad (62)$$

the operator L is singular if the corresponding homogeneous equation

$$Lf = 0 \quad (63)$$

has a nontrivial solution f_0 . For the electric current formulation, (29) and (30), we must show that there are some frequencies for which

$$\hat{n} \times [\bar{E}_e^+(\bar{J}_e, 0) - \bar{E}_i^-(\bar{J}_i, 0)] = 0 \quad (64)$$

$$\hat{n} \times [\bar{H}_e^+(\bar{J}_e, 0) - \bar{H}_i^-(\bar{J}_i, 0)] = 0 \quad (65)$$

are satisfied by $\bar{J}_e, \bar{J}_i \neq 0, 0$. In words, (64) and (65) state that we must seek nonzero \bar{J}_e such that $\hat{n} \times \bar{E}_e$ and $\hat{n} \times \bar{H}_e$ are zero on $S+$, or nonzero \bar{J}_i such that $\hat{n} \times \bar{E}_i$ and $\hat{n} \times \bar{H}_i$ are zero on $S-$, or both.

In the next paragraph, we assume that (64) and (65) are true. We use (64) and (65) to derive (66) and (67). Although (66) and (67) are true, there is no assurance that they are as restrictive as (64) and (65). Therefore, the set of all possible solutions to (64) and (65) will belong to the set of all possible solutions to (66) and (67).

Consider the composite situations where, in region e , $(\bar{E}_e, (\bar{J}_e, 0), \bar{H}_e(\bar{J}_e, 0))$ exists in medium (μ_e, ϵ_e) and, in region i , $(\bar{E}_i(\bar{J}_i, 0), \bar{H}_i(\bar{J}_i, 0))$ exists in medium (μ_i, ϵ_i) . Because of (64) and (65), the tangential components of both the electric and magnetic fields in the composite situation are continuous across S . Therefore,

the composite situation has no sources so that its fields collapse to zero. As a result, (64) and (65) imply that

$$\begin{aligned}\hat{n} \times \bar{E}_e^+(\bar{J}_e, 0) &= 0 \\ \hat{n} \times \bar{H}_e^+(\bar{J}_e, 0) &= 0\end{aligned}\quad (66)$$

$$\begin{aligned}\hat{n} \times \bar{E}_i^-(\bar{J}_i, 0) &= 0 \\ \hat{n} \times \bar{H}_i^-(\bar{J}_i, 0) &= 0\end{aligned}\quad (67)$$

Regarding (66), refer to Fig. 2. From our knowledge of cavity resonators, we know that there are resonances within S , with currents \bar{J}_e on S such that both tangential \bar{E} and tangential \bar{H} are zero on $S+$. Hence, at each resonant frequency, there will be a non-trivial \bar{J}_e which satisfies (66). A resonant frequency is a frequency at which S , when covered by a perfect electric conductor and filled with (μ_e, ϵ_e) forms a resonant cavity. Moving on to (67), refer to Fig. 3. Again from our knowledge of cavity resonators, we know that there can be resonances within S . However, this time we are evaluating $\hat{n} \times \bar{E}$ and $\hat{n} \times \bar{H}$ on $S-$ as denoted by the $-$ superscripts in (67). There are no resonances for which tangential \bar{E} and tangential \bar{H} are both zero on $S-$. Hence, (67) can never have a non-trivial solution \bar{J}_i .

In the previous paragraph, it was shown that the resonant frequencies were the only frequencies at which (66) and (67) could have a non-trivial solution (\bar{J}_e, \bar{J}_i) . This non-trivial solution is called $(\bar{J}_R, 0)$ where \bar{J}_R is the resonant current. Obviously, $(\bar{J}_R, 0)$ satisfies (64) and (65). It turned out (66) and (67) are as restrictive as (64) and (65). The solutions to (64) and (65) are the same as the solutions to (66) and (67). Therefore, the only frequencies for which the total operator of (64) and (65) is singular are the resonant frequencies. This is the statement made in Section III-A.

The homogeneous equations corresponding to the E -field formulation (56) and (57) are

$$\hat{n} \times \bar{E}_e^+(\bar{J}, \bar{M}) = 0 \quad (68)$$

$$\hat{n} \times \bar{E}_i^-(\bar{J}, \bar{M}) = 0 \quad (69)$$

In this paragraph and the next two paragraphs, we assume that (68) and (69) are true and investigate how (68) and (69) restrict (\bar{J}, \bar{M}) . Consider the composite situation of Fig. 6 where $(\bar{E}_i^-(\bar{J}, -\bar{M}), \bar{H}_i^-(\bar{J}, -\bar{M}))$ exists in (μ_i, ϵ_i) internal to S and $(\bar{E}_e^+(\bar{J}, \bar{M}), \bar{H}_e^+(\bar{J}, \bar{M}))$ exists in (μ_e, ϵ_e) external to S . The field in Fig. 6 is supported by equivalent electric and magnetic currents \bar{J} and \bar{M} on S given by

$$\bar{J} = \hat{n} \times (\bar{H}_e^+(\bar{J}, \bar{M}) - \bar{H}_i^-(\bar{J}, -\bar{M})) \quad (70)$$

$$\bar{M} = -\hat{n} \times (\bar{E}_e^+(\bar{J}, \bar{M}) - \bar{E}_i^-(\bar{J}, -\bar{M})) \quad (71)$$

In this paragraph, we find how (68) and (69) restrict \bar{J} and \bar{M} of (70) and (71). We have

$$\bar{J} = \hat{n} \times (\bar{H}_e^+(\bar{J}, \bar{M}) - \bar{H}_e^-(\bar{J}, \bar{M})) \quad (72)$$

$$\overline{M} = -\hat{n} \times (\overline{E}_e^+(\overline{J}, \overline{M}) - \overline{E}_e^-(\overline{J}, \overline{M})) \quad (73)$$

and

$$\overline{J} = \hat{n} \times (\overline{H}_i^+(\overline{J}, \overline{M}) - \overline{H}_i^-(\overline{J}, \overline{M})) \quad (74)$$

$$\overline{M} = -\hat{n} \times (\overline{E}_i^+(\overline{J}, \overline{M}) - \overline{E}_i^-(\overline{J}, \overline{M})) \quad (75)$$

Subtraction of (74) from (72) yields

$$\overline{J} = \hat{n} \times \overline{H}_i^+(\overline{J}, \overline{M}) + \hat{n} \times \overline{H}_e^-(\overline{J}, \overline{M}) \quad (76)$$

where \overline{J} is given by (70). Subtraction of (75) from (73) yields

$$\overline{M} = -\hat{n} \times \overline{E}_i^+(\overline{J}, \overline{M}) - \hat{n} \times \overline{E}_e^-(\overline{J}, \overline{M}) \quad (77)$$

where \overline{M} is given by (71). Since there are no external resonance, (69) implies that

$$\hat{n} \times \overline{H}_i^+(\overline{J}, \overline{M}) = 0 \quad (78)$$

Equation (68) implies that

$$\hat{n} \times \overline{H}_e^-(\overline{J}, \overline{M}) = \begin{cases} 0, & \text{no resonance} \\ \alpha \overline{J}_R, & \text{resonance} \end{cases} \quad (79)$$

where "resonance" means that the frequency is a resonant frequency and "no resonance" means that the frequency is not a resonant frequency. Substitution of (78) and (79) into (76) gives

$$\overline{J} = \begin{cases} 0, & \text{no resonance} \\ \alpha \overline{J}_R, & \text{resonance} \end{cases} \quad (80)$$

Substitution of (68) and (69) into (77) gives

$$\overline{M} = 0 \quad (81)$$

In this paragraph, we express $(\overline{J}, \overline{M})$ in terms of the field just inside S due to $(\overline{J}, \overline{M})$ of (80) and (81). Substitution of (78) and (69) into (74) and (75) gives

$$\overline{J} = \hat{n} \times \overline{H}_i^-(\overline{J}, \overline{M}) \quad (82)$$

$$\overline{M} = -\hat{n} \times \overline{E}_i^-(\overline{J}, \overline{M}) \quad (83)$$

Now, $(\overline{E}_i^-(\overline{J}, \overline{M}), \overline{H}_i^-(\overline{J}, \overline{M}))$ is the electromagnetic field just inside S due to \overline{J} in Fig. 6, so that (82) and (83) can be recast as

$$\overline{J} = \hat{n} \times \overline{H}_{ie}^-(\overline{J}, 0) \quad (84)$$

$$\overline{M} = -\hat{n} \times \overline{E}_{ie}^-(\overline{J}, 0) \quad (85)$$

where $(\overline{E}_{ie}^-(\overline{J}, 0), \overline{H}_{ie}^-(\overline{J}, 0))$ is the electromagnetic field just inside S in Fig. 6. This field is radiated by \overline{J} of (80) on S in the presence of (μ_i, ϵ_i) inside S and (μ_e, ϵ_e) outside S . If the frequency is a resonant frequency, then $(\overline{J}, \overline{M})$ of (84) and (85) is not trivial for $\alpha \neq 0$ because the non-trivial \overline{J} of (80) radiates a non-trivial field internal to S in Fig. 6. However, if the frequency is not a resonant frequency, then $\overline{J} = 0$ so that the composite field of Fig. 6 collapses to zero because it has no source. In this $\overline{J} = \overline{M} = 0$.

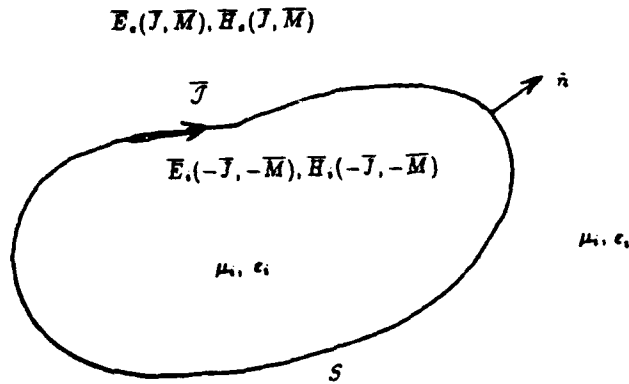


Figure 6. The composite situation used to prove that the E -field formulation fails at resonant frequencies.

VI. DISCUSSION

We have shown that there are many different boundary integral formulations for the problem of electromagnetic scattering from and transmission into a homogeneous material body. One class of formulations, called source formulations, leads to two equations in four unknown currents $\vec{J}_e, \vec{M}_e, \vec{J}_i, \vec{M}_i$. Two additional relationships among the currents must be postulated. When only a single type of current is used, say electric only or magnetic only, the formulations fail at certain resonant frequencies. The formulation remains valid at all frequencies only if both types of current, electric and magnetic, are used.

A second class of formulations, called field formulations, leads to four equations in two unknown currents \vec{J}, \vec{M} . We must then choose which two equations, or which two linear combinations of the four equations, to use. When only two of the equations are used, say the E -field or the H -field equations, the formulations fail at certain resonant frequencies. These are the same frequencies for which the single-source formulations fail. When we take linear combinations of the four equations, such that we are in effect forcing all four equations to be satisfied, we obtain formulations valid at all frequencies.

An extension of the source-type formulation has been made to give a *single-equation* formulation for the scattering problem [11,12]. This formulation is basically an electric current formulation of the type discussed in Section III-A, for which an additional relationship has been used to eliminate \vec{J}_i . The result is a single equation in terms of \vec{J}_e to give the scattered field. The solution does not give the transmitted field directly. This involves finding \vec{J}_i , the source of the internal field. Because this single-equation formulation is of the electric current type, it fails at those frequencies for which S , when covered by a perfect electric conductor and filled with the external medium, forms a cavity resonator. However, it is possible to establish a single-equation formulation in terms of combined sources to eliminate this problem [13].

ACKNOWLEDGMENTS

This work was supported by the U.S. Office of Naval Research under Contract No. N00014-88-K-0027, and by the New York State Center for Advanced Technology in Computer Applications and Software Engineering, Syracuse University. The author wishes to thank Dr. Joseph R. Mautz for his help with Section V.

The Editor thanks E. Arvas and N. Morita for reviewing the paper.

REFERENCES

1. Müller, C., *Foundations of the Mathematical Theory of Electromagnetic Waves*, Springer-Verlag, Berlin, 301, 1969.
2. Solodukhov, V. V., and E. N. Vasil'ev, "Diffraction of a plane electromagnetic wave by a dielectric cylinder of arbitrary cross section," *Soviet Physics Tech. Phys.*, Vol. 15, 32-36, 1970.
3. Morita, N., "Analysis of scattering by a dielectric rectangular cylinder by means of integral equation formulation," *Electron. and Comm. in Japan*, Vol. 57-B, 72-80, 1974.
4. Wu, T. K., and L. L. Tsai, "Scattering from arbitrarily cross-sectioned layered lossy dielectric cylinders," *IEEE Trans. Antennas Propagat.*, Vol. AP-25, 518-524, 1977.
5. Arvas, E., S. M. Rao, and T. K. Sarkar, "E-field solution of TM-scattering from multiple perfectly conducting and lossy dielectric cylinders of arbitrary cross-section," *Proc. IEEE*, Vol. 133, pt. H, 115-121, 1986.
6. Mautz, J. R., and R. F. Harrington, "Electromagnetic scattering from a homogeneous material body of revolution," *Archiv für Elektronik und Übertrag.*, Band 33, 71-80, 1979.
7. Wu, T. K., *Electromagnetic Scattering from Arbitrarily-Shaped Lossy Dielectric Bodies*, Ph.D. dissertation, University of Mississippi, 1976.
8. Umashankar, K., A. Tafflove, and S. M. Rao, "Electromagnetic scattering by arbitrarily shaped three-dimensional homogeneous lossy dielectric objects," *IEEE Trans. Antennas Propagat.*, Vol. AP-34, 758-766, 1986.
9. Harrington, R. F., *Time-Harmonic Electromagnetic Fields*, McGraw-Hill, New York, 1961.
10. Mautz, J. R., and R. F. Harrington, "A combined-source solution for radiation and scattering from a perfectly conducting body," *IEEE Trans. Antennas Propagat.*, Vol. AP-27, 445-454, 1979.
11. Marx, E., "Integral equation for scattering by a dielectric," *IEEE Trans. Antennas Propagat.*, Vol. AP-32, 166-172, 1984.
12. Glisson, A. W., "An integral equation for electromagnetic scattering from homogeneous dielectric bodies," *IEEE Trans. Antennas Propagat.*, Vol. AP-32, 173-175, 1984.
13. Mautz, J. R., "A stable integral equation for electromagnetic scattering from homogeneous dielectric bodies," *IEEE Trans. Antennas Propagat.*, In press, 1988.

Roger F. Harrington received the Ph.D. degree from the Ohio State University in 1952. While there, he was a Research Fellow in the Antenna Laboratory. Since 1952 he has been Professor of Electrical Engineering at Syracuse University. He has also served as Visiting Professor at the University of Illinois, the University of California at Berkeley, the Technical University of Denmark, and the East China Normal University. He is the author of "Time Harmonic Electromagnetic Fields" (McGraw-Hill) and "Field Computation by Moment Methods" (Krieger Publ. Co.).

The Excess Capacitance of a Microstrip Via in a Dielectric Substrate

TAOYUN WANG, STUDENT MEMBER, IEEE, JOSEPH R. MAUTZ, SENIOR MEMBER, IEEE,
AND ROGER F. HARRINGTON, FELLOW, IEEE

Abstract—The equivalent circuit of a via which connects two semi-infinitely long microstrip transmission lines imbedded in a dielectric medium above a ground plane is considered. The Γ -type equivalent circuit consists of an excess capacitance and an excess inductance. The excess inductance of the via is the same as the one computed in the case of free space (without a substrate). The excess capacitance of the via is computed quasi-statically by the method of moments and the image method from the integral equations. It converges rapidly as the number of image terms is increased. Parametric plots of the excess capacitance of the via are given for reference.

1. INTRODUCTION

A VERY important type of microstrip discontinuity in integrated circuits is a via connection. An often-used model for analysis of this type of discontinuity is a microstrip via connecting two semi-infinitely long transmission lines, as shown in Fig. 1. This problem has been investigated in [1]–[3] in the case of free space (i.e., without a substrate). The via effect on the transmission line (TEM) modes is approximated by an equivalent circuit in the previously mentioned literature. The components in the equivalent circuit are computed by the method of moments quasi-statically. The problem is more practical, however, if the transmission lines and the via are imbedded in a uniform dielectric, as shown in Fig. 2. Here, the widths of the microstrips are assumed to be very small compared to the heights so that the microstrips are replaced by wires of the equivalent radii which are one fourth the widths. This equivalence is justified in [4]. Let h_1 , h_2 be the heights of transmission line 1 (wire 1) and transmission line 2 (wire 2), and, a_1 , a_2 , a_3 be the radii of wire 1, wire 2, and the via (wire 3), respectively. By assumption, h_1 , h_2 , $h_1 - h_2 \gg a_1$, a_2 , a_3 . The interface of the dielectric of permittivity ϵ is assumed to be parallel to the ground plane. The coordinate system is so chosen that the x -axis is on the ground plane and parallel to wire 1 and wire 2 and that the y -axis coincides with the axis of wire 3 (see Fig. 2).

Manuscript received December 5, 1988; revised May 24, 1989. This work was supported by Digital Equipment Corporation, Marlboro, MA, and by the Office of Naval Research, Arlington, VA, under Contract N00014-88-K-0027. This paper was recommended by Associate Editor J. G. Fossum.

The authors are with the Department of Electrical and Computer Engineering, Syracuse University, Syracuse, NY 13244-1240.

IEEE Log Number 8931291.

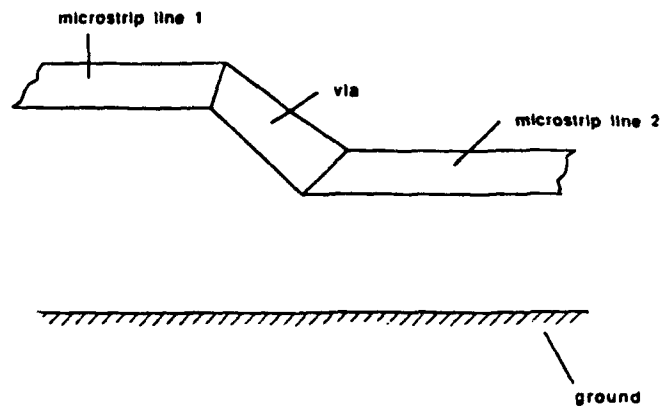


Fig. 1. A microstrip discontinuity: via connection.

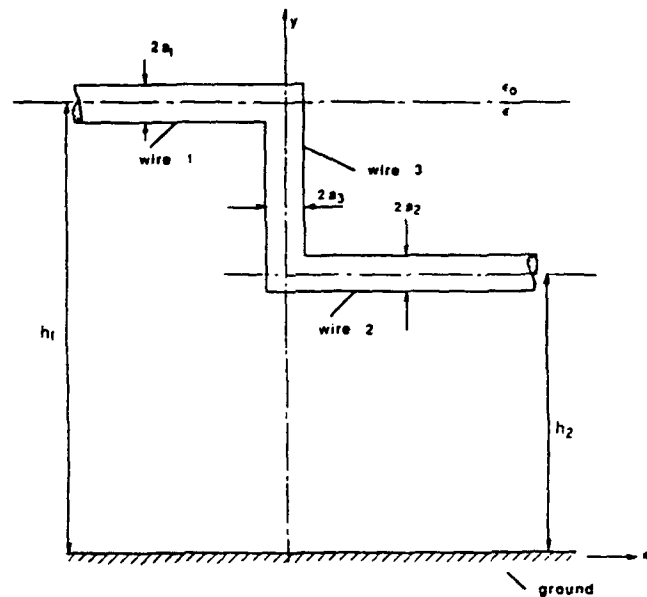


Fig. 2. A transmission line model of a microstrip via.

The equivalent circuit of the via for the quasi-TEM modes is shown in Fig. 3, where Z_{01} and Z_{02} are the characteristic impedance of the transmission lines 1 and 2, respectively. Since the dielectric is nonmagnetic, L_c is the same as that in free space, which was determined in [3]. We wish to determine C_c in this paper.

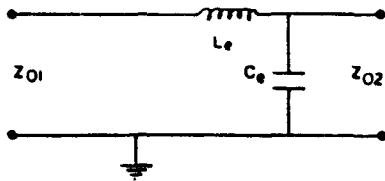


Fig. 3. The equivalent circuit of the via.

II. FORMULATION

The excess capacitance in Fig. 3 is a quasi-static quantity and is defined formally [1]:

$$C_e = \lim_{l_1, l_2 \rightarrow \infty} \frac{Q - l_1 q_{01} - l_2 q_{02}}{V} \quad (1)$$

where Q is the total charge on wire 1 of length l_1 (wire 1 truncated at $x = -l_1$), wire 2 of length l_2 (wire 2 truncated at $x = l_2$), and the via. V is the constant potential maintained on the surfaces of the wires with respect to ground. It is convenient to assume that V is 1 V throughout the following text. q_{01} and q_{02} are the uniform charge densities of single transmission lines 1 and 2. Numerical computation of C_e directly from (1) is not recommended because the numerator is the result of subtraction of large, nearly equal numbers as l_1 and l_2 get large. The more efficient method is to decompose the total charge density into the uniform charge density and the excess charge density. The latter is then determined by the method of moments.

Let q be the total charge distribution. Then we may write

$$q = \begin{cases} q_{01} + q_e, & \text{on wire 1} \\ q_{02} + q_e, & \text{on wire 2} \\ q_e, & \text{on wire 3.} \end{cases} \quad (2)$$

Here q_{01} is q_{01} existing on wire 1 and q_{02} is q_{02} existing on wire 2. If q_{01}^+ is defined as q_{01} existing on the extension of wire 1 to $x = \infty$ and if q_{02}^- defined as q_{02} existing on the extension of wire 2 to $x = -\infty$, we have

$$\psi(q_{01}^-) + \psi(q_{01}^+) = 1, \quad \text{on wire } i, \quad i = 1, 2 \quad (3)$$

where $\psi(\cdot)$ is the potential due to the charge density \cdot in the presence of the dielectric and the ground plane.

The total charge distribution q is governed by the following boundary condition

$$\psi(q) = 1, \quad \text{on wires 1, 2, 3.} \quad (4)$$

In view of (2) and (3), we write

$$\begin{aligned} \psi(q_e) &= \psi(q_{01}^+) - \psi(q_{02}^-), & \text{on wire 1} \\ \psi(q_e) &= \psi(q_{02}^-) - \psi(q_{01}^+), & \text{on wire 2} \\ \psi(q_e) &= 1 - \psi(q_{01}^-) - \psi(q_{02}^+), & \text{on wire 3.} \end{aligned} \quad (5)$$

Note that we replaced $1 - \psi(q_{01}^-)$ by $\psi(q_{01}^+)$ on wire 1 and $1 - \psi(q_{02}^+)$ by $\psi(q_{02}^-)$ on wire 2 to avoid possible significant round-off errors.

Equations (5) are integral equations to determine the excess charge distribution. In order to obtain a moment method solution for q_e , we first truncate q_e and (5) at $x = -K_1 h_1$ on wire 1 and $x = K_2 h_2$ on wire 2. This approximation is justified due to the fact that q_e and the right-hand sides of the first two equations in (5), called the residual potentials on wire 1 and wire 2, respectively, decay rapidly along wire 1 and wire 2. Experience has shown that K_1 and K_2 should be between 2 and 3.

Let

$$q_e = \begin{cases} \sum_{n=1}^{N_1} l_{n1} p_{n1}, & \text{on wire 1} \\ \sum_{n=1}^{N_2} l_{n2} p_{n2}, & \text{on wire 2} \\ \sum_{n=1}^{N_3} l_{n3} p_{n3}, & \text{on wire 3.} \end{cases} \quad (6)$$

where $\{l_{ni}, n = 1, 2, \dots, N_i, i = 1, 2, 3\}$ are expansion coefficients to be determined. p_{ni} are pulse expansion functions defined as follows:

$$p_{ni} = \begin{cases} 1 & x_{ni} < x < x_{ni} + \Delta x_i \\ 0 & \text{elsewhere,} \end{cases} \quad n = 1, 2, \dots, N_i; i = 1, 2$$

$$x_{n1} = -K_1 h_1 + (n-1) \Delta x_1, \quad \Delta x_1 = \frac{K_1 h_1 + a_3}{N_1}$$

$$x_{n2} = -a_3 + (n-1) \Delta x_2, \quad \Delta x_2 = \frac{K_2 h_2 + a_3}{N_2}$$

$$p_{n3} = \begin{cases} 1 & y_n < y < y_n + \Delta y \\ 0 & \text{elsewhere,} \end{cases} \quad n = 1, 2, \dots, N_3$$

$$y_n = h_2 + (n-1) \Delta y, \quad \Delta y = \frac{h_1 - h_2}{N_3}$$

In essence, we divide the truncated wires 1 and 2 and wire 3 into N_1 , N_2 , N_3 subsections, respectively, and assume uniform excess charge distribution on each subsection. A simple moment method solution is to satisfy (5) at the center of each subsection. This results in the following matrix equations:

$$\begin{aligned} L_{11} \bar{Q}_1 + L_{12} \bar{Q}_2 + L_{13} \bar{Q}_3 &= \bar{P}_1 \\ L_{21} \bar{Q}_1 + L_{22} \bar{Q}_2 + L_{23} \bar{Q}_3 &= \bar{P}_2 \\ L_{31} \bar{Q}_1 + L_{32} \bar{Q}_2 + L_{33} \bar{Q}_3 &= \bar{P}_3 \end{aligned} \quad (7)$$

where \bar{Q}_i are the column vectors of the coefficients l_{ni} . L_{ji} are matrices whose m th elements are the potentials due to the unit charge distribution in the m th subsection of wire i at the center of the m th subsection of wire j , in the pres-

ence of the dielectric and the ground plane. \vec{P}_j are the column vectors whose m th elements are residual potentials at the center of the m th subsection of wire j . After solving the above matrix equations, we sum up the excess charge and obtain the excess capacitance of the via. That is,

$$C_e = \sum_{i=1}^2 \Delta x_i \sum_{m=1}^{N_i} l_{im} + \Delta y \sum_{n=1}^{N_1} l_{in}. \quad (8)$$

In the next section, we will evaluate L_{ji} and \vec{P}_j .

III. COMPUTATION

To evaluate the moment matrices L_{ji} and the excitation vectors \vec{P}_j , one needs to find the potential distribution due to a uniform line charge in the presence of the dielectric and the ground plane. There are several approaches to this problem. One can place a surface polarization charge on the interface and solve the problem in free space. This is an efficient approach in the two-dimensional case (i.e., the line is infinitely long), as [5] demonstrated. However, in the three-dimensional case (i.e., the line is finite), one needs a huge number of expansion functions for the polarization charge and the method becomes too time-consuming. Another approach is to use the image method. Although the image method introduces an infinite set of image line charges and is difficult to generalize to the case of multilayered dielectrics, the solution is fairly straightforward and is obtainable numerically easily in the case of one dielectric interface. We take the second approach.

The electrostatic potential due to a unit point charge in the presence of a dielectric interface parallel to an infinite ground plane (i.e., the Green's function of our problem)

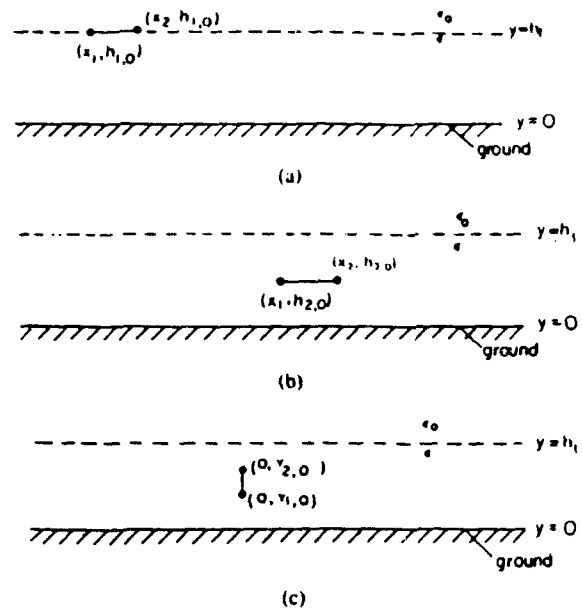


Fig. 4. Three cases of line charge sources.

using an integral representation of the free-space Green's function [10], [11]. Then, the potential distribution due to a uniform line charge is obtained by integration over the line source. Reference [6] gives the complete detailed derivation.¹

Case 1: A uniform line charge of finite length with unit line charge density lies on the dielectric interface. The location of the line is specified by its two end points $(X_1, h_1, 0)$ and $(X_2, h_1, 0)$, as is shown in Fig. 4(a). Call this line charge λ_1 . Then the potential due to λ_1 is given by [6]

$$\psi(\lambda_1)|_{r_{\text{inair}}} = \frac{1}{4\pi\epsilon_0} \frac{2}{1 + \epsilon_r} \left[\ln \frac{\sqrt{(X_2 - x)^2 + (y - h_1)^2 + z^2} + X_2 - x}{\sqrt{(X_1 - x)^2 + (y - h_1)^2 + z^2} + X_1 - x} - \frac{2\epsilon_r}{1 + \epsilon_r} \sum_{k=0}^{\infty} \left(\frac{1 - \epsilon_r}{1 + \epsilon_r} \right)^k \ln \frac{\sqrt{(X_2 - x)^2 + (y + (2k + 1)h_1)^2 + z^2} + X_2 - x}{\sqrt{(X_1 - x)^2 + (y + (2k + 1)h_1)^2 + z^2} + X_1 - x} \right] \quad (9)$$

$$\psi(\lambda_1)|_{r_{\text{indielectric}}} = \frac{1}{4\pi\epsilon_0} \frac{2}{1 + \epsilon_r} \sum_{k=0}^{\infty} \left(\frac{1 - \epsilon_r}{1 + \epsilon_r} \right)^k \cdot \ln \left[\frac{\sqrt{(X_2 - x)^2 + (y - (2k + 1)h_1)^2 + z^2} + X_2 - x}{\sqrt{(X_2 - x)^2 + (y + (2k + 1)h_1)^2 + z^2} + X_2 - x} \cdot \frac{\sqrt{(X_1 - x)^2 + (y + (2k + 1)h_1)^2 + z^2} + X_1 - x}{\sqrt{(X_1 - x)^2 + (y - (2k + 1)h_1)^2 + z^2} + X_1 - x} \right] \quad (10)$$

has been obtained by the image method in which the image charges are found directly [6], [8], by considering flux lines rather than the images themselves [9], and by

¹Note that many references such as [12] do not give the Green's function in all four combinations of source and field regions. Some references such as [7] give a complete form, which is not the simplest form.

where $r = (x, y, z)$ is the field point where the potential is to be evaluated and $\epsilon_r = \epsilon/\epsilon_0$ is the relative dielectric constant.

Case 2: A uniform line charge of finite length with unit line charge density is placed inside the dielectric. The location of the line is specified by its two end points $(X_1, h_2, 0)$ and $(X_2, h_2, 0)$, as is shown in Fig. 4(b). Call this line charge λ_2 . Then the potential due to λ_2 is given by [6]

$$\begin{aligned} \psi(\lambda_2)|_{r \text{ in air}} &= \frac{1}{4\pi\epsilon} \frac{2\epsilon_r}{1+\epsilon_r} \sum_{k=0}^{\infty} \left(\frac{1-\epsilon_r}{1+\epsilon_r} \right)^k \\ &\cdot \ln \left[\frac{\sqrt{(X_2-x)^2 + (y-h_2+2kh_1)^2 + z^2} + X_2-x}{\sqrt{(X_2-x)^2 + (y+h_2+2kh_1)^2 + z^2} + X_2-x} \right. \\ &\cdot \left. \frac{\sqrt{(X_1-x)^2 + (y+h_2+2kh_1)^2 + z^2} + X_1-x}{\sqrt{(X_1-x)^2 + (y-h_2+2kh_1)^2 + z^2} + X_1-x} \right] \end{aligned} \quad (11)$$

$$\begin{aligned} \psi(\lambda_2)|_{r \text{ in dielectric}} &= \frac{1}{4\pi\epsilon} \sum_{k=0}^{\infty} + \frac{1}{4\pi\epsilon} \sum_{k=1}^{\infty} \left(\frac{1-\epsilon_r}{1+\epsilon_r} \right)^k \\ &\cdot \ln \left[\frac{\sqrt{(X_2-x)^2 + (y-h_2-2kh_1)^2 + z^2} + X_2-x}{\sqrt{(X_2-x)^2 + (y+h_2-2kh_1)^2 + z^2} + X_2-x} \right. \\ &\cdot \left. \frac{\sqrt{(X_1-x)^2 + (y+h_2-2kh_1)^2 + z^2} + X_1-x}{\sqrt{(X_1-x)^2 + (y-h_2-2kh_1)^2 + z^2} + X_1-x} \right]. \end{aligned} \quad (12)$$

In (12), $\sum_{k=0}^{\infty}$ is the series in (11).

Case 3: A uniform line charge of finite length with unit line charge density is placed inside the dielectric. The location of the line is specified by its two end points $(0, Y_1, 0)$ and $(0, Y_2, 0)$, as is shown in Fig. 4(c). Call this line charge λ_3 . Then the potential due to λ_3 is given by [6]

$$\begin{aligned} \psi(\lambda_3)|_{r \text{ in air}} &= \frac{1}{4\pi\epsilon} \frac{2\epsilon_r}{1+\epsilon_r} \sum_{k=0}^{\infty} \left(\frac{1-\epsilon_r}{1+\epsilon_r} \right)^k \\ &\cdot \ln \left[\frac{\sqrt{x^2 + (Y_2-2kh_1-y)^2 + z^2} + Y_2-2kh_1-y}{\sqrt{x^2 + (Y_2+2kh_1+y)^2 + z^2} + Y_2+2kh_1+y} \right. \\ &\cdot \left. \frac{\sqrt{x^2 + (Y_1+2kh_1+y)^2 + z^2} + Y_1+2kh_1+y}{\sqrt{x^2 + (Y_1-2kh_1-y)^2 + z^2} + Y_1-2kh_1-y} \right] \end{aligned} \quad (13)$$

$$\begin{aligned} \psi(\lambda_3)|_{r \text{ in dielectric}} &= \frac{1}{4\pi\epsilon} \sum_{k=0}^{\infty} + \frac{1}{4\pi\epsilon} \sum_{k=1}^{\infty} \left(\frac{1-\epsilon_r}{1+\epsilon_r} \right)^k \\ &\cdot \ln \left[\frac{\sqrt{x^2 + (Y_2+2kh_1-y)^2 + z^2} + Y_2+2kh_1-y}{\sqrt{x^2 + (Y_2-2kh_1+y)^2 + z^2} + Y_2-2kh_1+y} \right. \\ &\cdot \left. \frac{\sqrt{x^2 + (Y_1-2kh_1+y)^2 + z^2} + Y_1-2kh_1+y}{\sqrt{x^2 + (Y_1+2kh_1-y)^2 + z^2} + Y_1+2kh_1-y} \right]. \end{aligned} \quad (14)$$

In (14), $\sum_{k=0}^{\infty}$ is the series in (13).

According to (3), the potential due to the charge density q_{01} on the line $(-\infty \leq x \leq \infty, y = h_1, z = 0)$ is unity. Since this potential is given by the product of q_{01} with the right-hand side of [6, (A-73)] with $x, h, y,$ and y' replaced

by $a_1, h_1, h_1,$ and $h_1,$ respectively, we obtain

$$\begin{aligned} \frac{2q_{01}}{4\pi\epsilon_0} \frac{2}{1+\epsilon_r} \left[\ln \left(\frac{2h_1}{a_1} \right) + \sum_{k=1}^{\infty} \left(\frac{1-\epsilon_r}{1+\epsilon_r} \right)^k \right. \\ \left. \cdot \ln \left(1 + \frac{1}{k} \right) \right] = 1. \end{aligned} \quad (15)$$

According to (3), the potential due to the charge density q_{02} on the line ($-\infty \leq x \leq \infty, y = h_2, z = 0$) is unity. Since this potential is given by the product of q_{02} with the right-hand side of [6, (A-75)] with $x, h, y,$ and y' replaced by $a_2, h_1, h_2,$ and $h_2,$ respectively, we obtain

$$\frac{2q_{02}}{4\pi\epsilon} \left[\ln \left(\frac{2h_2}{a_2} \right) + \sum_{k=1}^{\infty} \left(\frac{1 - \epsilon_r}{1 + \epsilon_r} \right)^k \ln \left(1 - \frac{h_2^2}{k^2 h_1^2} \right) \right] = 1 \quad (16)$$

The two-dimensional potentials on the left-hand sides of (15) and (16) are also given by Weeks [7].

Now, it is trivial to write out the expressions for the moment matrices and excitation vectors. In fact, we only need to use the formulas in the dielectric region. A small special consideration must be made when the diagonal elements of L_{ii} are evaluated. In that case, the $k = 0$ terms in the series in (10), (12), and (14) are replaced by

$$2 \ln \left[\frac{\sqrt{1 + \left(\frac{2a_i}{\Delta x_i} \right)^2} + 1}{\sqrt{1 + \left(\frac{4h_i}{\Delta x_i} \right)^2} + 1} \cdot \frac{2h_i}{a_i} \right], \quad i = 1, 2 \quad (17)$$

$$2 \ln \left[\left(\sqrt{1 + \left(\frac{2a_3}{\Delta y} \right)^2} + 1 \right) \frac{\Delta y}{2a_3} \sqrt{\frac{4Y_1 + \Delta y}{4Y_2 - \Delta y}} \right], \quad i = 3 \quad (18)$$

Results

$$4\pi\epsilon_0 L_{j1}(m, n) = \frac{2}{1 + \epsilon_r} \sum_{k=0}^{\infty} \left(\frac{1 - \epsilon_r}{1 + \epsilon_r} \right)^k \cdot \ln \left[\frac{\sqrt{\theta_1^2 + \beta_1^2} + \theta_1}{\sqrt{\theta_1^2 + \beta_2^2} + \theta_1} \cdot \frac{\sqrt{\theta_2^2 + \beta_2^2} + \theta_2}{\sqrt{\theta_2^2 + \beta_1^2} + \theta_2} \right]$$

$$\left. \begin{aligned} \theta_1 &= x_{n1} - x'_{m1} \\ \theta_2 &= x_{(n+1)1} - x'_{m1} \\ \beta_1 &= 2(k+1)h_1 \\ \beta_2 &= 2kh_1 \end{aligned} \right\} j = 1 \text{ (if } m = n, \text{ the } k = 0 \text{ term is replaced by (17).)}$$

$$\left. \begin{aligned} \theta_1 &= x_{n1} - x'_{m2} \\ \theta_2 &= x_{(n+1)1} - x'_{m2} \\ \beta_1 &= h_2 + (2k+1)h_1 \\ \beta_2 &= h_2 - (2k+1)h_1 \end{aligned} \right\} j = 2$$

$$\left. \begin{aligned} \theta_1 &= x_{n1} \\ \theta_2 &= x_{(n+1)1} \\ \beta_1 &= y'_m + (2k+1)h_1 \\ \beta_2 &= y'_m - (2k+1)h_1 \end{aligned} \right\} j = 3$$

$$4\pi\epsilon_0 L_{j2}(m, n) = \gamma_1 \sum_{k=0}^{\infty} \left(\frac{1 - \epsilon_r}{1 + \epsilon_r} \right)^k \cdot \ln \left[\frac{\sqrt{\theta_1^2 + \beta_1^2} + \theta_1}{\sqrt{\theta_1^2 + \beta_2^2} + \theta_1} \cdot \frac{\sqrt{\theta_2^2 + \beta_2^2} + \theta_2}{\sqrt{\theta_2^2 + \beta_1^2} + \theta_2} \right] + \gamma_2 \sum_{k=1}^{\infty} \left(\frac{1 - \epsilon_r}{1 + \epsilon_r} \right)^k \cdot \ln \left[\frac{\sqrt{\theta_1^2 + \beta_1^2} + \theta_1}{\sqrt{\theta_1^2 + \beta_2^2} + \theta_1} \cdot \frac{\sqrt{\theta_2^2 + \beta_2^2} + \theta_2}{\sqrt{\theta_2^2 + \beta_1^2} + \theta_2} \right]$$

$$\left. \begin{aligned} \gamma_1 &= \frac{2}{1 + \epsilon_r} \\ \gamma_2 &= 0 \\ \theta_1 &= x_{n2} - x'_{m1} \\ \theta_2 &= x_{(n+1)2} - x'_{m1} \\ \beta_1 &= (2k+1)h_1 + h_2 \\ \beta_2 &= (2k+1)h_1 - h_2 \end{aligned} \right\} j = 1$$

$$\left. \begin{aligned} \gamma_1 &= \frac{1}{\epsilon_r} \\ \gamma_2 &= \frac{1}{\epsilon_r} \\ \theta_1 &= x_{n2} - x'_{m2} \\ \theta_2 &= x_{(n+1)2} - x'_{m2} \\ \beta_1 &= 2kh_1 + 2h_2 \\ \beta_2 &= 2kh_1 \\ \beta_3 &= 2kh_1 - 2h_2 \\ \beta_4 &= 2kh_1 \end{aligned} \right\} j = 2 \text{ (if } m = n, \text{ the } k = 0 \text{ term is replaced by (17).)}$$

$$\left. \begin{aligned} \gamma_1 &= \frac{1}{\epsilon_r} \\ \gamma_2 &= \frac{1}{\epsilon_r} \\ \theta_1 &= x_{n2} \\ \theta_2 &= x_{(n+1)2} \\ \beta_1 &= 2kh_1 + h_2 + y'_m \\ \beta_2 &= 2kh_1 - h_2 + y'_m \\ \beta_3 &= 2kh_1 - h_2 - y'_m \\ \beta_4 &= 2kh_1 + h_2 - y'_m \end{aligned} \right\} j = 3$$

$$4\pi\epsilon_0 L_{j,1}(m, n)$$

$$= \gamma_1 \sum_{k=0}^{\infty} \left(\frac{1 - \epsilon_r}{1 + \epsilon_r} \right)^k \cdot \ln \left| \frac{\sqrt{\theta^2 + \beta_1^2} + \beta_1}{\sqrt{\theta^2 + \beta_2^2} + \beta_2} \cdot \frac{\sqrt{\theta^2 + \beta_3^2} + \beta_3}{\sqrt{\theta^2 + \beta_4^2} + \beta_4} \right| + \gamma_2 \sum_{k=1}^{\infty} \left(\frac{1 - \epsilon_r}{1 + \epsilon_r} \right)^k \cdot \ln \left| \frac{\sqrt{\theta^2 + \beta_5^2} + \beta_5}{\sqrt{\theta^2 + \beta_6^2} + \beta_6} \cdot \frac{\sqrt{\theta^2 + \beta_7^2} + \beta_7}{\sqrt{\theta^2 + \beta_8^2} + \beta_8} \right|$$

$$\gamma_1 = \frac{2}{1 + \epsilon_r}$$

$$\gamma_2 = 0$$

$$\theta = x'_{m1}$$

$$\beta_1 = (2k + 1)h_1 + y_n$$

$$\beta_2 = (2k + 1)h_1 - y_{n+1}$$

$$\beta_3 = (2k + 1)h_1 - y_n$$

$$\beta_4 = (2k + 1)h_1 + y_{n-1}$$

$j = 1$

$$\gamma_1 = \frac{1}{\epsilon_r}$$

$$\gamma_2 = \frac{1}{\epsilon_r}$$

$$\theta = x'_{m2}$$

$$\beta_1 = 2kh_1 + h_2 + y_n$$

$$\beta_2 = 2kh_1 + h_2 - y_{n+1}$$

$$\beta_3 = 2kh_1 + h_2 - y_n$$

$$\beta_4 = 2kh_1 + h_2 + y_{n+1}$$

$$\beta_5 = 2kh_1 - h_2 - y_{n+1}$$

$$\beta_6 = 2kh_1 - h_2 + y_n$$

$$\beta_7 = 2kh_1 - h_2 + y_{n+1}$$

$$\beta_8 = 2kh_1 - h_2 - y_n$$

$j = 2$

$$\gamma_1 = \frac{1}{\epsilon_r}$$

$$\gamma_2 = \frac{1}{\epsilon_r}$$

$$\theta = 0$$

$$\beta_1 = 2kh_1 + y'_m + y_n$$

$$\beta_2 = 2kh_1 + y'_m - y_{n+1}$$

$$\beta_3 = 2kh_1 + y'_m - y_n$$

$$\beta_4 = 2kh_1 + y'_m + y_{n+1}$$

$$\beta_5 = 2kh_1 - y'_m - y_{n+1}$$

$$\beta_6 = 2kh_1 - y'_m + y_n$$

$$\beta_7 = 2kh_1 - y'_m + y_{n+1}$$

$$\beta_8 = 2kh_1 - y'_m - y_n$$

$j = 3$ (if $m = n$, the $k = 0$ term is replaced by (18).)

$$P_1(m) = \frac{2\hat{q}_{01}}{1 + \epsilon_r} \sum_{k=0}^{\infty} \left(\frac{1 - \epsilon_r}{1 + \epsilon_r} \right)^k \ln \frac{\sqrt{\theta^2 + \beta_1^2} + \theta}{\sqrt{\theta^2 + \beta_2^2} + \theta} - \frac{2\hat{q}_{02}}{1 + \epsilon_r} \sum_{k=0}^{\infty} \left(\frac{1 - \epsilon_r}{1 + \epsilon_r} \right)^k \ln \frac{\sqrt{\theta^2 + \beta_3^2} + \theta}{\sqrt{\theta^2 + \beta_4^2} + \theta}$$

$$\theta = -x'_{m1}$$

$$\beta_1 = 2(k + 1)h_1; \quad \beta_2 = 2kh_1$$

$$\beta_3 = (2k + 1)h_1 + h_2; \quad \beta_4 = (2k + 1)h_1 - h_2$$

$$P_2(m) = -\frac{2\hat{q}_{01}}{1 + \epsilon_r} \sum_{k=0}^{\infty} \left(\frac{1 - \epsilon_r}{1 + \epsilon_r} \right)^k \ln \frac{\sqrt{\theta^2 + \beta_1^2} + \theta}{\sqrt{\theta^2 + \beta_2^2} + \theta} + \frac{\hat{q}_{02}}{\epsilon_r} \left[\sum_{k=0}^{\infty} \left(\frac{1 - \epsilon_r}{1 + \epsilon_r} \right)^k \ln \frac{\sqrt{\theta^2 + \beta_3^2} + \theta}{\sqrt{\theta^2 + \beta_4^2} + \theta} + \sum_{k=1}^{\infty} \left(\frac{1 - \epsilon_r}{1 + \epsilon_r} \right)^k \ln \frac{\sqrt{\theta^2 + \beta_5^2} + \theta}{\sqrt{\theta^2 + \beta_6^2} + \theta} \right]$$

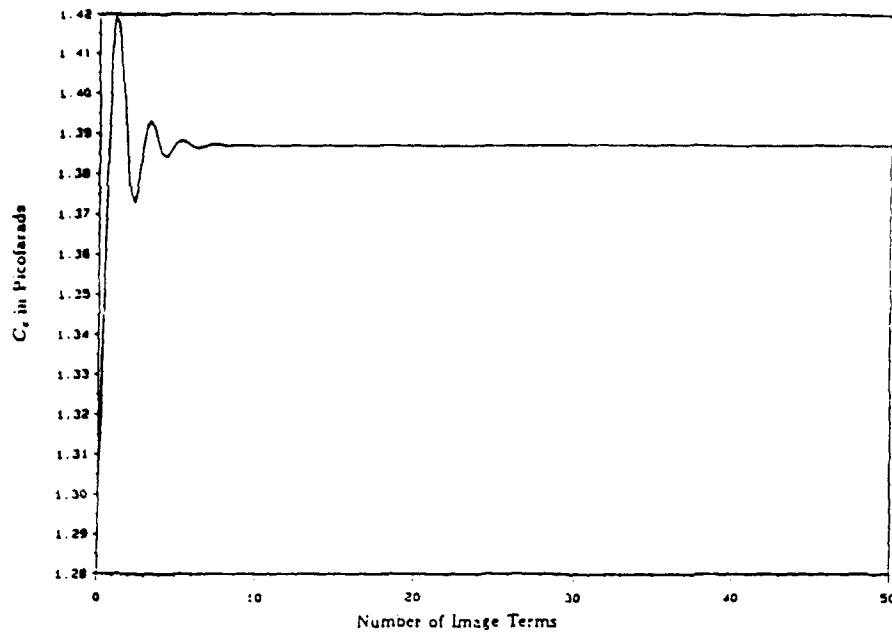
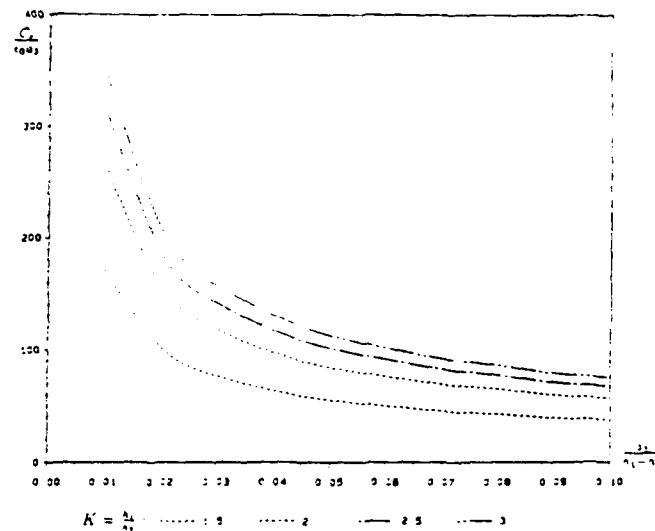
$$\theta = x'_{m2}$$

$$\beta_1 = (2k + 1)h_1 + h_2; \quad \beta_2 = (2k + 1)h_1 - h_2$$

$$\beta_3 = 2kh_1 + 2h_2; \quad \beta_4 = 2kh_1$$

$$\beta_5 = 2kh_1 - 2h_2; \quad \beta_6 = 2kh_1$$

$$P_3(m) = 1 - \frac{2\hat{q}_{01}}{1 + \epsilon_r} \sum_{k=0}^{\infty} \left(\frac{1 - \epsilon_r}{1 + \epsilon_r} \right)^k \ln \frac{\sqrt{\theta^2 + \beta_1^2} + \theta}{\sqrt{\theta^2 + \beta_2^2} + \theta} - \frac{\hat{q}_{02}}{\epsilon_r} \left[\sum_{k=0}^{\infty} \left(\frac{1 - \epsilon_r}{1 + \epsilon_r} \right)^k \ln \frac{\sqrt{\theta^2 + \beta_3^2} + \theta}{\sqrt{\theta^2 + \beta_4^2} + \theta} + \sum_{k=1}^{\infty} \left(\frac{1 - \epsilon_r}{1 + \epsilon_r} \right)^k \ln \frac{\sqrt{\theta^2 + \beta_5^2} + \theta}{\sqrt{\theta^2 + \beta_6^2} + \theta} \right]$$

Fig. 5. Convergence of excess capacitance ($\epsilon_r = 4$).Fig. 6. Normalized excess capacitance of the via ($\epsilon_r = 4$, $\ln(2h_1/a_1) = \ln(2h_2/a_2) = 5$).

$$\theta = 0$$

$$\beta_1 = (2k + 1)h_1 + y'_m; \quad \beta_2 = (2k + 1)h_1 - y'_m$$

$$\beta_3 = 2kh_1 + h_2 + y'_m; \quad \beta_4 = 2kh_1 - h_2 + y'_m$$

$$\beta_5 = 2kh_1 - h_2 - y'_m; \quad \beta_6 = 2kh_1 + h_2 - y'_m$$

In the above equations, the primed coordinates denote the center of each subsection and $\hat{q}_{0i} = q_{vi}/(4\pi\epsilon_0)$, $i = 1, 2$. Note that the expressions given above are not numerically most efficient but show some patterns for easy programming. The following section gives some numerical results.

IV. NUMERICAL RESULTS AND DISCUSSION

The computer program to calculate the excess capacitance of the via was written in Fortran and was run in an IBM AT/PC machine with Microsoft Fortran. It only took 10 s to run a case (with 29 subsections and 10 image terms in the series). To verify our code, we made two basic checks.

Check 1: If the dielectric constant is 1 (i.e., there is no dielectric medium at all), then the problem is identical to the one in [3]. For the following geometry:

$$h_1 = 0.08 \text{ m} \quad a_1 = 0.002 \text{ m}$$

$$h_2 = 0.04 \text{ m} \quad a_2 = 0.001 \text{ m}$$

$$a_3 = 0.002 \text{ m}$$

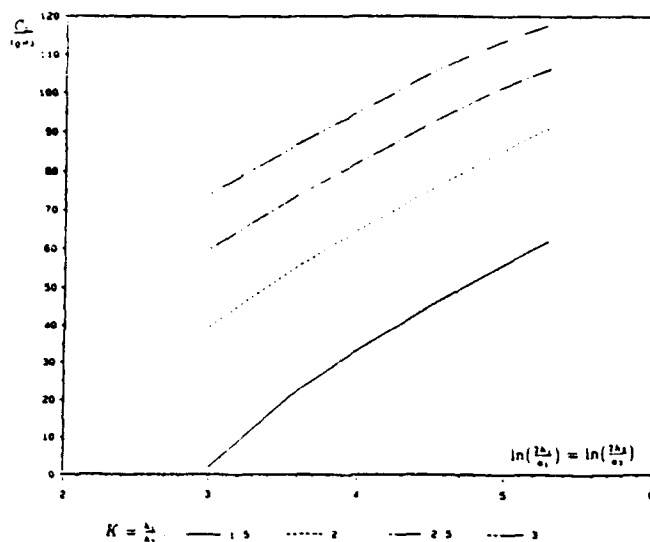


Fig. 7. Normalized excess capacitance of the via ($\epsilon_r = 4$, $a_1/(h_1 - h_2) = 0.05$).

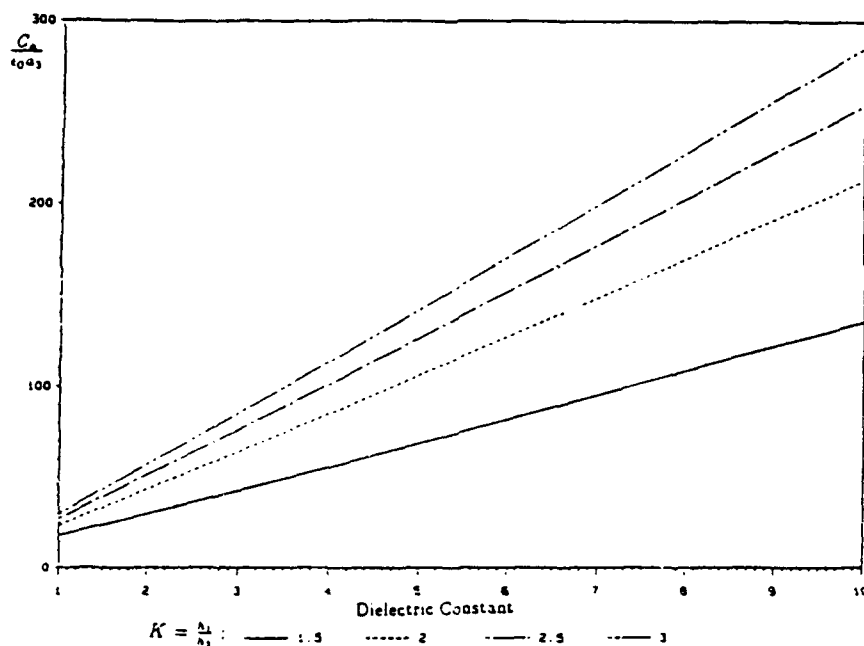


Fig. 8. Normalized excess capacitance of the via ($a_1/(h_1 - h_2) = 0.05$, $\ln(2h_1/a_1) = \ln(2h_2/a_2) = 5$).

we calculated the excess capacitance:

$$C_v = 0.3701 \text{ pF}$$

With the same data, [3] gives $C_v = 0.3776 \text{ pF}$.

Check 2: The excess capacitance should be convergent as the number of the image terms in the series used in the calculation gets large. With the above data and $\epsilon_r = 4$, we plot the excess capacitance versus the number of the image terms in Fig. 5. We observe rapid convergence.

To be consistent with [3], we plot the normalized excess capacitance of the via in various cases, as shown in Figs. 6-8. Figs. 6 and 7 replace figs. 4 and 5 in [3] and help design a reflectionless via together with the curves of figs. 6 and 8 in [3]. See [3] for detailed discussion.

In conclusion, we used a simple wire model to compute the excess capacitance of a via connecting two semi-infinitely long microstrips. The approximation deteriorates when the microstrips are not narrow in comparison to the heights of the microstrips above ground. In this case, one can divide the microstrips into rectangles or triangles and can still follow the same approach (the method of moments and the image method) as that in this paper.

REFERENCES

- [1] J. R. Mautz and R. F. Harrington, "Calculation of the excess capacitance of a microstrip discontinuity," Tech. Rep. TR-84-2, Dep. Elect. Comput. Eng., Syracuse Univ., Syracuse, NY, Jan. 1984.
- [2] —, "Calculation of the excess inductance of a microstrip discontinuity," Tech. Rep. SYRU/DICE/TR-84/5, Dep. Elect. Comput. Eng., Syracuse Univ., Syracuse, NY, May 1984.

- [13] T. Wang, R. F. Harrington, and J. R. Mautz, "The equivalent circuit of a via," *Trans. Soc. Comput. Simulation*, vol. 4, pp. 97-123, Apr. 1987.
- [14] C. M. Butler, "The equivalent radius of a narrow conducting strip," *IEEE Trans. Antennas Propagat.*, vol. AP-30, pp. 755-758, July 1982.
- [15] C. Wei, R. F. Harrington, J. R. Mautz, and T. K. Sarkar, "Multi-conductor transmission lines in multilayered dielectric media," *IEEE Trans. Microwave Theory Tech.*, vol. MTT-32, pp. 439-450, Apr. 1984.
- [16] T. Wang, J. R. Mautz, and R. F. Harrington, "The excess capacitance of a microstrip via in a dielectric substrate," Tech. Rep. TR-88-10, Dep. Elect. Comput. Eng., Syracuse Univ., Syracuse, NY, Aug. 1988.
- [17] W. T. Weeks, "Calculation of coefficients of capacitance of multi-conductor transmission lines in the presence of a dielectric interface," *IEEE Trans. Microwave Theory Tech.*, vol. MTT-18, pp. 35-43, Jan. 1970.
- [18] Y. M. Hill, N. O. Reckord, and D. R. Winner, "A general method for obtaining impedance and coupling characteristics of practical microstrip and triplate transmission line configurations," *IBM J. Res. Develop.*, vol. 13, pp. 314-322, May 1969.
- [19] P. Silvester, "TEM wave properties of microstrip transmission lines," *Proc. Inst. Elec. Eng.*, vol. 115, pp. 43-48, Jan. 1968.
- [10] S. Coen, "A note on Green's function for microstrip," *IEEE Trans. Microwave Theory Tech.*, vol. MTT-23, pp. 591-593, July 1975.
- [11] R. Crampagne and J.-L. Guiraud, "A two- or three-dimensional Green's function which can be applied to hyperequency microelectronic transmission lines," *IEEE Trans. Microwave Theory Tech.*, vol. MTT-25, pp. 442-444, May 1977.
- [12] A. Farrar and A. T. Adams, "Matrix methods for microstrip three-dimensional problems," *IEEE Trans. Microwave Theory Tech.*, vol. MTT-20, pp. 497-504, Aug. 1972.



Joseph R. Mautz (S'66-M'67-SM'75) received the B.S., M.S., and Ph.D. degrees in electrical engineering from Syracuse University in 1961, 1965, and 1969, respectively.

He is currently a Research Engineer in the Department of Electrical Engineering, Syracuse University, where he works on radiation and scattering problems. He is currently working in the area of numerical methods for solving field problems. His main interests include electromagnetic theory and applied mathematics.

*



Taoyun Wang (S'84) received the B.S. degree in 1982 from Xian Jiaotong University, China, and the M.S. and Ph.D. degrees in electrical engineering from Syracuse University in 1984 and 1989, respectively.

Since 1983, he has been actively involved with the electromagnetic research group at Syracuse University. His research interests include electromagnetic scattering and transmission, microstrip circuits, and numerical methods.



Roger F. Harrington (S'48-A'53-M'57-SM'62-F'68) received the B.E.E. and M.E.E. degrees from Syracuse University in 1948 and 1950, respectively, and the Ph.D. degree from Ohio State University in 1952.

From 1945 to 1946, he served as an Instructor at the U.S. Naval Radio Materiel School, Dearborn, MI, and from 1948 to 1950, he was an Instructor and Research Assistant at Syracuse University. Since 1952, he has been on the faculty of Syracuse University, where he is currently a Professor of Electrical Engineering.

Dr. Harrington is a member of Tau Beta Pi, Sigma Xi, and the American Association of University Professors.

Dr. Harrington is a member of Tau Beta Pi, Sigma Xi, and the American Association of University Professors.

Communications

A Stable Integral Equation for Electromagnetic Scattering from Homogeneous Dielectric Bodies

JOSEPH R. MAUTZ, SENIOR MEMBER, IEEE

Abstract—It is shown that a previously derived integral equation for electromagnetic scattering from a homogeneous dielectric body does not have a unique solution at resonant frequencies of the cavity formed by making the surface S of the body perfectly conducting and filling the region internal to S with the external medium. This integral equation was formulated so that an equivalent electric current radiates in the presence of the homogeneous external medium to produce the scattered field external to the body. A combination of equivalent electric and magnetic currents is used to formulate an integral equation whose solution is always unique.

I. INTRODUCTION

Consider electromagnetic scattering from a homogeneous dielectric body immersed in a homogeneous medium. The surface of the body is S . Assuming that the scattered field can be produced by equivalent electric current \mathbf{J}_e placed on S and radiating into a homogeneous medium having the material parameters of the external ambient medium, Marx [1] derived an integral equation for \mathbf{J}_e and Glisson [2] put this equation into familiar notation. A resonant frequency is a frequency for which S , when covered by a perfect electric conductor and filled with the external medium forms a resonant cavity. At a resonant frequency, this integral equation does not uniquely determine the pure electric current that supposedly produces the scattered field external to S . Actually, at a resonant frequency, a pure electric current is not sufficient to produce an arbitrary scattered field; a magnetic current is also needed [3, pp. 351–362].

II. FORMULATION OF THE INTEGRAL EQUATION

Continuity of the tangential electric field across S is expressed as [2, eq. (9)]

$$\hat{n} \times (\mathbf{E}_e^+ + \mathbf{E}^i) = \hat{n} \times \mathbf{E}_d^- \quad (1)$$

Except for the superscripts plus and minus, our notation is that of [2]. The superscript plus denotes field evaluation on the side of S facing the external region and the superscript minus denotes field evaluation on the side of S facing the region internal to the body. We assume that the electromagnetic field $(\mathbf{E}_e, \mathbf{H}_e)$ is radiated not by \mathbf{J}_e alone but by the combination of the electric current \mathbf{J}_e and the magnetic current $\alpha \hat{n} \times \mathbf{J}_e$, both exactly on S :

$$\mathbf{E}_e = \mathbf{E}_e(\mathbf{J}_e, \alpha \hat{n} \times \mathbf{J}_e) \quad (2)$$

$$\mathbf{H}_e = \mathbf{H}_e(\mathbf{J}_e, \alpha \hat{n} \times \mathbf{J}_e) \quad (3)$$

Here, α is an arbitrary constant. The source $(\mathbf{J}_e, \alpha \hat{n} \times \mathbf{J}_e)$ is similar to the combined source in [4]. If $\alpha = 0$, then the integral equation in the process of being derived will be the one presented in [2]. The field $(\mathbf{E}_d, \mathbf{H}_d)$ is radiated by the combination of electric and magnetic currents \mathbf{J}_d and \mathbf{M}_d exactly on S :

$$\mathbf{E}_d = \mathbf{E}_d(\mathbf{J}_d, \mathbf{M}_d) \quad (4)$$

$$\mathbf{H}_d = \mathbf{H}_d(\mathbf{J}_d, \mathbf{M}_d) \quad (5)$$

If, as in [2], $(\mathbf{J}_d, \mathbf{M}_d)$ is to radiate no field in the external region, then

$$\mathbf{J}_d = -\hat{n} \times (\mathbf{H}_e^+ + \mathbf{H}^i) \quad (6)$$

$$\mathbf{M}_d = -(\mathbf{E}_e^+ + \mathbf{E}^i) \times \hat{n} \quad (7)$$

The original scattering problem, the simulation of the field in the exterior region, and the simulation of the field in the interior region are as illustrated in [2, Fig. 1] with \mathbf{M}_d replaced by $\alpha \hat{n} \times \mathbf{J}_e$.

Substituting (2), (4), (6), and (7) into (1) and rearranging terms, we obtain an integral equation similar to [2, eq. (24)]:

$$\hat{\mathbf{M}}_d - \hat{n} \times \mathbf{E}_d^-(\mathbf{J}_d, \hat{\mathbf{M}}_d) = -\hat{n} \times [\mathbf{E}^i + \mathbf{E}_d^-(\hat{n} \times \mathbf{H}^i, \mathbf{E}^i \times \hat{n})] \quad (8)$$

where

$$\hat{\mathbf{J}}_d = -\hat{n} \times \mathbf{H}_e^+(\mathbf{J}_e, \alpha \hat{n} \times \mathbf{J}_e) \quad (9)$$

$$\hat{\mathbf{M}}_d = \hat{n} \times \mathbf{E}_e^+(\mathbf{J}_e, \alpha \hat{n} \times \mathbf{J}_e) \quad (10)$$

The homogeneous equation associated with (8) is

$$\hat{\mathbf{M}}_d - \hat{n} \times \mathbf{E}_d^-(\hat{\mathbf{J}}_d, \hat{\mathbf{M}}_d) = 0 \quad (11)$$

where $\hat{\mathbf{J}}_d$ and $\hat{\mathbf{M}}_d$ are given by (9) and (10). If a solution \mathbf{J}_e to (8) exists, then it is unique if and only if the homogeneous equation (11) with supporting equations (9) and (10) has only the trivial solution $\mathbf{J}_e = 0$.

If $\alpha = 0$, then the integral equation (8) with supporting equations (9) and (10) is the same as [2, eq. (24)] and, of course, the homogeneous equation (11) with supporting equations (9) and (10) is the same as the homogeneous equation associated with [2, eq. (24)]. When the frequency is a resonant frequency, there is a nontrivial electric current \mathbf{J}_R such that

$$\hat{n} \times \mathbf{E}_e^+(\mathbf{J}_R, 0) = 0 \quad (12)$$

$$\hat{n} \times \mathbf{H}_e^+(\mathbf{J}_R, 0) = 0 \quad (13)$$

Assuming that $\alpha = 0$, it is evident from (12) and (13) that $\mathbf{J}_e = \mathbf{J}_R$ is a nontrivial solution to the homogeneous equation (11) with supporting equations (9) and (10). Therefore, even if [2, eq. (24)] had a solution at a resonant frequency, then this solution would not be unique.

Can a different choice of α cause (8)–(10) to have not more than one solution? Otherwise stated, can α be chosen such that the homogeneous equation (11) with supporting equations (9) and (10) has only the trivial solution $\mathbf{J}_e = 0$?

Assuming that (9)–(11) hold, consider the composite situation where, in the internal region, $(\mathbf{E}_d(\hat{\mathbf{J}}_d, \hat{\mathbf{M}}_d), \mathbf{H}_d(\hat{\mathbf{J}}_d, \hat{\mathbf{M}}_d))$ exists in

Manuscript received January 27, 1988; revised May 10, 1988. This work was supported by the Office of Naval Research, Arlington VA, under Contract N00014-85-K-0082, and by the New York State Center for Advanced Technology in Computer Applications and Software Engineering (CASE), Syracuse University.

The author is with the Department of Electrical and Computer Engineering, Syracuse University, Syracuse, NY 13244-1240.

IEEE Log Number 8927717.

(μ_e, ϵ_d) and, in the external region, $(\mathbf{E}_e(\mathbf{J}_e, \alpha \hat{\mathbf{n}} \times \mathbf{J}_e), \mathbf{H}_e(\mathbf{J}_e, \alpha \hat{\mathbf{n}} \times \mathbf{J}_e))$ exists in (μ_e, ϵ_e) . The sources of the above defined composite field are electric and magnetic currents \mathbf{J} and $\hat{\mathbf{M}}$ on S given by

$$\mathbf{J} = \hat{\mathbf{n}} \times (\mathbf{H}_d^+(\mathbf{J}_d, \alpha \hat{\mathbf{n}} \times \mathbf{J}_d) - \mathbf{H}_d^-(\mathbf{J}_d, \hat{\mathbf{M}}_d)) \quad (14)$$

$$\hat{\mathbf{M}} = (\mathbf{E}_d^+(\mathbf{J}_e, \alpha \hat{\mathbf{n}} \times \mathbf{J}_e) - \mathbf{E}_d^-(\mathbf{J}_d, \hat{\mathbf{M}}_d)) \times \hat{\mathbf{n}}. \quad (15)$$

Equations (10) and (11) reduce (15) to

$$\hat{\mathbf{M}} = \mathbf{0}. \quad (16)$$

Equation (11) is recast as

$$\hat{\mathbf{n}} \times \mathbf{E}_d^-(\mathbf{J}_d, \hat{\mathbf{M}}_d) = \mathbf{0}. \quad (17)$$

Since there are no external resonances, (17) implies that

$$\hat{\mathbf{n}} \times \mathbf{H}_d^+(\mathbf{J}_d, \hat{\mathbf{M}}_d) = \mathbf{0}. \quad (18)$$

From (18), we obtain

$$\hat{\mathbf{n}} \times \mathbf{H}_d^-(\mathbf{J}_d, \hat{\mathbf{M}}_d) = -\mathbf{J}_d. \quad (19)$$

Equations (9) and (19) reduce (14) to

$$\mathbf{J} = \mathbf{0}. \quad (20)$$

According to (16) and (20), the composite field defined in the paragraph containing (14) has no sources. Therefore, this field collapses to zero. In particular,

$$\hat{\mathbf{n}} \times \mathbf{E}_e^+(\mathbf{J}_e, \alpha \hat{\mathbf{n}} \times \mathbf{J}_e) = \mathbf{0}. \quad (21)$$

It is shown in [4, eqs. (4)-(8)] that, if $\text{Re}(\alpha) > 0$, then the only solution to (21) is $\mathbf{J}_e = \mathbf{0}$. Here, Re denotes the real part. Thus, if $\text{Re}(\alpha) > 0$, then only $\mathbf{J}_e = \mathbf{0}$ can satisfy (9)-(11). Therefore, if $\text{Re}(\alpha)$

> 0 , then the integral equation (8) with supporting equations (9) and (10) can not have more than one solution \mathbf{J}_e .

REFERENCES

- [1] E. Marx, "Integral equation for scattering by a dielectric," *IEEE Trans. Antennas Propagat.*, vol. AP-32, pp. 166-172, Feb. 1984.
- [2] A. W. Glisson, "An integral equation for electromagnetic scattering from homogeneous dielectric bodies," *IEEE Trans. Antennas Propagat.*, vol. AP-32, pp. 173-175, Feb. 1984.
- [3] H. Hönl, A. W. Maue, and K. Westphal, *Handbuch der Physik*, vol. 25, pt. 1. Berlin: Springer-Verlag, 1961.
- [4] J. R. Mautz and R. F. Harrington, "A combined-source solution for radiation and scattering from a perfectly conducting body," *IEEE Trans. Antennas Propagat.*, vol. AP-27, pp. 445-454, July 1979.

Correction to "A Useful Approximation for the Flat Surface Impulse Response"

RONALD J. POGORZELSKI, SENIOR MEMBER, IEEE

The above work was erroneously included as a full paper. It should have appeared as a communication.

The author is Editor of IEEE TRANSACTIONS ON ANTENNAS AND PROPAGATION.

IEEE Log Number 8930281.

¹ G. S. Brown, *IEEE Trans. Antennas Propagat.*, vol. 37, no. 6, pp. 764-767, June 1989.

On the location of leaky wave poles for a grounded dielectric slab

by

Chung-I G. Hsu, Student Member IEEE

Roger F. Harrington, Fellow IEEE

Joseph R. Mautz, Senior Member IEEE

Tapan K. Sarkar, Senior Member IEEE

Abstract — A simple numerical procedure is implemented to find the loci of the TE and TM leaky wave poles for a grounded dielectric slab as the thickness is varied. The information of how these complex poles are distributed is very important when various deformed integration paths for Sommerfeld integrals are considered.

¹This work was supported by the Office of Naval Research, Arlington, VA 22217, under contract No. N00014-88-K-0027, and by the New York State Center for Advanced Technology in Computer Applications and Software Engineering (CASE), Syracuse University, Syracuse, NY 13244.

²The authors are with the Department of Electrical and Computer Engineering, Syracuse University, N. Y. 13244-1240.

1 Introduction

It is well known that the electromagnetic fields due to a dipole in a layered media in an open region can be expressed in terms of an improper integral [1] to account for the continuous spectra. In order to perform this integration accurately and efficiently, the integration path must be deformed off the real axis in some cases. Various deformed paths have been considered by many researchers, e.g., Newman and Forrai [2], Michalski and Zheng [3], Fang and Chew [4], and Sarkar [5], to name a few. For half-space problems, there are only two surface wave poles located on either Sheets I and IV or Sheets II and III of the Riemann surface [3, 6], depending on the constitutive parameters of the two media. For a grounded dielectric slab, besides a finite number of surface wave poles, there are an infinite number of leaky wave poles [7-9]. If the branch cut is properly chosen [3, 7, 9], then all the surface wave poles are located on the top sheet (proper sheet or Sheet I), whereas all the leaky wave poles are located on the bottom sheet (improper sheet or Sheet II) of the Riemann surface. The locations of the leaky wave poles are immaterial if the integration path stays on Sheet I. In order to improve the computational efficiency, deforming the path to Sheet II is desirable in some cases, e.g., the steepest descent method of integration for far fields, where part of the path enters Sheet II [9, 10, 13]. In this case, precise information on how these leaky wave poles are distributed is very important unless the residues of these leaky wave poles are negligible. Some researchers [10, 11], when applying the steepest descent method of integration, or its approximate version the so called saddle point method, only take into account surface wave poles. Their results are correct if the dielectric slab is thin and if the observation point is not too close to the interface, which is shown in next section. However, when the thickness of the slab is moderate, or when the observation point is close to the interface, some of the leaky wave poles, not too far away from the

saddle point, may have been captured.

The locations of the TE and TM leaky wave poles can be found by solving for the roots of two simultaneous transcendental equations [7, 9], which are then mapped to the complex plane of the integration variable. Although standard root searching routines could be applied, we gain no idea how these roots are distributed on the complex plane, since there are infinite number of them. It is the purpose of this short communication to show a simple numerical procedure of finding the loci of the leaky wave poles as the thickness is varied, which in turn gives us the desired information.

2 Root Loci

For simplicity, we assume that the grounded dielectric slab is non-magnetic and lossless. The constitutive parameters for the half space and the slab are (μ_o, ϵ_o) and $(\mu_o, \epsilon_o \epsilon_r)$, respectively. The thickness of the slab is d . The locations of the surface and leaky wave poles are the roots of [9, 10, 12],

$$D_{\text{TE}} = j\sqrt{1 - \xi^2} + \sqrt{\epsilon_r - \xi^2} \cot(\sqrt{\epsilon_r - \xi^2} k_o d) \quad (1)$$

for the TE case, and

$$D_{\text{TM}} = j\epsilon_r \sqrt{1 - \xi^2} - \sqrt{\epsilon_r - \xi^2} \tan(\sqrt{\epsilon_r - \xi^2} k_o d) \quad (2)$$

for the TM case. Here ξ is the normalized parameter such that $k_p = \xi k_o$ is the transverse wave number or integration variable for the Sommerfeld integral in terms of a transmission line representation in the z direction [9, 10], where z is perpendicular to the interface. For convenience, the branch cut is chosen to be the line such that $\text{Im}\{\sqrt{1 - \xi^2}\} = 0$ [3, 9, 10, 13], as shown in Fig. 1. When this branch cut is chosen, the roots of (1) and (2) on Sheets I and II of complex ξ plane

are the surface wave and leaky wave poles, respectively. It is well known that the surface wave poles are real and confined in the region $(1, \sqrt{\epsilon_r})$, and the number of them is finite [10, 12]. Furthermore, it can be shown that the leaky wave poles assume both real and complex values, and the number of them is infinite [7, 9]. A simple graphical procedure [9, 12] can be employed to find the real roots of (1) and (2), as shown in Figures 2(a) and 2(b), respectively. In these two figures,

$$X = k_0 d \sqrt{\epsilon_r - \xi^2} \quad \text{and} \quad B = k_0 d \sqrt{\epsilon_r - 1}. \quad (3)$$

The intersecting points on the upper and the lower parts are related to the surface and leaky wave poles on the $\text{Re}(\xi)$ axis, respectively.

There is only one pole associated with curve (1) in Fig. 2(a). It is a surface wave pole if $B > \pi/2$, a leaky wave pole in the regions $1 < \xi < \sqrt{\epsilon_r}$ and $\sqrt{\epsilon_r} < \xi < \infty$ if $1 < B < \pi/2$ and $B < 1$, respectively [7], [9]. Likewise, the pole associated with curve (1) in Fig. 2(b) is always a surface wave pole. Clearly, there are two poles associated with the rest of the curves in both figures. As an illustration, let curve (2) in Fig. 2(a) be examined. If $B > 3\pi/2$, the semi-circle intersects with curve (2) at two points, one for the surface wave pole and the other for the leaky wave pole. As B is reduced and becomes smaller than $3\pi/2$, the surface wave pole falls down to Sheet II from Sheet I through $\xi = 1$, which is the branch point. It then becomes a leaky wave pole and moves toward the right, whereas the original leaky wave poles stays on the same sheet and moves toward the left. As B reaches a value B_0 , such that the semi-circle is tangent to curve (2), these two leaky wave poles merge into one. If we reduce B further, then the semi-circle does not intersect with curve (1) any more, and the poles move symmetrically off the $\text{Re}(\xi)$ axis on Sheet II. It is understood that the poles move smoothly as B is varied. Based on the above observation, the numerical procedure of finding the locus of the leaky wave poles in the ξ plane associated with each curve in Figures 2(a) and 2(b) is as follows.

1. Find B_0 and the corresponding ξ , called ξ_0 . Since ξ_0 is real, this step is straight forward.
2. Search for a new root ξ_1 for the parameter $B_1 = B_0 - \Delta B$ with $\xi_0 - j\delta$ as the initial searching point, where both ΔB and δ are small positive numbers.
3. Search for new roots ξ_{n+1} for the parameters $B_{n+1} = B_n - \Delta B_n$, $n = 1, 2, 3, \dots$, with ξ_n as the initial searching points.

If the ΔB_n are reasonably small, a few iterations of steps 2 and 3 give satisfactory results using a Newton-Raphson algorithm. The same procedure can be repeated to generate the locus associated with each curve in Figures 2(a) and 2(b). Since when ξ is a root of (1) or (2), then $-\xi$ and $\pm\xi^*$ are also roots, we only show the loci in the fourth quadrant (these are the leaky wave poles that matter for a time dependence $e^{j\omega t}$). Figures 3 to 6 show the loci of the leaky wave poles for $\epsilon_r = 4$ and 9, respectively. Careful scrutiny of these figures reveals that the TM poles approach the real axis faster than do the TE poles as B increases from zero. Furthermore, for both the TE and TM cases, the pole associated with the lower numbered curve in Figures 2(a) and 2(b) approach the real axis faster than that associated with the higher numbered curve. This explains why only the lower ordered leaky poles are important for a thin slab when steepest descent path is adopted. A comparison of Fig. 1, which shows steepest decent paths for various observation angles, with Figures 3 to 6 demonstrates that many leaky wave poles can be captured by the deformation, depending on the observation angle and physical parameters of the slab. The residues of the leaky wave poles are highly attenuated in the far field as claimed by Fang and Chow [4]. In fact, they completely ignored the residues of the leaky poles for separation distance $k_0 r > 2\pi$ and observation angle $\theta = \pi/2$, i.e., on the interface. However, it is clear from [14] that for some values of the dielectric constant and height, the closeness of

the leaky wave poles to the steepest descent path still has to be taken into account even for $k_0 r = 100$ and $0 < \theta < \pi/2$. Although the physical parameters employed in [4] and [14] are different, our purpose is to emphasize that care must be taken when ignoring the residues of the leaky waves poles. Moreover, without knowing the locations or the loci of the leaky wave poles, this cannot be done satisfactorily.

3 Concluding Remarks

A simple numerical procedure for finding the loci of TE and TM leaky wave poles as the thickness of the slab is varied is presented. These loci provide important information when the integration path of the Sommerfeld integral for grounded dielectric slab problem is deformed into the "improper" sheet of the Riemann surface. The accuracy of the loci has been checked extensively against contour plots for expressions (1) and (2) with the B 's as parameters.

4 Acknowledgement

The authors would like to thank Dr. D. Zheng at Texas A&M University for valuable discussions.

References

- [1] L. B. Felsen and N. Marcuvitz, *Radiation and Scattering of Waves*. Englewood Cliffs, N.J.: Prentice Hall, 1973.
- [2] E. H. Newman and D. Forrai, "Scattering from a microstrip patch," *IEEE Trans. Antennas Propagat.*, vol. AP-35, pp. 245-251, Mar. 1987.
- [3] K. Michalski and D. Zheng, "Modeling antennas and scatterers of arbitrary shape embedded in layered dielectric media," Technical Report, Dept. Elec. Eng., Texas A&M University, Nov. 1989.
- [4] D. G. Fang and Y. L. Chow, "The Green's function along the microstrip substrate from a horizontal magnetic dipole," *J. Appl. Phys.*, vol. 54, pp. 33-38, Jan., 1983.
- [5] T. K. Sarkar, "Analysis of arbitrarily oriented thin wire antennas over a plane imperfect ground," *Arch. Elek. Übertragung.*, vol. 31, pp. 449-457, 1977.
- [6] A. Banõs, *Dipole Radiation in the presence of a Conducting Half-Space*. New York: Pergamon Press, 1966.
- [7] S. Barkeshli, "Efficient Approaches for Evaluating the Planar Microstrip Green's Function and its Applications to the Analysis of Microstrip Antennas," Ph.D. dissertation, Dept. Elec. Eng., Ohio State Univ., 1988.
- [8] M. Marin, S. Barkeshli, and P. H. Pathak, "On the location of proper and improper surface wave poles for the grounded dielectric slab," *IEEE Trans. Antennas Propagat.*, vol. 38, pp. 570-573, Apr. 1990.
- [9] R. E. Collin, *Field Theory of Guided Waves*. New York: McGraw-Hill, 1960.

- [10] J. R. Mosig and F. E. Gardiol, "A dynamical radiation model for microstrip structures," in *Advances in Electronics and Electron Physics*, vol. 59, pp. 139-237. New York: Academic Press, 1982.
- [11] G. N. Tsandoulas, "Excitation of a grounded dielectric slab by a horizontal dipole," *IEEE Trans. Antennas Propagat.*, vol. AP-17, pp. 156-161, Mar., 1969.
- [12] R. F. Harrington, *Time-Harmonic Electromagnetic Fields*. New York: McGraw-Hill, 1961.
- [13] T. Tamir and A. A. Oliner, "Guided complex waves, Part 1" *Proc. IEE*, vol. 110, pp. 310-324, Feb, 1963.
- [14] G. D. Bernard and A. Ishimaru, "On complex waves," *Proc. IEE*, vol. 114, pp. 43-49, Jan, 1967.

Figure captions

Fig. 1. Steepest descent paths in the complex ξ plane for different observation angles, where the solid line is on the top sheet, the dotted line is on the bottom sheet, and the zigzag line is the branch cut.

Fig. 2. Graphic solution for the TE and TM surface and leaky wave modes.

Fig. 3. Loci of the TE leaky wave poles in the complex ξ plane, $\epsilon_r = 4$.

Fig. 4. Loci of the TM leaky wave poles in the complex ξ plane, $\epsilon_r = 4$.

Fig. 5. Loci of the TE leaky wave poles in the complex ξ plane, $\epsilon_r = 9$.

Fig. 6. Loci of the TM leaky wave poles in the complex ξ plane, $\epsilon_r = 9$.

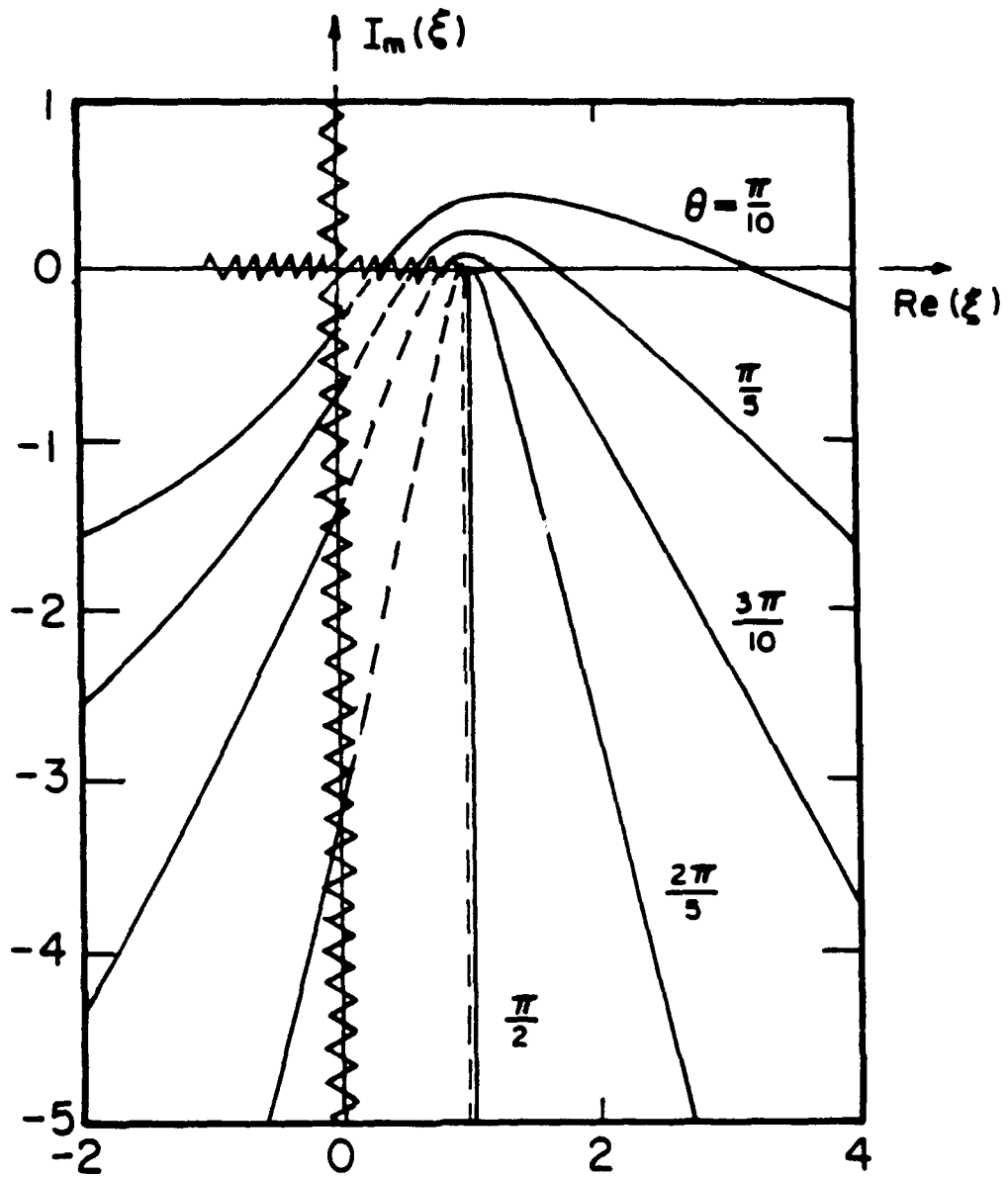
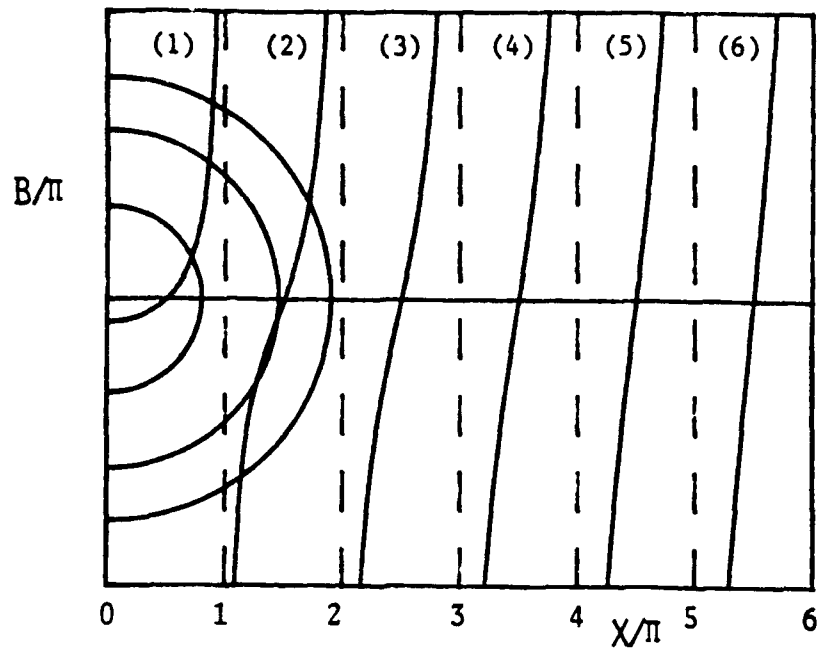
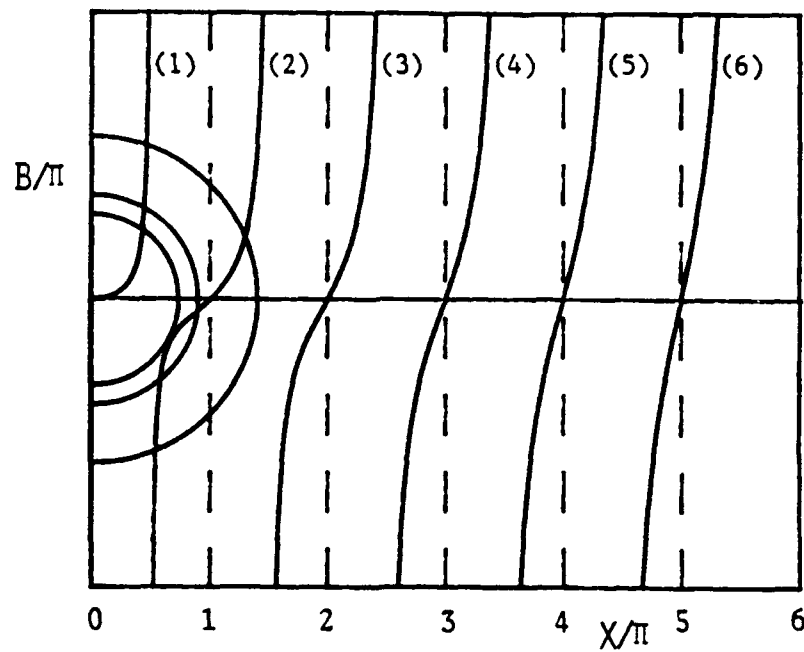


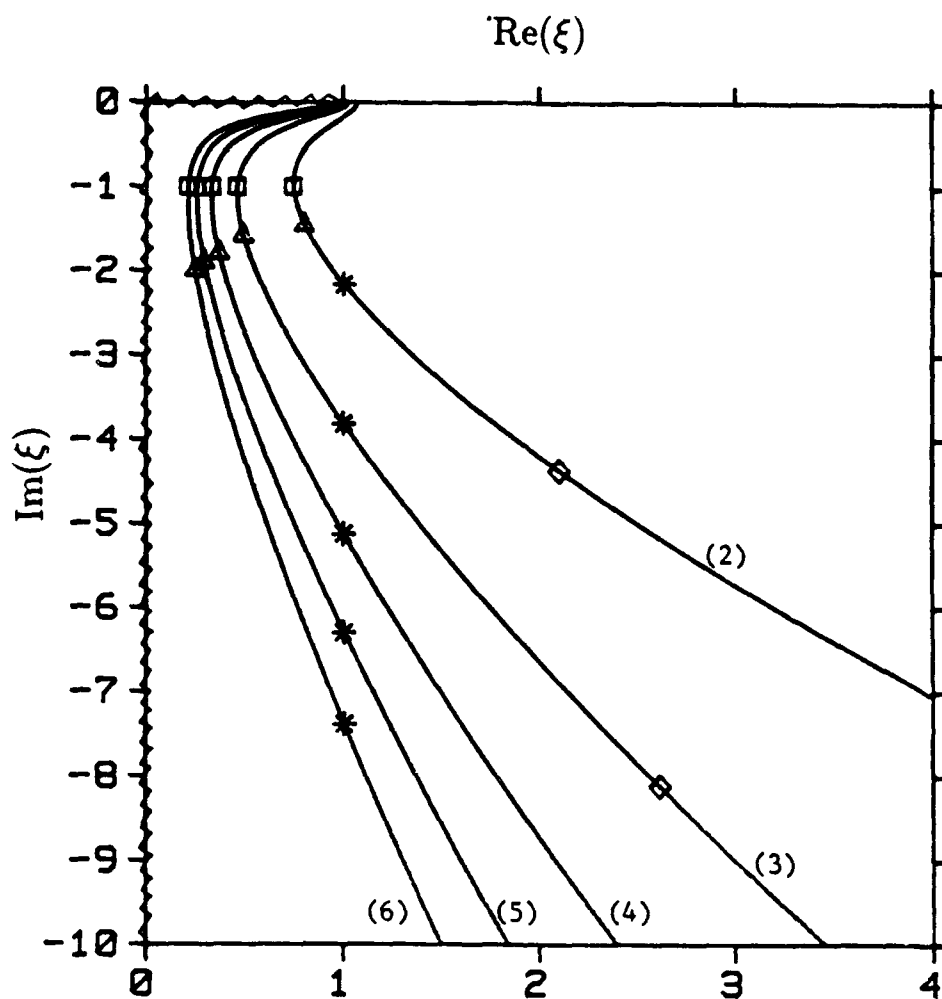
FIG. 1



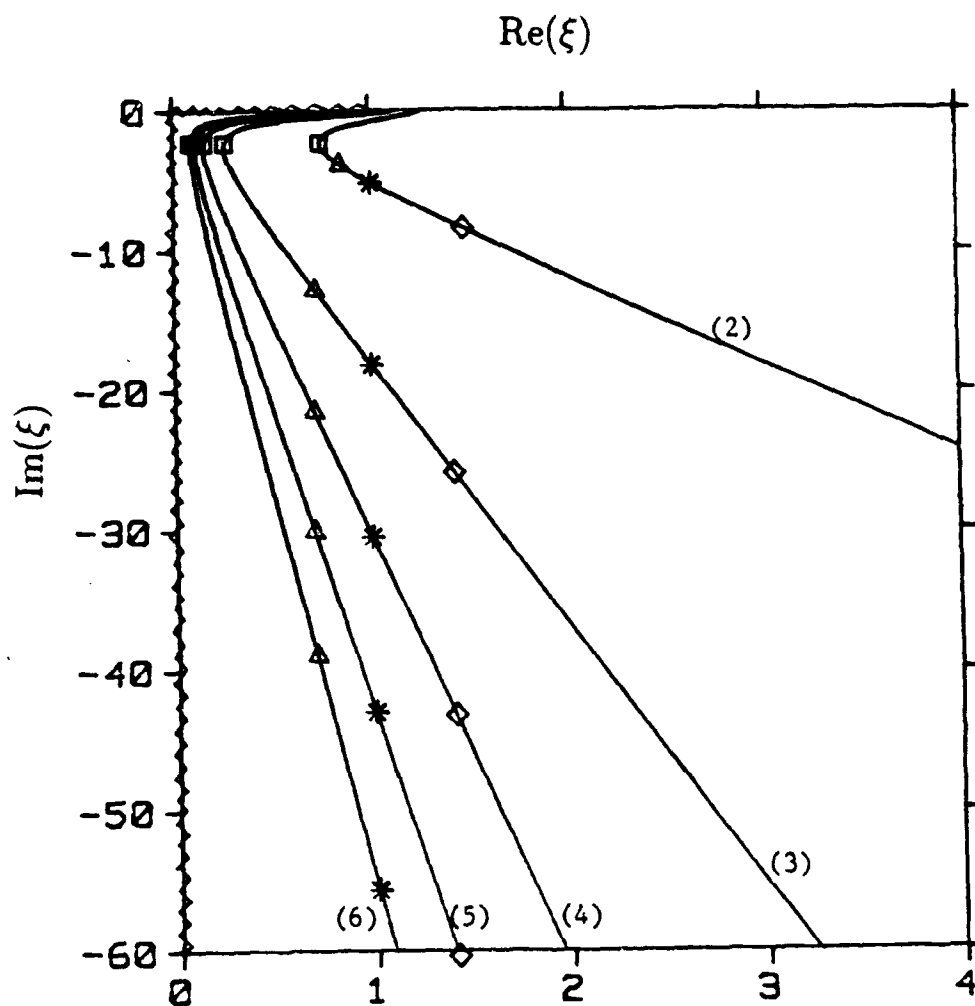
(a) TE, $\sqrt{B^2 - X^2} = -X \cot X$



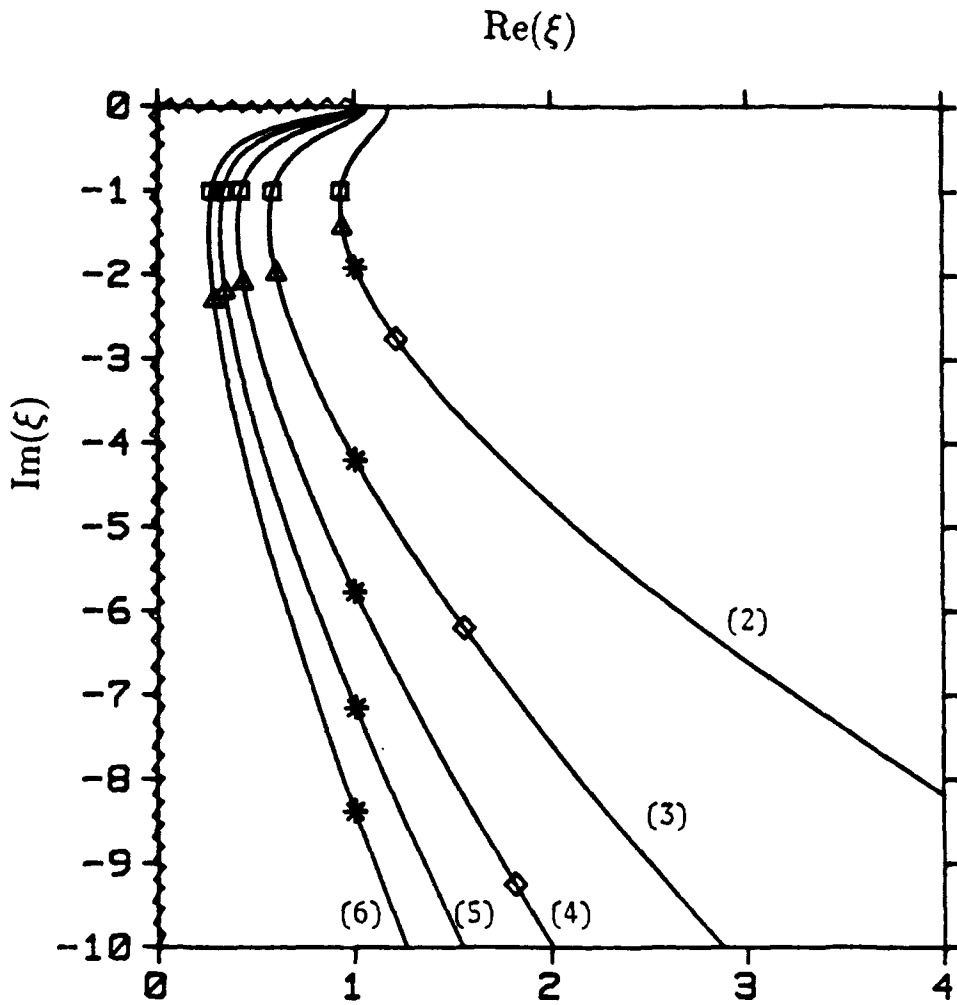
(b) TM, $\sqrt{B^2 - X^2} = \frac{X}{\epsilon_r} \tan X$



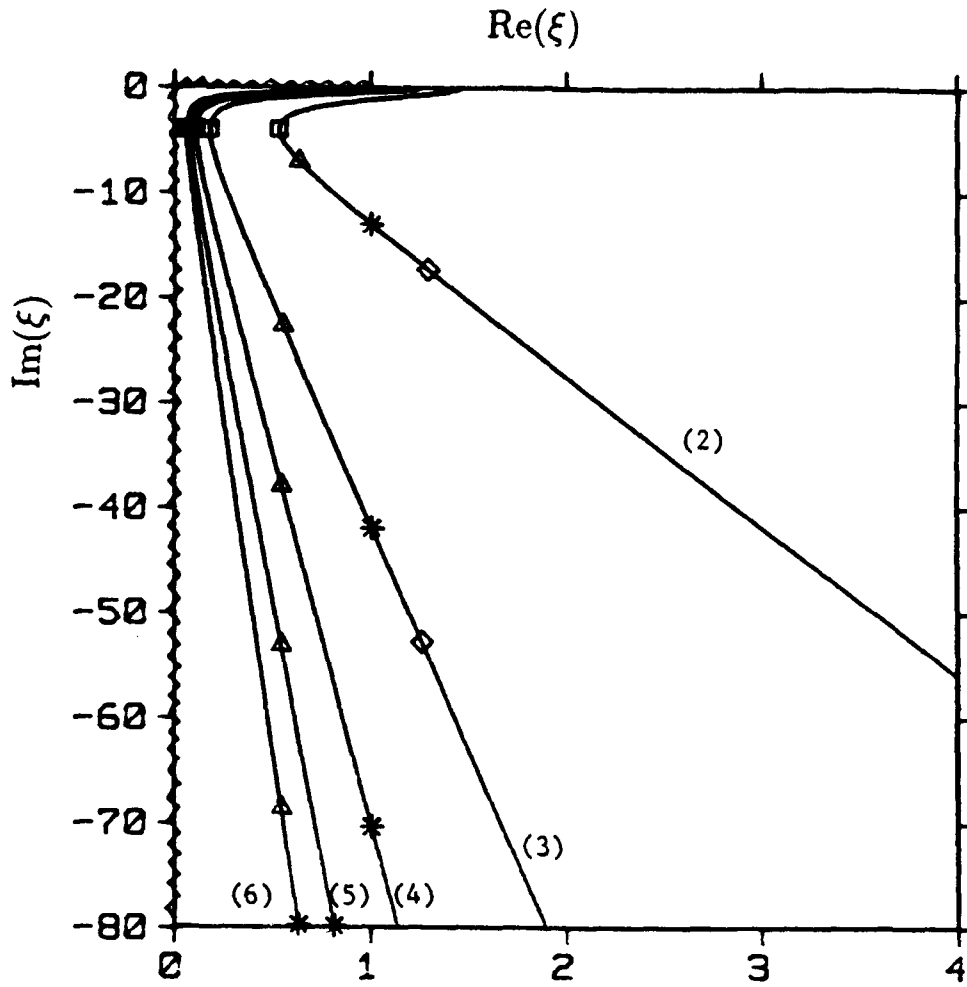
B/π	(2)	(3)	(4)	(5)	(6)
□	1.1484	1.9309	2.7060	3.4798	4.2553
Δ	1.0202	1.6768	2.2394	2.8111	3.3562
*	0.8425	0.9794	1.0848	1.1671	1.2354
◇	0.5003	0.4990	—	—	—



B/π	(2)	(3)	(4)	(5)	(6)
□	0.2954	0.8623	1.4343	2.0072	2.5856
△	0.2013	0.2003	0.2004	0.2011	0.2002
*	0.1578	0.1421	0.1417	0.1409	0.1400
◇	0.1001	0.1001	0.1001	0.1004	—



B/π	(2)	(3)	(4)	(5)	(6)
□	1.3261	2.2285	3.1282	4.0230	4.9142
△	1.2473	1.9433	2.6882	3.4058	4.9075
*	1.1576	1.3421	1.5031	1.6272	1.7365
◇	1.0000	1.0011	1.0021	—	—



B/π	(2)	(3)	(4)	(5)	(6)
□	0.2860	0.8547	1.4239	1.9939	2.5609
△	0.1856	0.1851	0.1855	0.1859	0.1853
*	0.1053	0.1006	0.1003	0.1240	0.1596
◇	0.0801	0.0801	—	—	—

SYRU/DECE/TR89/10

**FUNDAMENTAL MODE DISPERSION OF
A MICROSTRIP TRANSMISSION LINE**

Report TR-89-10

by

**Chung-I G. Hsu
Roger F. Harrington
Joseph R. Mautz
Ing-Chieh Jan**

November 1989

Department of
Electrical and Computer Engineering
Syracuse University
Syracuse, New York 13244-1240

Fundamental mode dispersion of a microstrip transmission line

Abstract — A spectral domain type solution with nonuniform subdomain basis function is implemented to investigate the dispersion characteristics of the fundamental mode of a microstrip transmission line. Agreement with the data available in the literature is demonstrated in several plots, where only the longitudinal current is used in numerical computation. This numerical scheme proves to be an alternative, or rather a supplement, to various well-developed methods in this area.

TABLE OF CONTENTS

	Page
1. INTRODUCTION	1
2. BASIC FORMULATION	1
3. NUMERICAL PROCEDURES	5
4. NUMERICAL RESULTS	10
5. CONCLUDING REMARKS	11
BIBLIOGRAPHY	12

1 Introduction

The dispersion characteristics of an open microstrip line have been an active research topic over the past two decades. Various methods and numerical results have been reported [1]–[12]. Although these methods appeared rigorous, some discrepancies among their results were noticed by Kuester and Chang [6] in 1979. Since then, the accuracies have been improved a lot. However, the spectral domain solutions are all employed with entire domain expansion functions [1], [2], [8], [12], whereas the space domain solutions are associated with subdomain expansion functions [5], [10], [11]. In this report, a spectral domain solution using nonuniform subdomain basis function is implemented to investigate the dispersion characteristics of the fundamental mode of a microstrip line. Agreement with the existing data in the literature is demonstrated in several plots, where we have used only the longitudinal current in numerical computation. This numerical scheme proves to be an alternative, or rather a supplement, to various well developed methods in this area.

2 Basic formulation

The microstrip line under consideration is shown in Fig. 1. The conductor sitting on the air–dielectric interface is assumed to be of zero thickness, and the structure is assumed lossless. The ground plane and the dielectric slab are of infinite extent in the x and the y direction, whereas the strip extends from $-\infty$ to ∞ in the y direction. The parameters of interest are the phase constant and the current densities on the strip. For simplicity, we only consider the fundamental mode, which is the lowest order mode propagating unattenuated in the z direction. The problem is basically a two dimensional one. A phase factor $e^{-j\beta y}$, where β is

between the wave numbers of the air and the dielectric, is common to all the field and current distributions, and is the only factor depending on the y coordinate. Hence,

$$f(x, y, z) = f(x, z)e^{-j\beta y} \quad (1)$$

follows through the entire analysis.

To account for the continuous spectrum of the open structure, we express the field and the current in terms of the improper integral [13, Ch. 4]

$$f(x, z) = \frac{1}{2\pi} \int_{-\infty}^{\infty} \tilde{f}(\xi, z) e^{-j\xi x} d\xi \quad (2)$$

which is identified as an inverse Fourier Transform. Thus, the Fourier transform of f , denoted by \tilde{f} , is obviously defined as

$$\tilde{f}(\xi, z) = \int_{-\infty}^{\infty} f(x, z) e^{j\xi x} dx \quad (3)$$

It is known that the fields can be decomposed into TE and TM components with respect to any direction [13, ch. 3]. The most natural choice for our problem is the direction perpendicular to the dielectric interface, i.e., the z direction. The z components of the magnetic and electric vector potentials, i.e., $A(x, y, z)$ and $F(x, y, z)$, which give rise to TM to z and TE to z fields, respectively, can be expressed by

$$A(x, y, z) = \begin{cases} e^{-j\beta y} \int_{-\infty}^{\infty} B_1 e^{-j\alpha_1(z-d)} e^{-j\xi x} d\xi, & d \leq z \\ e^{-j\beta y} \int_{-\infty}^{\infty} B_2 \frac{\cos \alpha_2 z}{\sin \alpha_2 d} e^{-j\xi x} d\xi, & 0 \leq z \leq d \end{cases} \quad (4)$$

$$F(x, y, z) = \begin{cases} e^{-j\beta y} \int_{-\infty}^{\infty} D_1 e^{-j\alpha_1(z-d)} e^{-j\xi x} d\xi, & d \leq z \\ e^{-j\beta y} \int_{-\infty}^{\infty} D_2 \frac{\sin \alpha_2 z}{\sin \alpha_2 d} e^{-j\xi x} d\xi, & 0 \leq z \leq d \end{cases} \quad (5)$$

where

$$\begin{aligned}\xi^2 + \beta^2 + \alpha_1^2 &= \omega^2 \mu_o \epsilon_o \\ \xi^2 + \beta^2 + \alpha_2^2 &= \omega^2 \mu_o \epsilon_o \epsilon_r\end{aligned}\quad (6)$$

are the dispersion relations. In (4) and (5), B_1, B_2, D_1 and D_2 are unknown functions of ξ that can be determined, if desired. Furthermore, to have field which decays from the dielectric and satisfies the radiation condition, we require that

$$\text{Re}(\alpha_1) \geq 0 \quad \text{and} \quad \text{Im}(\alpha_1) < 0 \quad (7)$$

The electric Dyadic Green's function in spectral domain, evaluated at the dielectric interface, has been found by many authors, e.g., Farrar [5], Faché [10], and Itoh [7], to name a few. In spectral domain, we have [7]

$$\begin{bmatrix} \tilde{Z}_{yy}(\xi, d) & \tilde{Z}_{yx}(\xi, d) \\ \tilde{Z}_{xy}(\xi, d) & \tilde{Z}_{xx}(\xi, d) \end{bmatrix} \begin{bmatrix} \tilde{J}_y(\xi, d) \\ \tilde{J}_x(\xi, d) \end{bmatrix} = \begin{bmatrix} \tilde{E}_y(\xi, d) \\ \tilde{E}_x(\xi, d) \end{bmatrix} \quad (8)$$

where

$$\tilde{Z}_{yy}(\xi, d) = \frac{1}{\omega \epsilon_o} \frac{\beta^2}{\xi^2 + \beta^2} \frac{\alpha_1 \alpha_2}{D_m} + \omega \mu_o \frac{\xi^2}{\xi^2 + \beta^2} \frac{1}{D_e} \quad (9)$$

$$\tilde{Z}_{yx}(\xi, d) = \tilde{Z}_{xy}(\xi, d) = \frac{\xi \beta}{\xi^2 + \beta^2} \left[\frac{1}{\omega \epsilon_o} \frac{\alpha_1 \alpha_2}{D_m} - \omega \mu_o \frac{1}{D_e} \right] \quad (10)$$

$$\tilde{Z}_{xx}(\xi, d) = \frac{1}{\omega \epsilon_o} \frac{\xi^2}{\xi^2 + \beta^2} \frac{\alpha_1 \alpha_2}{D_m} + \omega \mu_o \frac{\beta^2}{\xi^2 + \beta^2} \frac{1}{D_e} \quad (11)$$

are the spectral impedance functions evaluated at the interface. In equations (9) - (11),

$$D_m = \alpha_2 - j \epsilon_r \alpha_1 \cot \alpha_2 d \quad (12)$$

$$D_e = \alpha_1 - j \alpha_2 \cot \alpha_2 d \quad (13)$$

The spatial counterparts of the spectral currents $\tilde{J}_y(\xi, d)$ and $\tilde{J}_x(\xi, d)$, can be expressed as

$$J_y(x) = \sum_n a_n J_{yn}(x) \quad (14)$$

and

$$J_x(x) = \sum_n b_n J_{xn}(x) \quad (15)$$

respectively, where a_n and b_n are unknown coefficients. Using the method of moment [14], we enforce the boundary condition

$$\underline{E}_t = 0, \quad \text{on strip} \quad (16)$$

by taking the inner product of the tangential electric field at the interface, obtained from the inverse Fourier transform of (8), with J_{ym} and J_{xm} for all m . Doing so, we obtain the homogeneous matrix equation

$$\begin{bmatrix} [M_{mn}^{yy}] & [M_{mn}^{yx}] \\ [M_{mn}^{xy}] & [M_{mn}^{xx}] \end{bmatrix} \begin{bmatrix} [a_n] \\ [b_n] \end{bmatrix} = \begin{bmatrix} [0] \\ [0] \end{bmatrix} \quad (17)$$

The eigenvalues could be found by searching the β 's such that the determinant of the matrix in (17) is zero.

By virtue of Parsavel's theorem

$$\int_{-\infty}^{\infty} f(x)g^*(x)dx = \frac{1}{2\pi} \int_{-\infty}^{\infty} \tilde{f}(\xi)\tilde{g}^*(\xi)d\xi \quad (18)$$

each element of the matrix in (17) reads

$$M_{mn}^{pq} = \frac{1}{2\pi} \int_{-\infty}^{\infty} \tilde{J}_{pm}^* \tilde{Z}_{pq}(\xi, d) \tilde{J}_{qn} d\xi, \quad p, q = y, x \quad (19)$$

Notice that some authors [4], [8] have neglected the conjugate sign in (19). That is because the eigenvalues remain the same if either even or odd entire domain basis functions are chosen.

3 Numerical Procedure

3.1 Integration path

Equation (19) is an improper integral, whose integrand contains α_1 and α_2 , both being double-valued functions. Since the integrands for $p, q = y, x$ are all even functions of α_2 , only α_1 introduces the branch points and the branch cuts to the ξ plane. For bound mode in lossless structure, the branch points are always on the imaginary axis of the ξ plane. Fig. 2 shows the branch points and branch cuts chosen by Kowalski [2], Fache [10] and Zheng [11].

Since

$$D_m = \begin{cases} \sqrt{\epsilon_r k_o^2 - \beta^2 - \xi^2} - \epsilon_r \sqrt{\beta^2 + \xi^2 - k_o^2} \cot(\sqrt{\epsilon_r k_o^2 - \beta^2 - \xi^2} d), & k_o^2 < \beta^2 + \xi^2 < \epsilon_r k_o^2 \\ -j\sqrt{\beta^2 + \xi^2 - \epsilon_r k_o^2} - j\epsilon_r \sqrt{\beta^2 + \xi^2 - k_o^2} \coth(\sqrt{\beta^2 + \xi^2 - \epsilon_r k_o^2} d), & \epsilon_r k_o^2 < \xi^2 + \beta^2 \end{cases} \quad (20)$$

and

$$D_e = \begin{cases} -j\sqrt{\beta^2 + \xi^2 - k_o^2} - j\sqrt{\epsilon_r k_o^2 - \beta^2 - \xi^2} \cot(\sqrt{\epsilon_r k_o^2 - \beta^2 - \xi^2} d), & k_o^2 < \beta^2 + \xi^2 < \epsilon_r k_o^2 \\ -j\sqrt{\beta^2 + \xi^2 - k_o^2} - j\sqrt{\beta^2 + \xi^2 - \epsilon_r k_o^2} \coth(\sqrt{\beta^2 + \xi^2 - \epsilon_r k_o^2} d), & \epsilon_r k_o^2 < \xi^2 + \beta^2 \end{cases} \quad (21)$$

those roots of D_m and D_e , corresponding to the surface TM and TE waves of the grounded dielectric slab, respectively, must be in the interval $k_o^2 < \beta^2 + \xi^2 < \epsilon_r k_o^2$.

Letting [13], [15]

$$X = d\sqrt{\epsilon_r k_o^2 - \beta^2 + \xi^2} > 0 \quad (22)$$

$$\Delta = k_o d\sqrt{\epsilon_r - 1} > 0 \quad (23)$$

the roots of

$$\frac{X}{\epsilon_r} \tan X = (\Delta^2 - X^2)^{1/2} \quad (24)$$

and

$$-X \cot X = (\Delta^2 - X^2)^{1/2} \quad (25)$$

then correspond to those of D_m and D_e , respectively. It is seen from Fig. 3 and Fig. 4 that there will be at least one surface wave pole, which is TM_o , on the ξ plane, whereas the cut-off frequency for TE_1 mode is

$$f_c = \frac{c_o}{4d\sqrt{\epsilon_r - 1}} \quad (26)$$

To find the desired phase constant, we must try different β 's in (17). Since the phase constant of the fundamental bound mode is always larger than that of the TM_o surface wave [16], [17], the surface wave poles are understood to be on the imaginary axis of the ξ plane. The β 's can be restricted in the region between c^2 and the phase constant of the TM_o mode in the root searching process. Hence, we can keep the path of integration along the real axis. In general, if the higher order bound modes are investigated, and if the frequency is greater than the cutoff's of the other surface wave modes, there are some poles on the real ξ axis. In this case, the deformed path, as shown in Fig. 5, is proposed. A major advantage of deforming the contour off the real axis is that we do not have to search the surface wave poles. Slight inaccuracy in the locations of the poles on the real axis may result in large errors, if real axis integration is employed. Of course, the tradeoff is that the integrand becomes more complicated if we deform the path to the complex plane.

3.2 Expansion function

For a single microstrip structure, entire domain basis functions have proven to be efficient. However, in consideration of the extendibility to multiple strip structure, subdomain basis functions may be more suitable. Furthermore, to retrieve the edge condition of the current, non-uniform discretization of the strip is employed. The chosen basis functions are

$$J_{yn}(x) = \begin{cases} 1, & x_{n-1} < x < x_n \\ 0, & \text{otherwise} \end{cases} \quad (27)$$

$$J_{xn}(x) = \begin{cases} \frac{x - x_{n-1}}{x_n - x_{n-1}}, & x_{n-1} < x < x_n \\ \frac{x_{n+1} - x}{x_{n+1} - x_n}, & x_n < x < x_{n+1} \\ 0, & \text{otherwise} \end{cases} \quad (28)$$

Their Fourier transforms are

$$\tilde{J}_{yn}(\xi) = \frac{\sin(\xi\Delta_n/2)}{\xi/2} e^{j\xi x_{n-1/2}} \quad (29)$$

$$\tilde{J}_{xn}(\xi) = \frac{2j}{\xi^2} \left[\frac{\sin(\xi\Delta_n/2)}{\Delta_n} e^{j\xi x_{n-1/2}} - \frac{\sin(\xi\Delta_{n+1}/2)}{\Delta_{n+1}} e^{j\xi x_{n+1/2}} \right] \quad (30)$$

where $\Delta_n = x_n - x_{n-1}$ and $x_{n-1/2} = (x_{n-1} + x_n)/2$. Thus

$$M_{mn}^{yy} = M_{nm}^{yy} = \frac{4}{\pi} \int_0^\infty \tilde{Z}_{yy} \frac{F(m,n)}{\xi^2} d\xi \quad (31)$$

$$M_{mn}^{yx} = -M_{nm}^{xy} = \frac{4j}{\pi} \int_0^\infty \tilde{Z}_{yx} \frac{1}{\xi^3} \cdot \left[\frac{F(m,n)}{\Delta_n} - \frac{F(m,n+1)}{\Delta_{n+1}} \right] d\xi \quad (32)$$

$$M_{mn}^{xx} = M_{nm}^{xx} = \frac{4j}{\pi} \int_0^{\infty} \tilde{Z}_{xx} \frac{1}{\xi^4} \cdot \left[\frac{F(m, n)}{\Delta_m \Delta_n} - \frac{F(m+1, n)}{\Delta_{m+1} \Delta_n} - \frac{F(m, n+1)}{\Delta_m \Delta_{n+1}} + \frac{F(m+1, n+1)}{\Delta_{m+1} \Delta_{n+1}} \right] d\xi \quad (33)$$

where

$$F(m, n) = \sin\left(\frac{\xi x_{m-1/2}}{2}\right) \sin\left(\frac{\xi x_{n-1/2}}{2}\right) \cos[(x_{m-1/2} - x_{n-1/2})\xi] \quad (34)$$

3.3 Computations of matrix elements

It is clear that the efficiency and the accuracy are based upon how each matrix element, in terms of the improper integral, is evaluated. The improper integral is a function of frequency, dielectric constant, width and height of the slab, width and location of the subsegment, and β used in the computation. The behavior of the integrand is very different from one set of parameters to another. Hence, care must be exercised in performing the integrals.

Close scrutiny shows that all the integrands are of the order $O(1/\xi^3)$ as $\xi \rightarrow \infty$. At $\xi = 0$, the integrands are of finite values. As discussed in the previous subsection, if β is restricted to be larger than the phase constant of the TM_0 mode of the grounded dielectric slab, then there is no singularity on the real axis of the ξ plane. Hence, the convergence of the integrals is guaranteed, as the physics of the system should be.

Due to nonuniform discretization of the strip, $\Delta_m \neq \Delta_n$, in general. The oscillatory terms $F(m, n)$, which is a product of three sinusoidal functions with different periods, may behave quite irregular. The integration thus become quite difficult. As a remedy, we decompose $[0, \infty]$ into $[0, L]$ and $[L, \infty]$, where L is less than the first zero of $F(m, n)$. The integrand over $[L, \infty]$ is further decomposed

according to the identity

$$\begin{aligned} \sin A \cdot \sin B \cdot \cos C &= \frac{1}{4} [\cos (A - B - C) \\ &+ \cos (A - B + C) - \cos (A + B - C) - \cos (A + B + C)] \end{aligned} \quad (35)$$

Each integrand now contains only one sinusoidal function, where its zeros are periodic. Therefore, it is easier to perform the integration. As an example, for each M_{mn}^{vy} , we have to perform 4 integrals of the form

$$\int_L^\infty \tilde{Z}_{yy}(\xi) \cos\left(\frac{2\pi}{q}\xi\right) d\xi \quad (36)$$

where q is the period determined by (35). We can separate the above integral over $[L, \infty]$ into two parts, over $[L, U]$ and $[U, \infty]$, where

$$U = \max \left[50k_o \sqrt{\epsilon_r}, \sqrt{\left(\frac{3.2\pi}{d}\right)^2 + \epsilon_r k_o^2 - \beta^2} \right] \quad (37)$$

Filon's algorithm [18] is applied to the integral over $[L, U]$. For the integrals over $[U, \infty]$, the asymptotic expression of $\tilde{Z}_{yy}(\xi)$ is substituted into the integrands, which makes the integrals proportional to

$$B(x) = \int_x^\infty \frac{\cos u}{u^3} du \quad (38)$$

The strategy for performing this integral depends on the value of x . If $x < 1$, then

$$B(x) = \frac{\cos x}{2x^2} - \frac{\sin x}{2x} - \frac{1}{2} C_i(x) \quad (39)$$

where $C_i(x)$ is the cosin integral defined by

$$C_i(x) = \int_x^\infty \frac{\cos u}{u} du = -\gamma - \ln x + \sum_{n=1}^{\infty} \frac{(-1)^{n+1} x^{2n}}{2n \cdot (2n)!} \quad (40)$$

where $\gamma = 0.5772$ is Euler's constant. If $1 \leq x < 30\pi$, then

$$C_i(x) = -\gamma - \ln x + \int_0^x \frac{1 - \cos u}{u} du \quad (41)$$

where the last integral is performed using Filon's algorithm. If $x \geq 30\pi$, then

$$B(x) = \frac{\sin x}{2x} \sum_{n=0}^{N_1} \frac{(-1)^n (2n)!}{x^{2n}} - \frac{\cos x}{2x} \sum_{n=0}^{N_2} \frac{(-1)^n (2n+1)!}{x^{2n+1}} \quad (42)$$

where N_1 and N_2 are such that $(2N_1+2)(2N_1+1) < x^2$ and $(2N_2+3)(2N_2+2) < x^2$ respectively. It is known that both series in (42) are asymptotic series which diverge as N_1 and N_2 approach infinity [19]. If x is very large, 3 or 4 may be more than appropriate for N_1 and N_2 . Furthermore, using Filon's algorithm for the integral over $[L, U]$, we need to divide $[L, U]$ into subintervals, over each the Gaussian-Legendre quadrature can be used. The number of subintervals needed is $M = [2(U-L)/q] + 1$. If M is greater than 30, the method of average [15] is suggested to perform the integral over $[L, \infty]$. Usually, M is likely to be large if frequency is high, or if the width of the strip is wide. However, the method of average is not implemented in our computer program.

4 Numerical results

A computer program with only the longitudinal current has been implemented to check the validity and the accuracy of the present numerical scheme. The symmetric property of the longitudinal current has been used. We restrict the numerical results to some typical configurations that can be found in the literature. In Figures 6 to 11, the effective dielectric constants for several structures are presented. In these figures, the solid lines represent our solutions using only 5 expansion functions, the long dashed line the solutions from entire domain expansion functions of the type of the Maxwellian charge distribution, and the short dashed lines the surface wave modes of the grounded dielectric slab. Furthermore, the square and triangle represent the results sampled from the literature. Attention could be paid

to Fig. 10, which structure has been tested by many researchers, and their discrepancies were detected by Kuester and Chang [6]. In Figures 6 and 7, the results from subdomain and entire domain expansion functions are almost identical, and are very close to those obtained by Getsinger [3], whose dispersion model is based on approximating the microstrip line as suitable waveguides. Although some deviations between our solutions and Getsinger's are observed in Figures 8 and 9, it does not necessarily imply that our solutions are less accurate. From Figures 10 and 11, it is clear that ~~the~~ subdomain basis function yields better results than ~~do~~ ~~the~~ entire domain basis function.

Figures 12 and 13 show the normalized longitudinal currents for $d = 3.048mm$, $w = 3.175mm$ and $\epsilon_r = 11.7$. In Fig. 12, the square and the triangle are the currents at the center at each subdomain for 5 and 10 expansion functions, respectively, whereas the solid line is for 20 expansion functions. In Fig. 13, the currents are computed for three different frequencies, 0.001 GHz, 2 GHz and 12 GHz, all with 10 expansion functions. Although the frequency vary quite a lot, the current profiles remain close to the Maxwellian charge distribution. Notice, we have used more expansion functions near the edge than near the center of the strip, in order to retrieve the edge condition.

5 Concluding remarks

We have shown that the numerical scheme based on spectral domain analysis with non-uniform subdomain expansion functions could be an alternative, or at least a supplement, to the existing methods. Although, we only investigate single-strip structures, this approach is suitable to asymmetric multiple-strip structures as well. To improve the accuracy, the transverse current component should not be

neglected. However, the improvement by incorporating the transverse current and the extension to multiple structure are warranted.

References

- [1] E. J. Delinger, "A frequency dependent solution for microstrip transmission lines," *IEEE Trans. Microwave Theory Tech.*, vol. MTT-19, pp. 30-39, Jan. 1971.
- [2] G. Kowalski and R. Prella, "Dispersion characteristics of single and coupled microstrips," *AEU*, pp. 276-280, 1972.
- [3] W. J. Getsinger, "Microstrip dispersion model," *IEEE Trans. Microwave Theory Tech.*, vol. MTT-21, Jan., 1973.
- [4] T. Itoh and R. Mittra, "Spectral domain approach for calculating the dispersion characteristics of microstrip lines," *IEEE Trans. Microwave Theory Tech.*, vol. MTT-21, pp. 496-499, July, 1973.
- [5] A. Farrar, *Fourier Integral Methods for Static and Dynamic problems in microstrip*, Dissertation, Syracuse University, 1975.
- [6] E. F. Kuester, D. C. Chang, "An appraisal of methods for computation of the dispersion characteristics of open microstrip," *IEEE Trans. Microwave Theory Tech.*, vol. MTT-27, pp. 691-694, July 1979.
- [7] T. Itoh, "Spectral domain immittance approach for dispersion characteristics of generalized printed transmission line," *IEEE Trans. Microwave Theory Tech.*, vol. MTT-28, pp. 733-736, July 1980.

- [8] M. Kobayashi and F. Ando, "Dispersion characteristics of open microstrip lines," *IEEE Trans. Microwave Theory Tech.*, vol. MTT-35, pp. 101-105, Feb. 1987.
- [9] C. Shin, R. B. Wu, S. K. Jeng and C. H. Chen, "A full-wave analysis of microstrip lines by variational conformal mapping techniques," *IEEE Trans. Microwave Theory Tech.*, vol. 36, pp. 576-581, Mar. 1988.
- [10] N. Faché and D. De Zutter, "Rigorous full-wave space-domain solution for dispersive microstrip lines," *IEEE Trans. Microwave Theory Tech.*, vol. 36, pp. 731-737, Apr. 1988.
- [11] D. Zheng, *Radiation, Scattering and guidance of electromagnetic fields by conducting objects of arbitrary shape in layered media*, Ph.D. dissertation, Dept. Elec. Eng., Univ. Mississippi, 1988.
- [12] K. Uchida, T. Noda and T. Matsunaga, "New type of spectral domain analysis of a microstrip line," *IEEE Trans. Microwave Theory Tech.*, vol. 37, pp. 947-952, June 1989.
- [13] R. F. Harrington, *Time-Harmonic Electromagnetic Fields*, McGraw Hill, 1961.
- [14] R. F. Harrington, *Field Computation by Moment Methods*, New York: Macmillan, 1968. Reprinted by Krieger Publishing Co., Melbourne, FL, 1982
- [15] J. R. Mosig and F. E. Gardiol, "A dynamical radiation model for microstrip structures," in *Advances in Electronics and Electron Physics*, vol. 59, pp. 139-237, New York: Academic Press, 1982.

- [16] H. Erment, "Guiding and radiation characteristics of planar waveguides," *IEE Microwave, Optics and Acoustics*, vol. 3, pp. 59-62, Mar. 1979.
- [17] A. A. Oliner and K. S. Lee, "The nature of the leakage from higher modes on microstrip line," *IEEE MTT-S Digest*, pp. 57-60, 1986.
- [18] L. N. G. Filon, "On a quadrature formula for trigonometric integrals," *Proc. R. Soc. Edinburgh*, vol. 49, pp. 38-47, 1928.
- [19] N. Bleistein and R. A. Handelsman, *Asymptotic Expansions of Integrals*, New York: Dover, 1975.

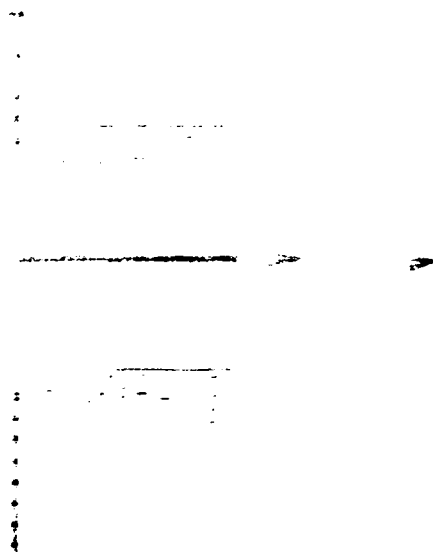
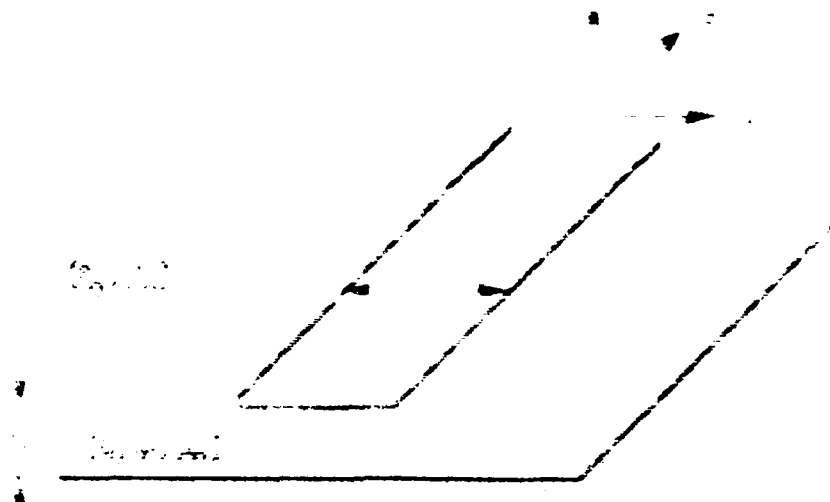
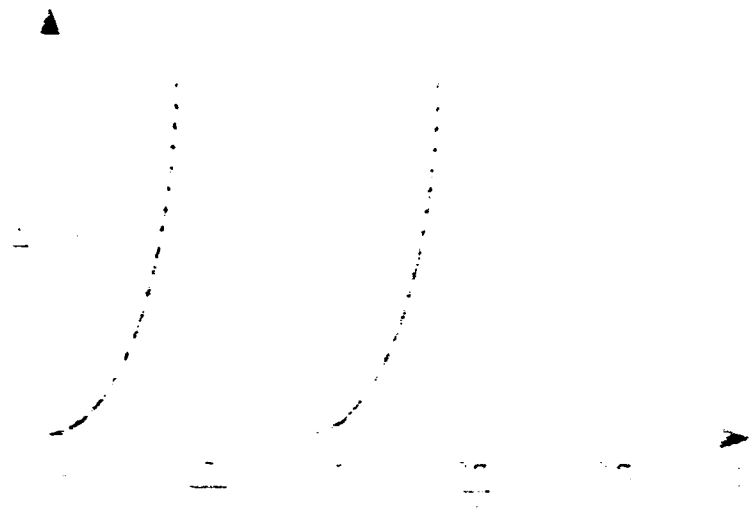
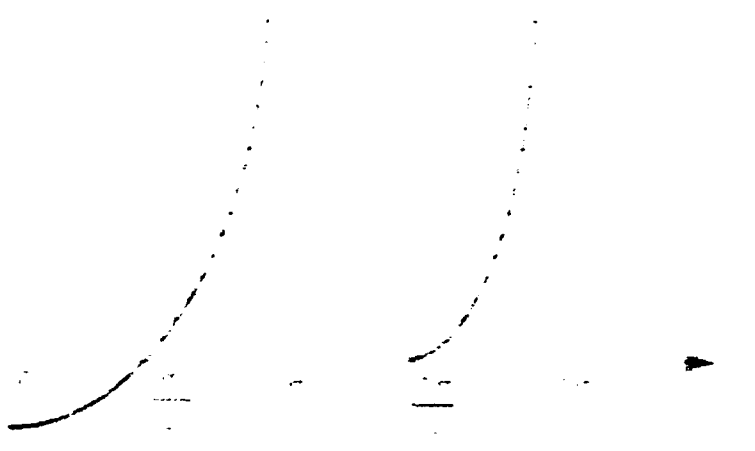


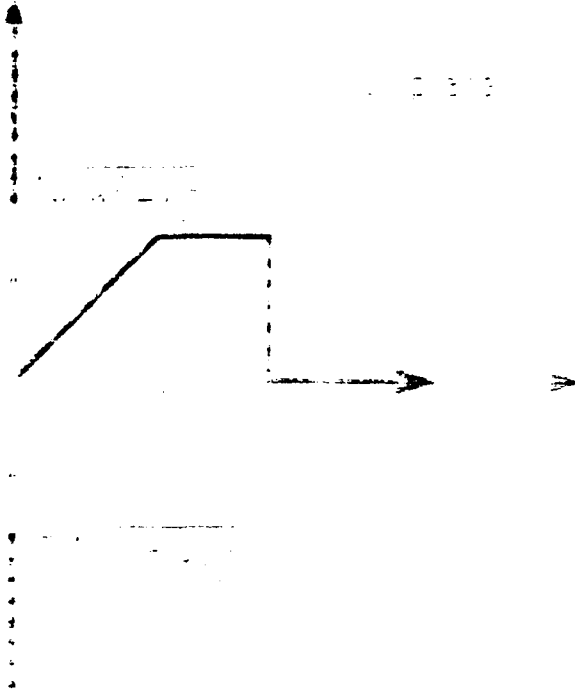
Fig. 1. Perspective view of a rectangular object.



$y = \frac{1}{x}$



$y = \frac{1}{x}$



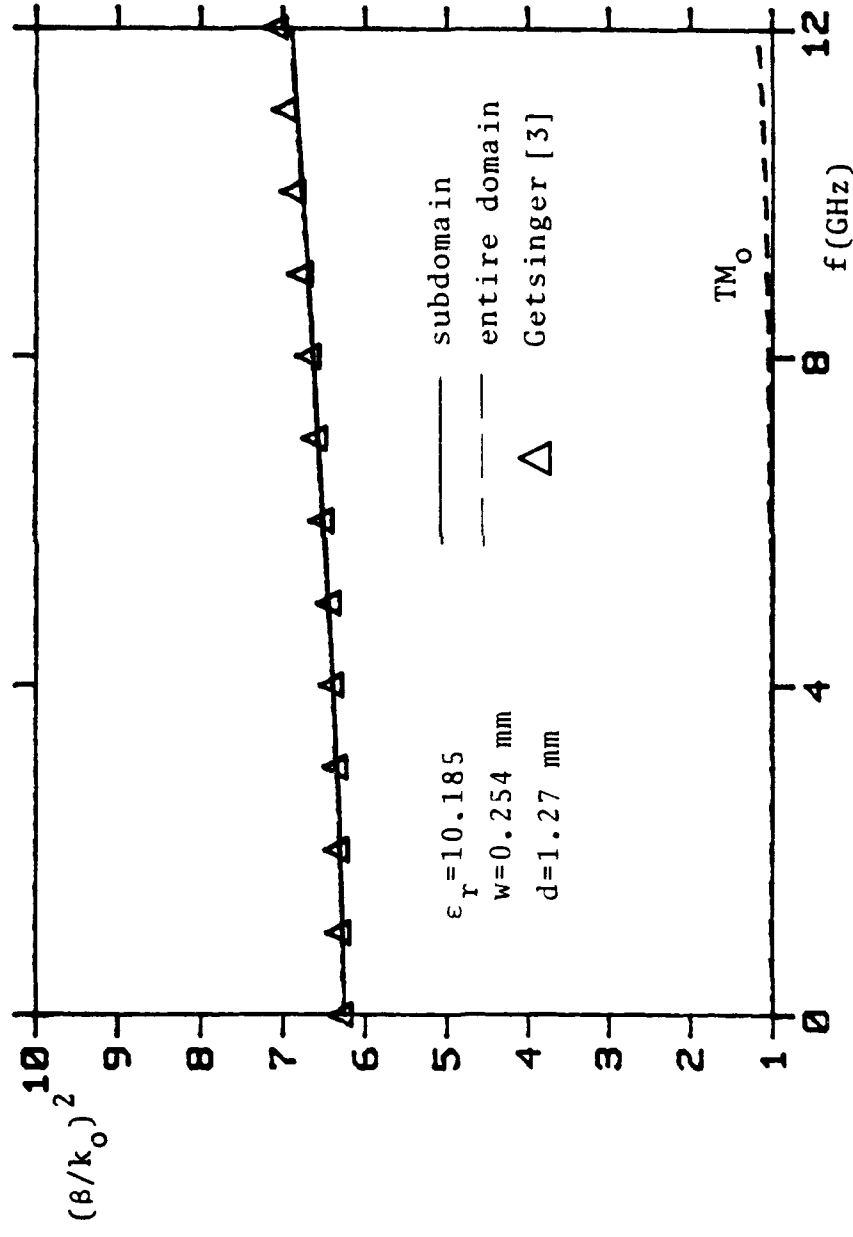


Fig. 6. Variation of the normalized phase constant of the fundamental mode versus frequency.

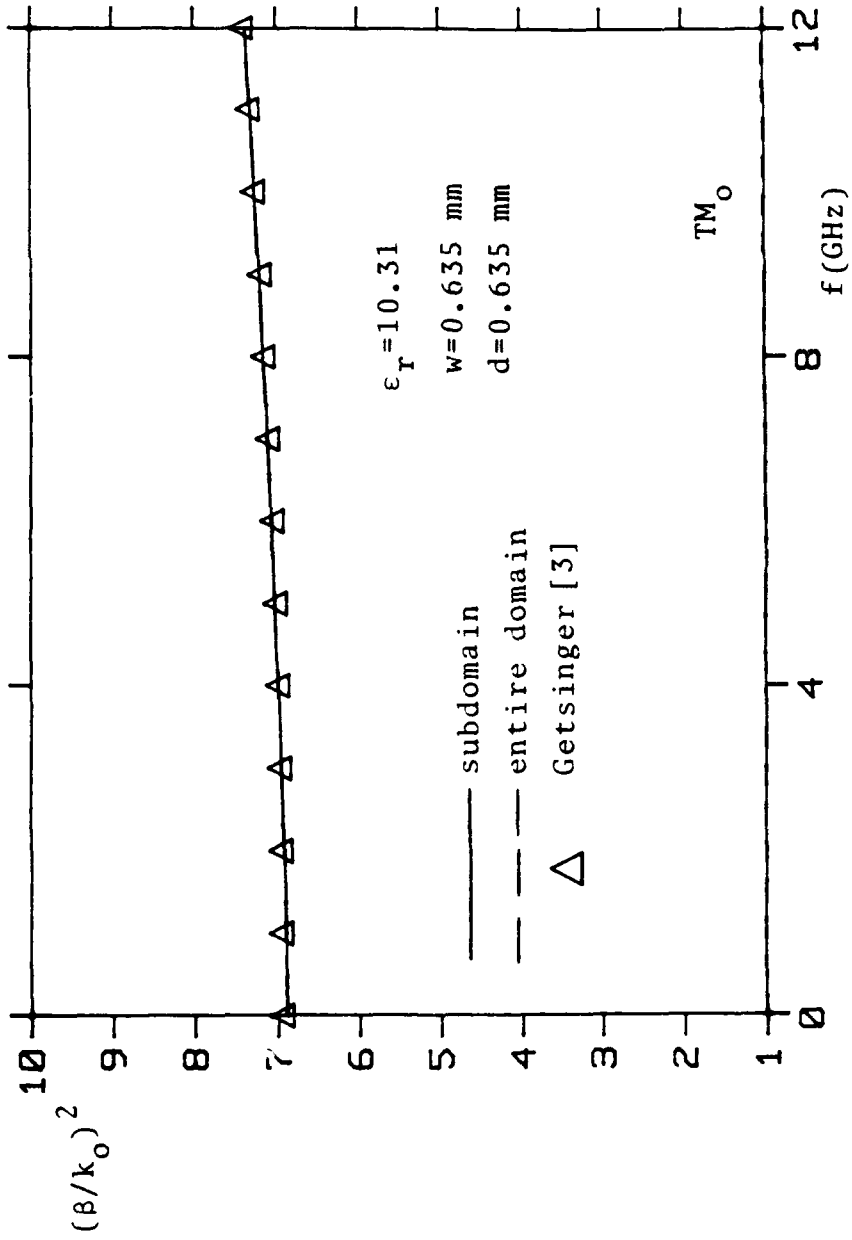


Fig. 7. Variation of the normalized phase constant of the fundamental mode versus frequency.

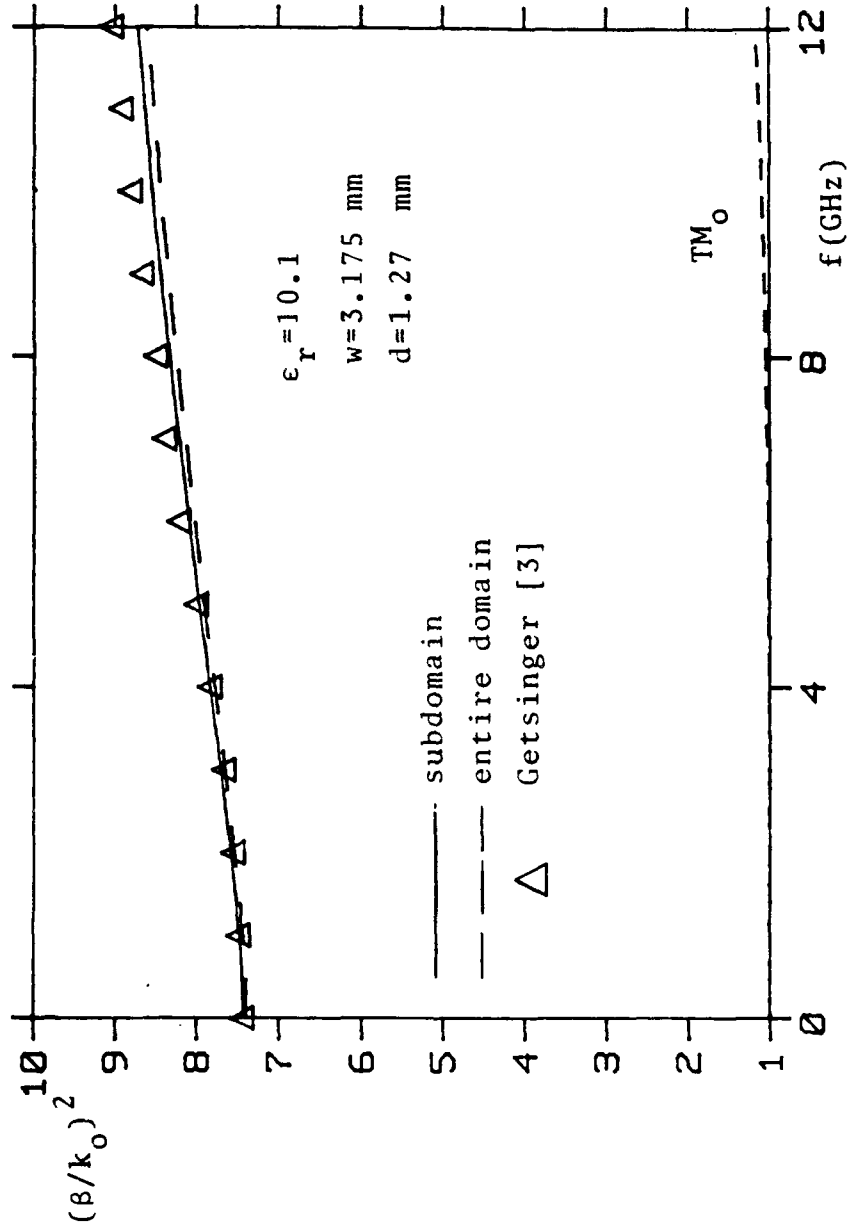


Fig. 8. Variation of the normalized phase constant of the fundamental mode versus frequency.

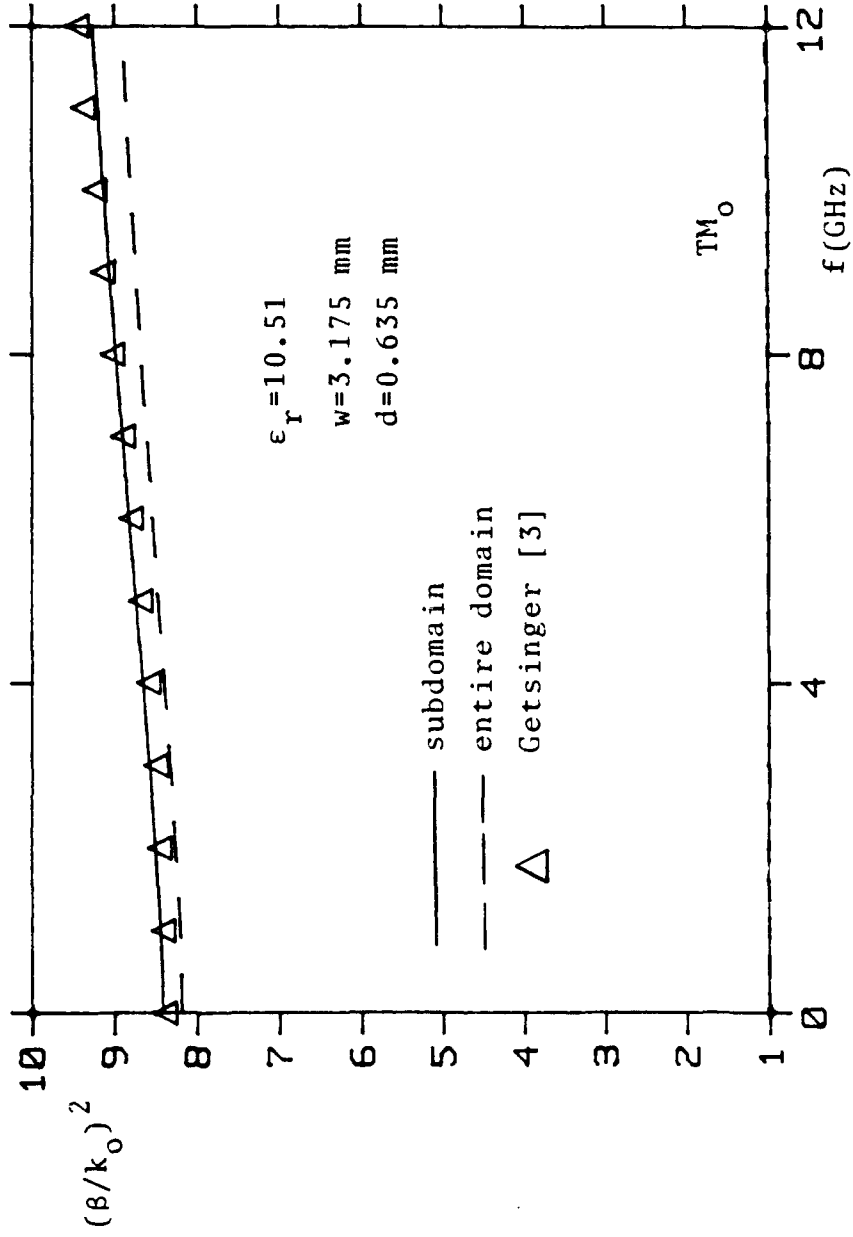


Fig. 9. Variation of the normalized phase constant of the fundamental mode versus frequency.

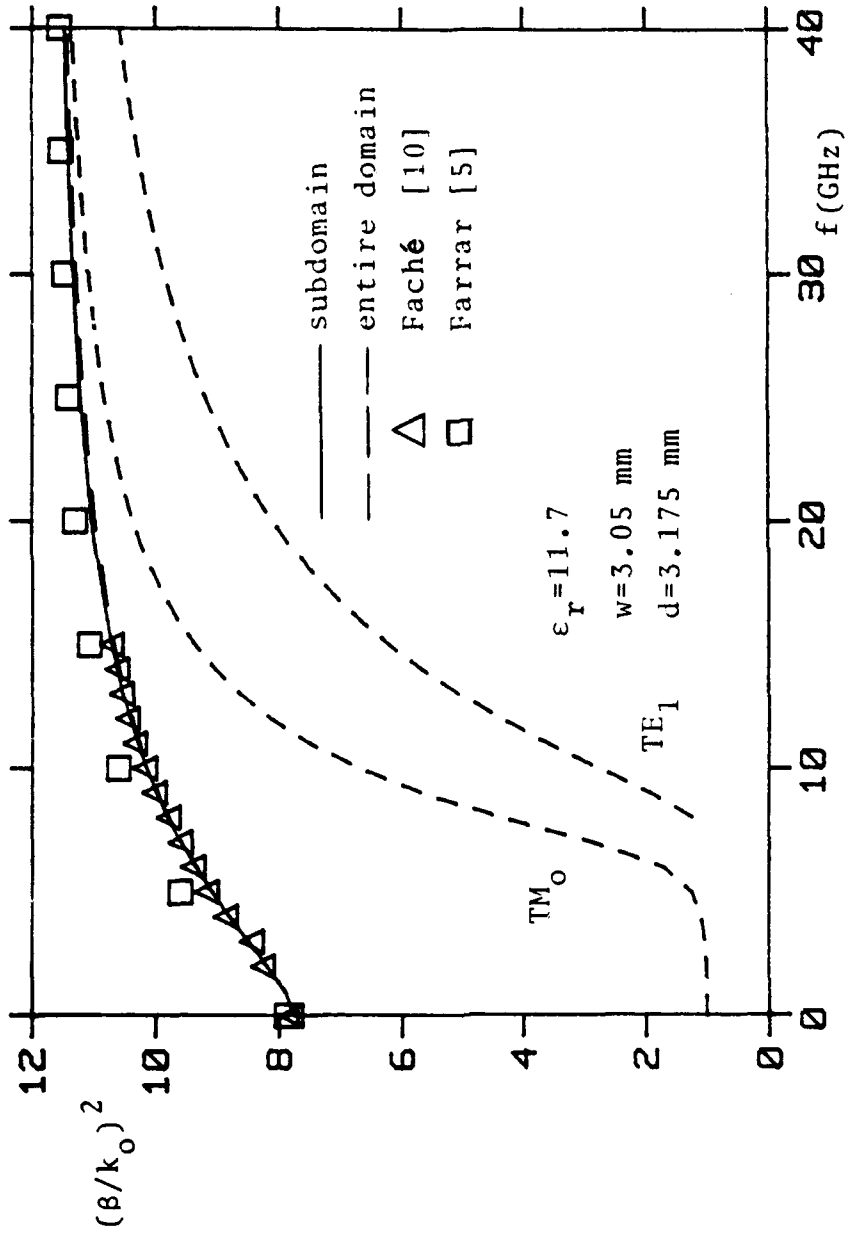


Fig. 10. Variation of the normalized phase constant of the fundamental mode versus frequency.

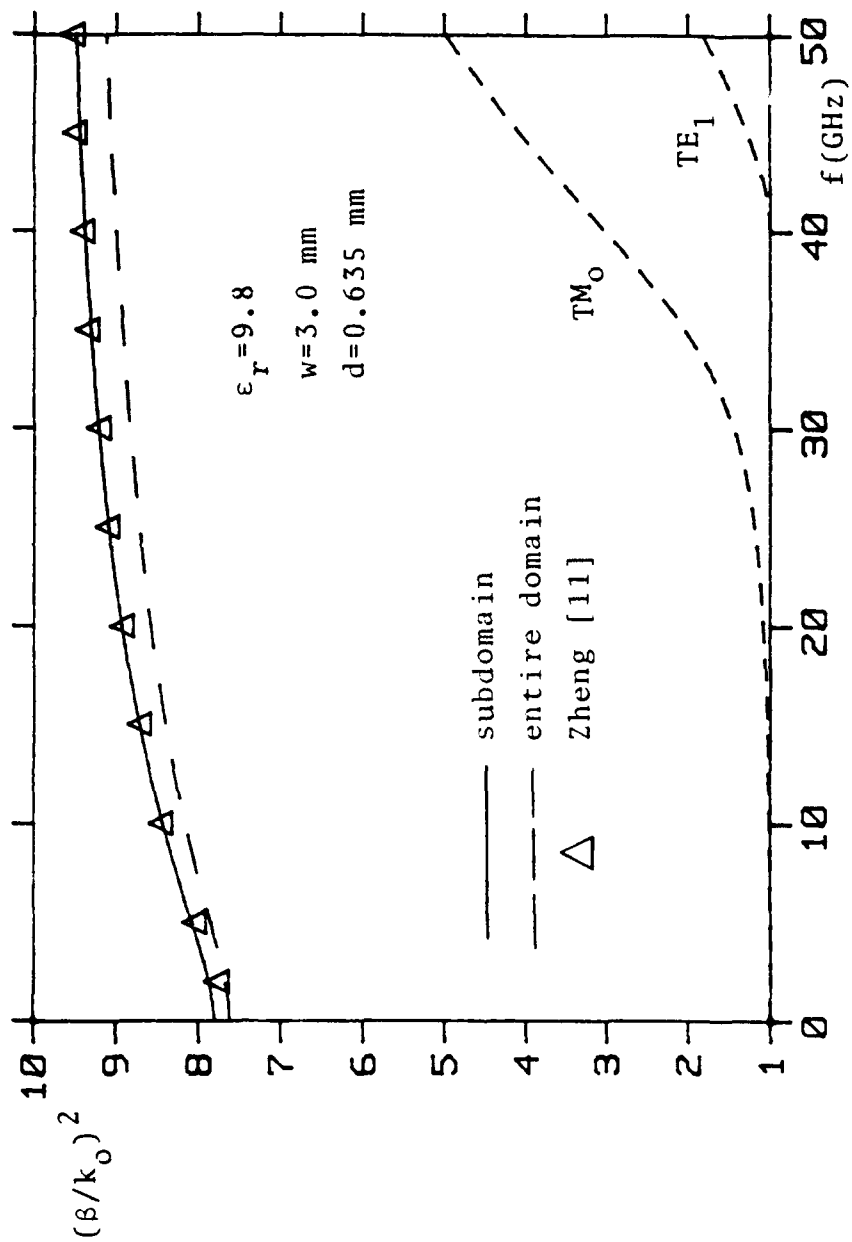


Fig. 11. Variation of the normalized phase constant of the fundamental mode versus frequency.

**On the dynamic model for
passive microwave printed circuits**

by

Chung-I G. Hsu

A dissertation proposal

Department of Electrical and Computer Engineering
Syracuse University

June, 1990

1 Introduction

Due to the advantage of low cost, small size, light weight, and high reliability [1–4], the microwave printed circuit (MPC) has become more and more popular during the past three decades. The theories of the MPC have been widely discussed in the literature. An extensive listing of reference papers can be found in [3]. Most models and numerical schemes that have been proposed and published regarding the MPC are valid at low frequencies [5], [6]. Many numerical techniques, excluding quasi-static analysis, are summarized in [7]. A rigorous approach using an integral equation formulation, which takes into account the radiation and the surface wave that are excited at the discontinuities of a microstrip, has been proposed by Katehi and Alexopoulos [8]. In this study, we seek the same objectives but with different computational schemes.

The basic structures under consideration are shown in Fig. 1(a) and Fig. 1(b) for two and three layered MPC's, respectively. All the media are assumed isotropic, lossless, and non-magnetic. The first layer is free space, whereas the second and the third layers are characterized by (ϵ_1, μ_0) and (ϵ_2, μ_0) , respectively. The planar circuits are printed on the interfaces. For the three layered structure, a via connecting the circuits on the two different interfaces is allowed, although this may not be a practical structure.

The method of moments [9] is employed to investigate various MPC problems. The electric field integral equation is formulated in the space domain. Instead of computing the electric field directly, we use the mixed potential integral equation (MPIE) approach [10], [11], where the vector and the scalar potentials are computed in the solution process. The mixed potential approach has been explored very thoroughly for free space problems [9], and its advantage over the original EFIE is well known. Mosig and Gardiol [10] extended the MPIE approach to

printed antennas on a grounded dielectric slab. Later, Michalski and Zheng [11] systematically developed this approach for problems of arbitrarily shaped conducting bodies embedded in layered media. In general, there are many different choices for the vector potentials. However, Sommerfeld's choice has been found to have advantages over the others [11], and is adopted here.

2 Green's function and integration path

To begin with, we only deal with the two layered structure, as shown in Fig. 1(a). Due to an x directed electric dipole on the interface, various components of the magnetic vector potential and the scalar potential are as follows [10], [11], [16].

$$G_{xz}^A \propto \int_0^\infty J_0(k_\rho \rho) \frac{k_\rho}{D_e} \left\{ \frac{\exp(-jk_{z_0}z)}{\sin k_{z_1}(z+d)/\sin k_{z_1}d} \right\} dk_\rho, \quad (1)$$

$$G_{zz}^A \propto \int_0^\infty J_0(k_\rho \rho) \frac{k_\rho}{D_e D_m} \left\{ \frac{\exp(-jk_{z_0}z)}{\cos k_{z_1}(z+d)/\cos k_{z_1}d} \right\} dk_\rho, \quad (2)$$

$$G_x^\phi \propto \int_0^\infty J_0(k_\rho \rho) \frac{k_\rho [jk_{z_0} - k_{z_1} \tan k_{z_1}d]}{D_e D_m} \left\{ \frac{\exp(-jk_{z_0}z)}{\sin k_{z_1}(z+d)/\sin k_{z_1}d} \right\} dk_\rho, \quad (3)$$

where the upper and the lower terms in the curly brackets are for $z > 0$ and $-d < z < 0$, respectively. Furthermore, the roots of

$$D_e = jk_{z_0} + k_{z_1} \cot k_{z_1}d \quad (4)$$

and

$$D_m = j\epsilon \cdot k_{z_0} - k_{z_1} \tan k_{z_1}d, \quad (5)$$

respectively, correspond to the TE and TM surface or leaky wave poles in the complex k_ρ plane. Notice that $\pm k_0$ are the only branch points. In general, the

branch cut is artificial and can be chosen arbitrarily. However, the most natural one is shown in Figures 2 and 3, in which the numbers of the surface wave poles, located on the upper half sheet of the Riemann surface, and the leaky wave poles, located on the bottom sheet of the Riemann surface, are finite and infinite, respectively [12], [13]. If the integration path is deformed off the real axis, the residues of the poles captured must be taken into account. Some researchers [10], [14] have implemented the real axis integration algorithm, which is not easy to perform in two extremely cases, i.e., if $B = k_o d \sqrt{\epsilon_r - 1}$ is very small or very large. If the parameter B is very small, the first TM surface wave pole is very close to the branch point k_o , where the integrand exhibits a derivative discontinuity [10], [16]. If B is very large, then some leaky wave poles are close to the real axis [15], making the integrand oscillate irregularly. We choose the integration path shown in Fig. 2 to avoid the complication caused by the poles. However, if $k_o \rho$ gets larger, this integration scheme gets less efficient due to the oscillation of the Bessel function along the path. For $k_o \rho > 5$, we make the following substitution for the integrands of (1) to (3),

$$J_o(k_o \rho) = \frac{1}{2} [H_o^{(2)}(k_o \rho) - H_o^{(2)}(-k_o \rho)] \quad (6)$$

The integration path is then deformed to be along the branch cut as shown in Fig. 3. Choosing this path, Mosig and Gardiol [16] has shown that the integral can be decomposed into three parts, i.e., the static term which is purely real, the space wave term, and the surface wave term. If $k_o \rho$ is very large, the efficiency is again degraded by the rapid oscillation of the Bessel function in the interval $k_p \in [0, k_o]$. In this case, the steepest descent path may be a better candidate.

3 Numerical results for printed dipoles

Figures 4 to 9 show the current distribution, and the input and mutual impedances of some printed wire and strip dipoles. The results agree with those available in the literature [13], [17], [18]. Attention should be paid to Fig. 10, where we use 49 unknowns in the solution process for a strip dipole of width $0.005\lambda_o$, and Barkeshli uses only three unknowns for a dipole of width $0.01\lambda_o$. Inaccuracy in Barkeshli's solution is suspected, since in Fig. 10(a), the results can hardly be differentiated from those of a wire dipole of radius $0.00125\lambda_o$.

4 Proposed study for microwave printed circuits

In the MPC, a microstrip line always serves as a transmission line. The number of ideal transmission lines needed to represent the microstrip must be the same as that of the bound modes that can be excited [3]. For simplicity, we restricted ourselves to the frequency range in which the fundamental mode is the only bound mode. Furthermore, we assume that $w \ll \lambda_o$, where w and λ_o are the width of the microstrip and the free space wavelength, respectively. Hence, the transverse current can be ignored with little error introduced. The axial current has singularities at the two edges of the microstrip. The transverse variations of the axial current at several frequencies are shown in Fig. 11, where the Maxwellian function is plotted for comparison. In general, if the frequency gets higher, the current distribution deviates from the Maxwellian function more. Figures 12 and 13 give curves of $(\lambda_o/\lambda_g)^2$ versus frequency, which are compared with those obtained by Getsinger [19], Farrar [20], and Faché and De Zutter [21]. It is obvious that if

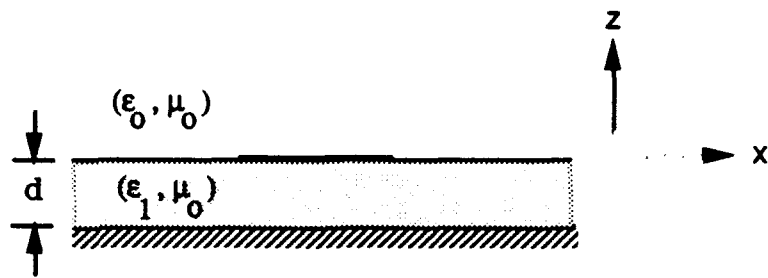
$w/d < 1$ and if the frequency is not too high, the Maxwellian function for the current gives a reasonably accurate result for the propagation constant. To further improve the accuracy, we assume the transverse variation of the current to be of the form

$$J_x(y) \propto \frac{1}{\sqrt{1 - (2y/w)^2}} [T_0(2y/w) + bT_2(2y/w)] \quad (7)$$

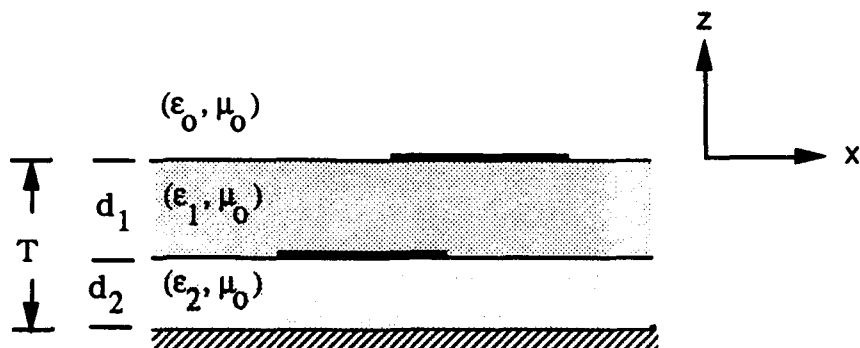
where T_n is the Chebyshev polynomials of the first kind of order n . After the propagation constant is found, the unknown coefficient b can be easily solved. The characteristic impedance can be computed according to [22]

$$Z_c = \frac{P}{|I|^2} \quad (8)$$

where P is the real power propagating in the axial direction. Fig. 14 shows the normalized propagation constant and the characteristic impedance computed from one ($b = 0$) and two ($b \neq 0$) expansion functions. The results computed from the commercial software SUPERCOMPACT and from quasi-static analysis are also plotted for comparison. The power ratio in the dielectric and the b in (7) are shown in Fig. 15. The modeling of the discontinuity is illustrated in Figs. 16 and 17. By observing the standing wave pattern exhibited in Fig. 17(a), several parameters can be computed. Notice that we need to compute two sets of currents with two different L_2 's in Fig. 17(a) in order to determine the scattering matrix.



(a) Two layered configuration



(b) Three layered configuration

Fig. 1. Side view of microwave printed circuit.

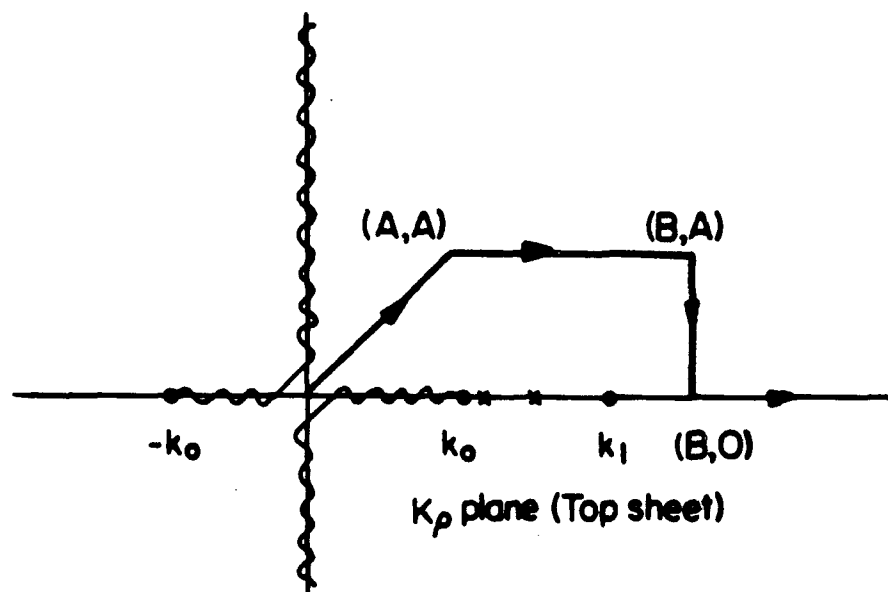


Fig. 2. Deformed integration path in the complex k_ρ plane.

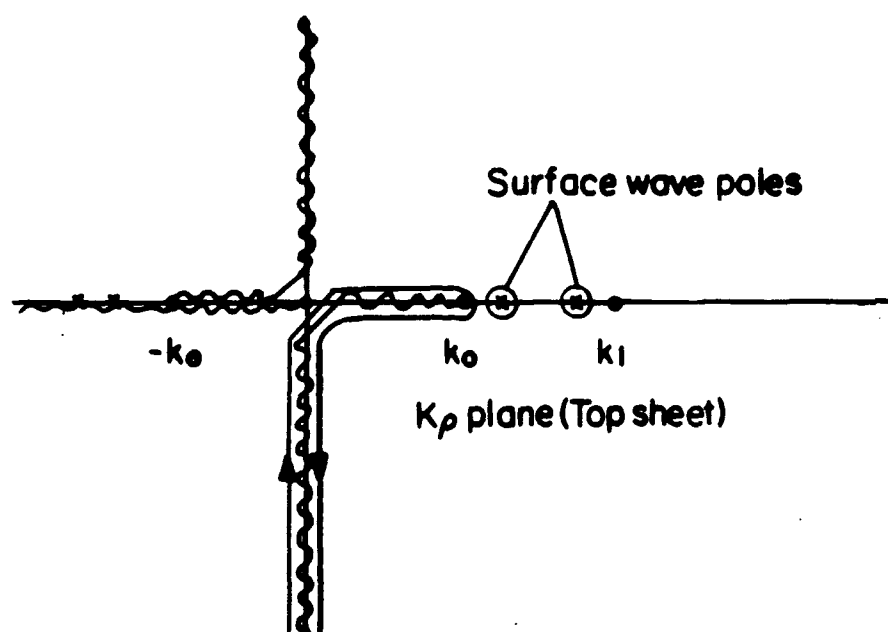


Fig. 3. Integration path along the branch cut in the complex k_ρ plane.

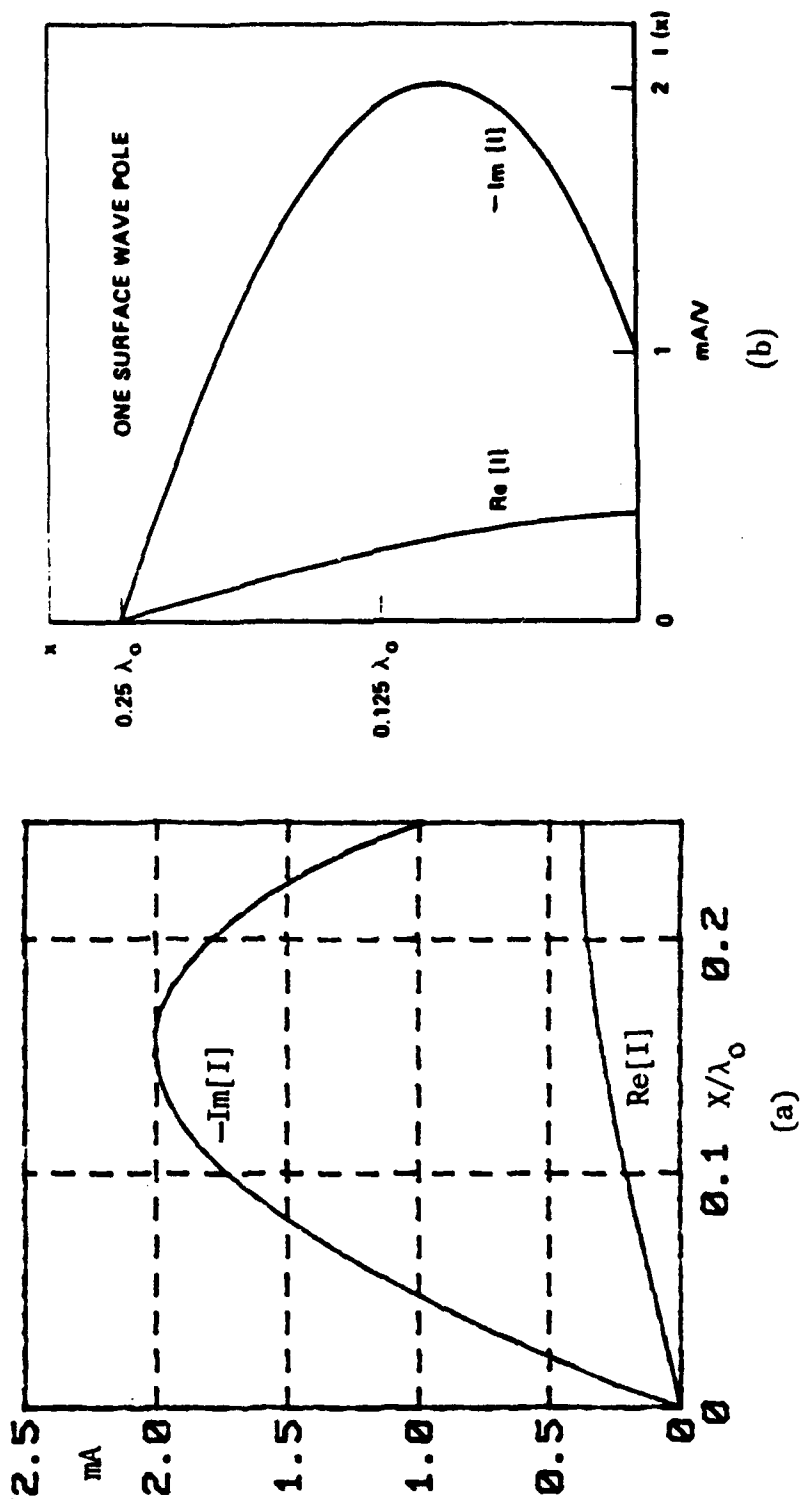


Fig. 4. Current distribution of a center-fed wire dipole, $L = 0.5\lambda_0$, $\epsilon_r = 3.25$, $d = 0.1016\lambda_0$, $a = 0.0001\lambda_0$, (a) our result, (b) after Rana (1981).

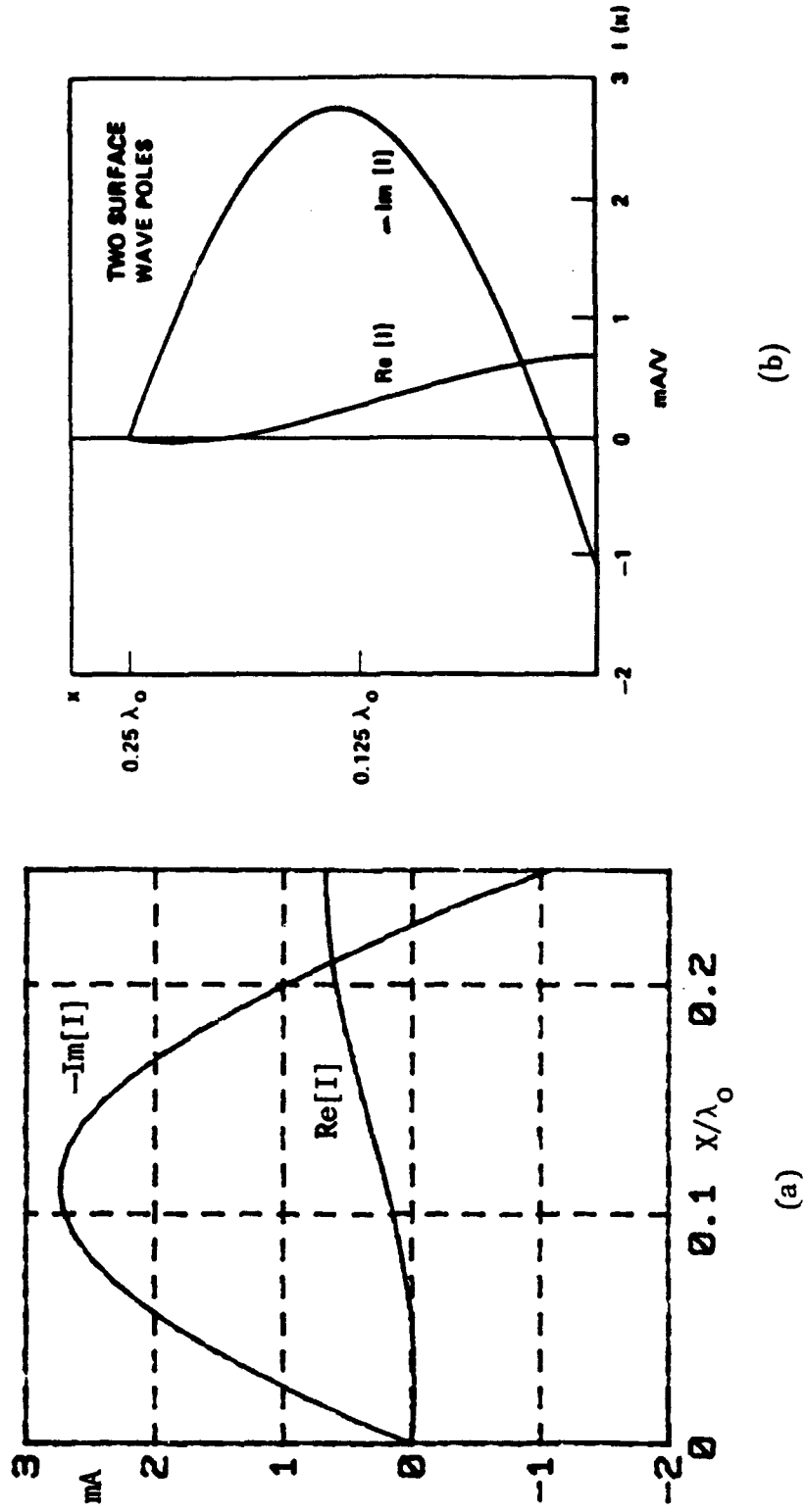
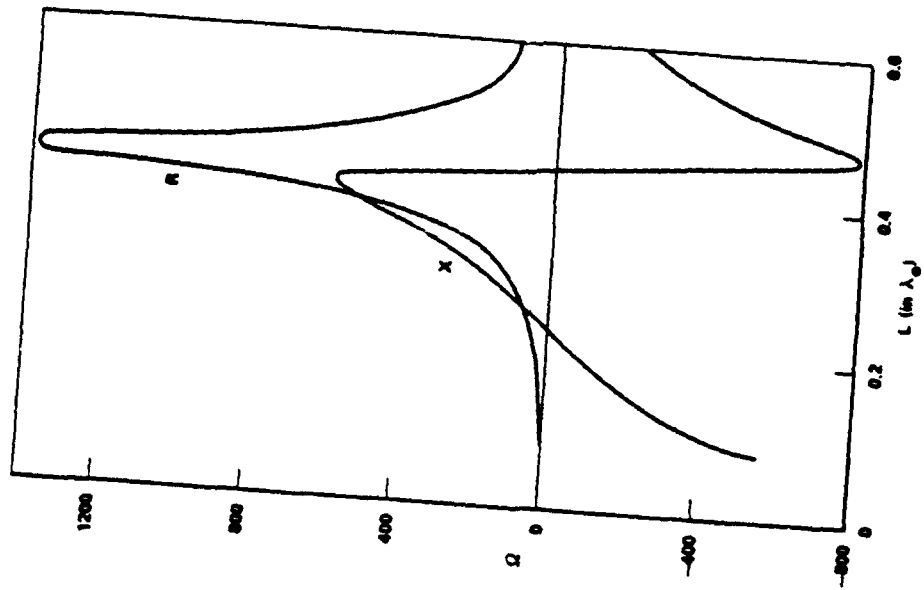
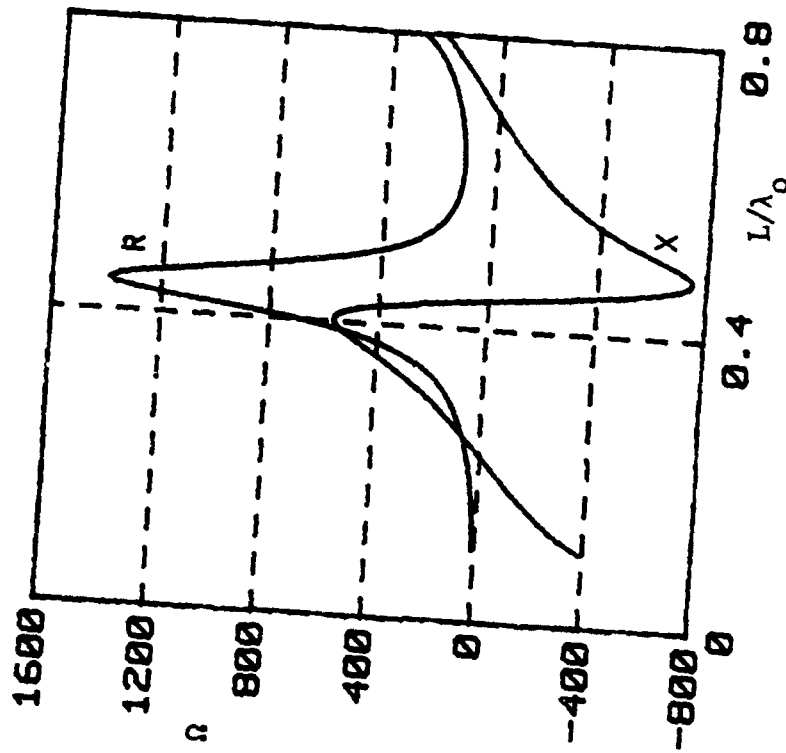


Fig. 5. Current distribution of a center-fed wire dipole, $L = 0.5\lambda_0$, $\epsilon_r = 8.5$, $d = 0.15\lambda_0$, $a = 0.00005\lambda_0$, (a) our result, (b) after Rana (1981).



(b)



(a)

Fig. 6. Input impedance of a center-fed wire dipole, $\epsilon_r = 8.5$, $d = 0.15\lambda_0$, $a = 0.00005\lambda_0$, (a) our result, (b) after Rana (1981).

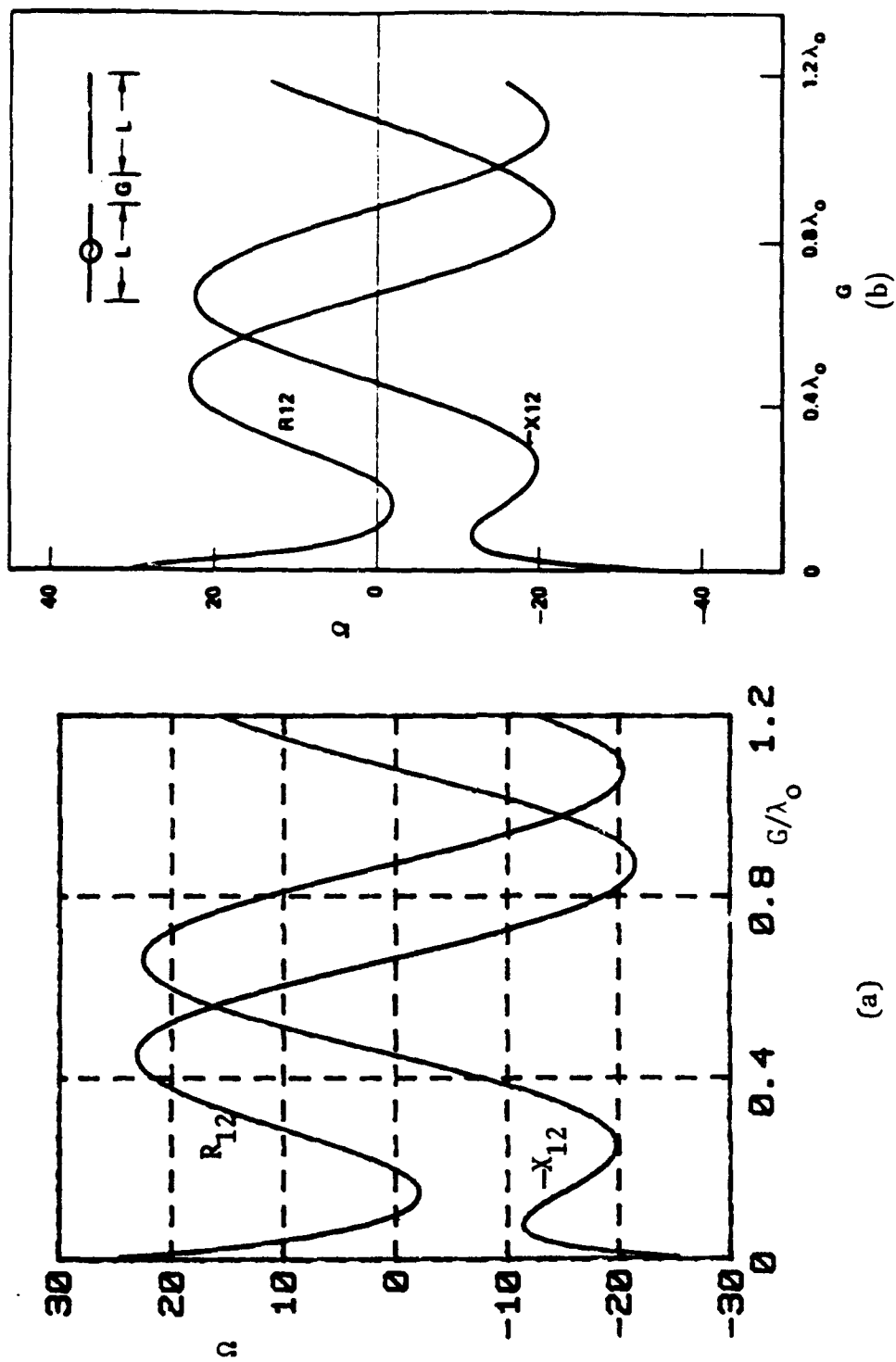


Fig. 7. Mutual impedance between two collinear wire dipoles, $\epsilon_r = 3.25, d = 0.127\lambda_0, a = 0.0001\lambda_0, L = 0.4\lambda_0$, (a) our result, (b) after Alexopoulos (1981).

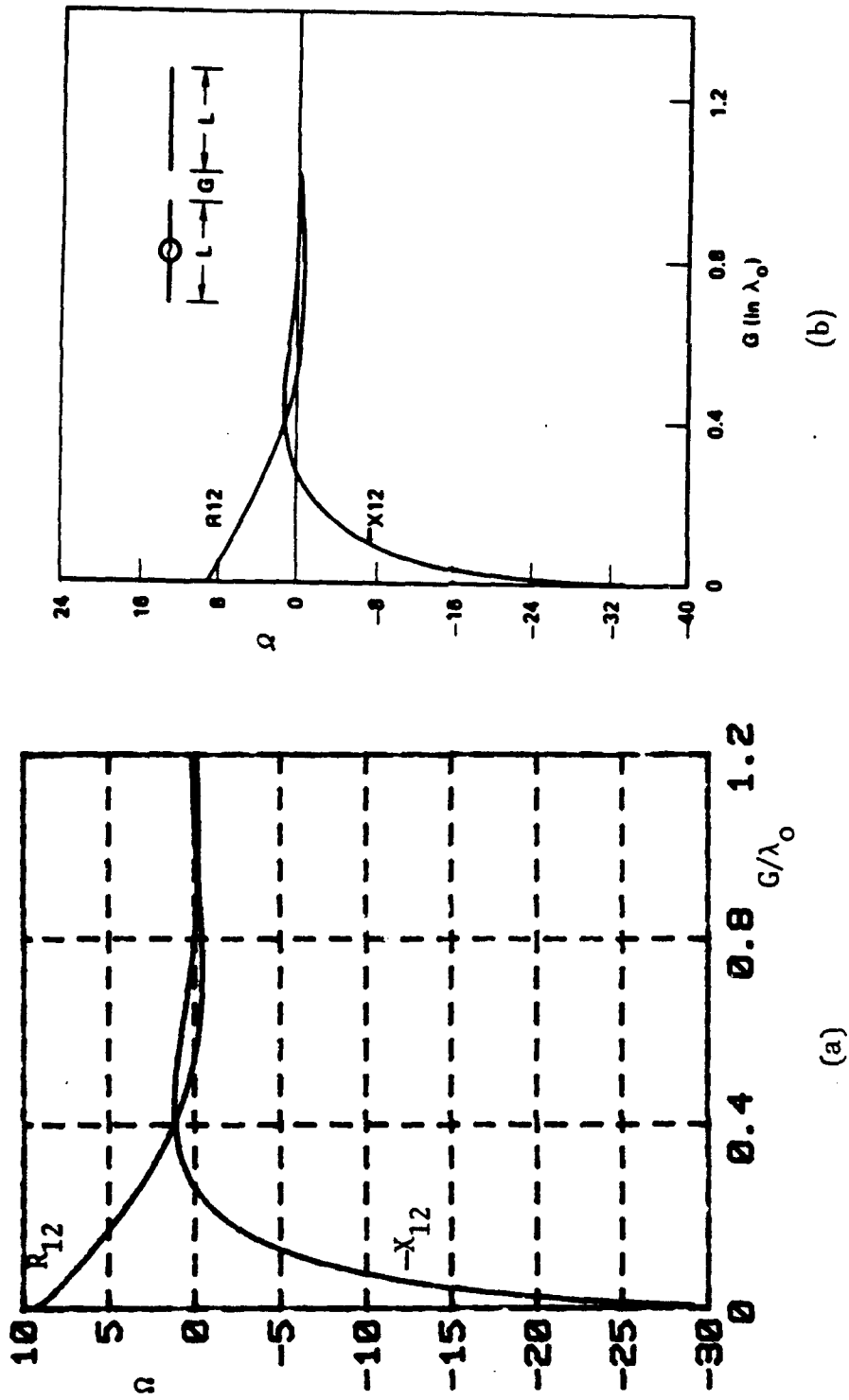


Fig. 8. Mutual impedance between two collinear wire dipoles, $\epsilon_r = 1, d = 0.1016\lambda_0, a = 0.0001\lambda_0, L = 0.25\lambda_0$, (a) our result, (b) after Alexopoulos (1981).

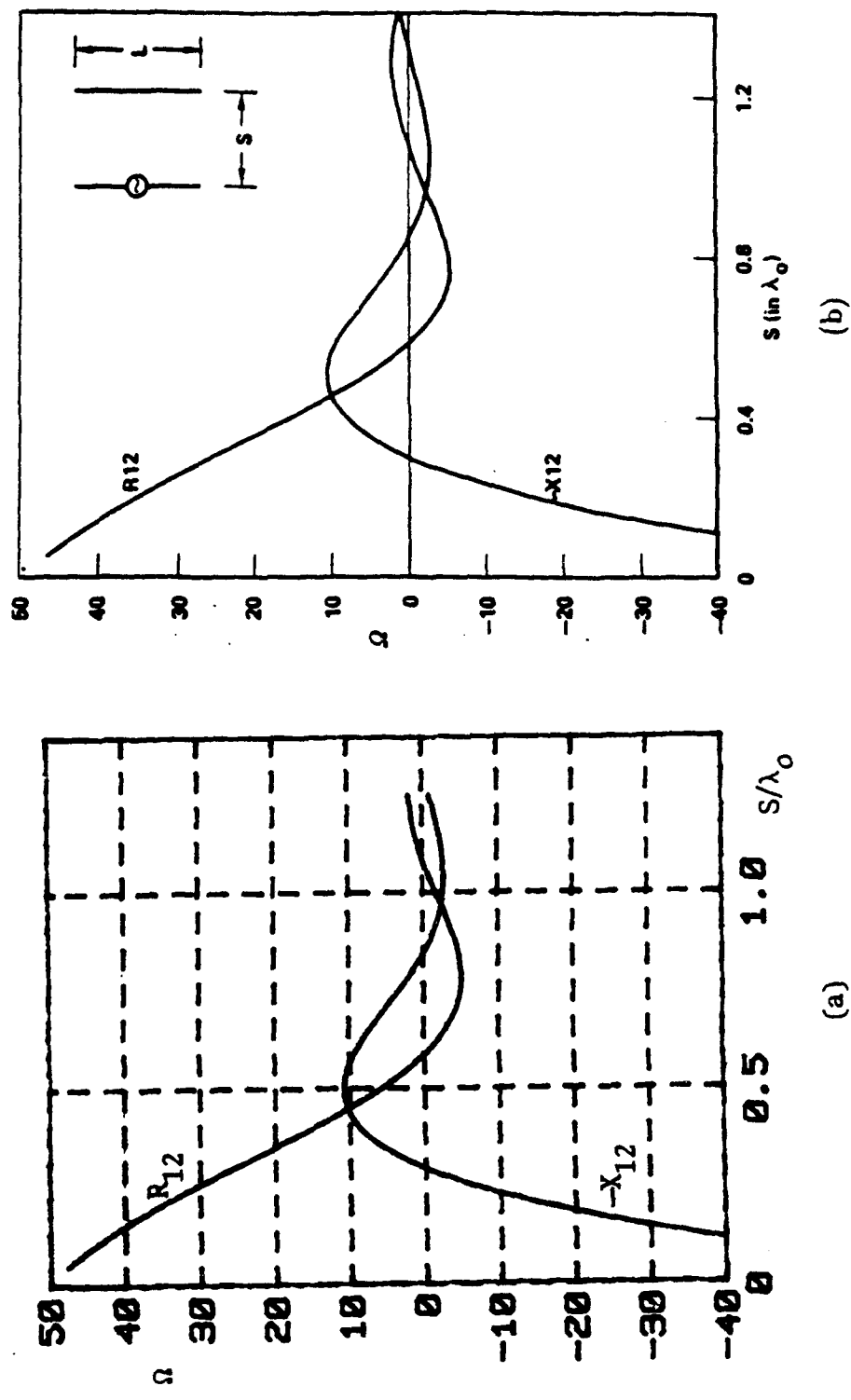
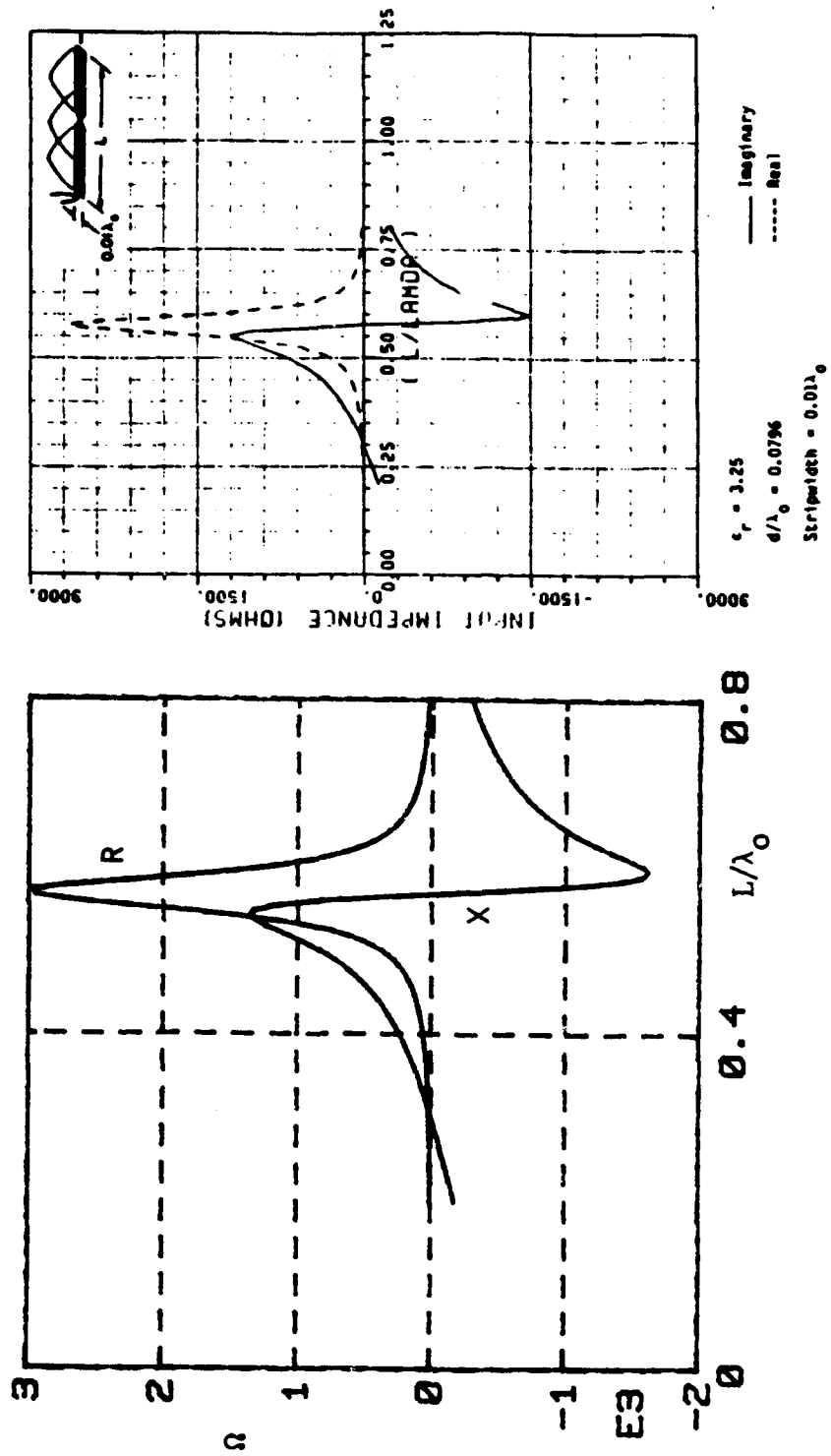


Fig. 7. Mutual impedance between two broadside wire dipoles, $\epsilon_r = 3.25$, $d = 0.1016\lambda_0$, $a = 0.0001\lambda_0$, $L = 0.333\lambda_0$, (a) our result, (b) after Alexopoulos (1981).



(a) (b)

Fig. 10. Input impedance of the center-fed strip and wire dipoles, $\epsilon_r = 3.25$, $d = 0.0796\lambda_0$, $w = 0.005\lambda_0$, $a = 0.00125\lambda_0$, (a) our result with strip (—) and wire (---), (b) after Barkeshli (1988).

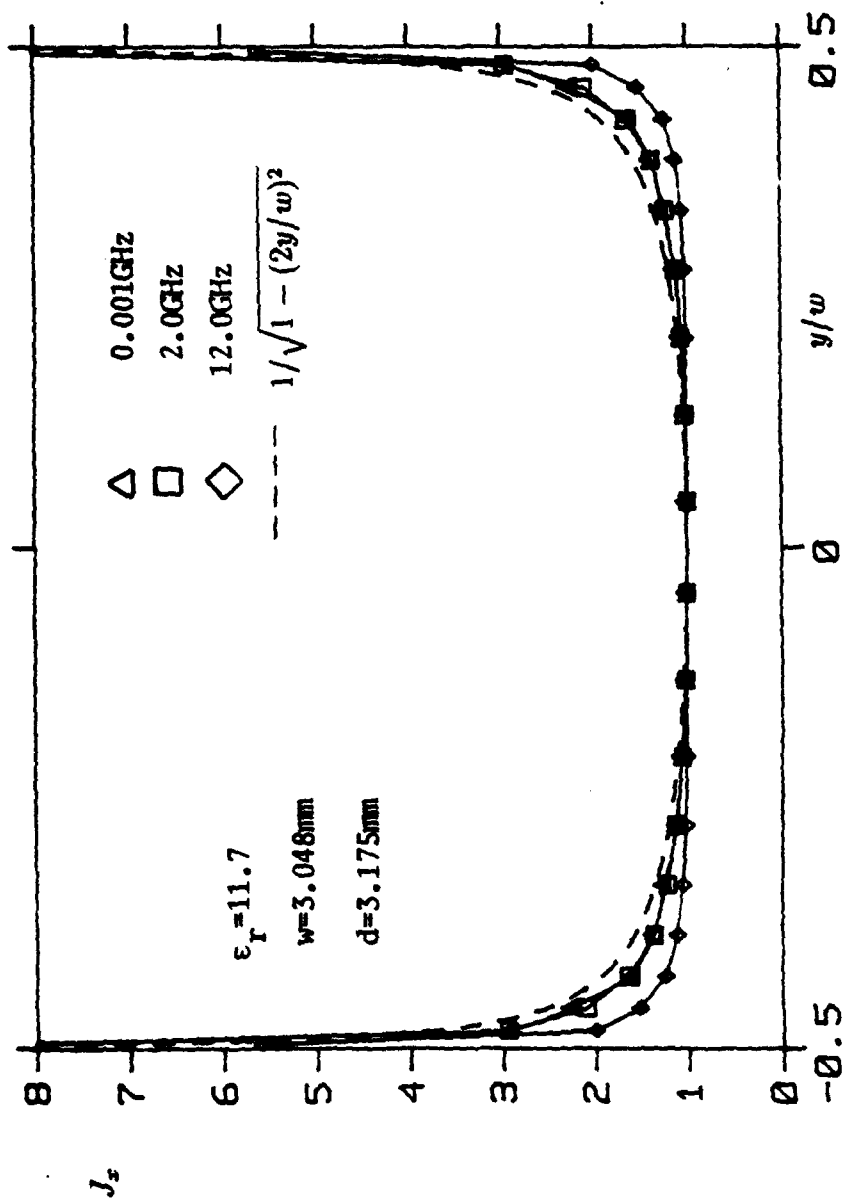


Fig. 11. Transverse variation of the longitudinal current distribution of the fundamental mode for a microstrip.

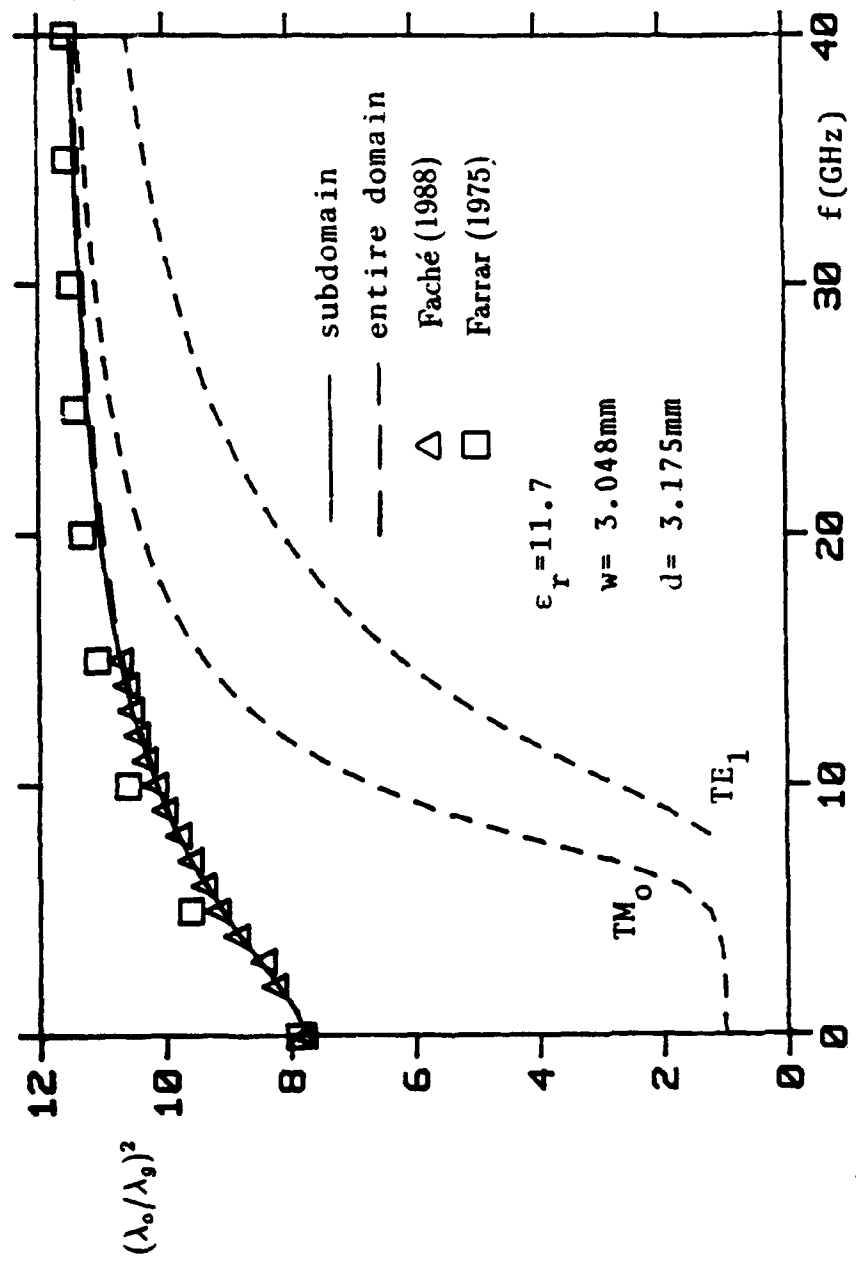


Fig. 12 Dispersion characteristics of the fundamental mode, where λ_0 and λ_g are the free space and guide wavelengths, respectively.

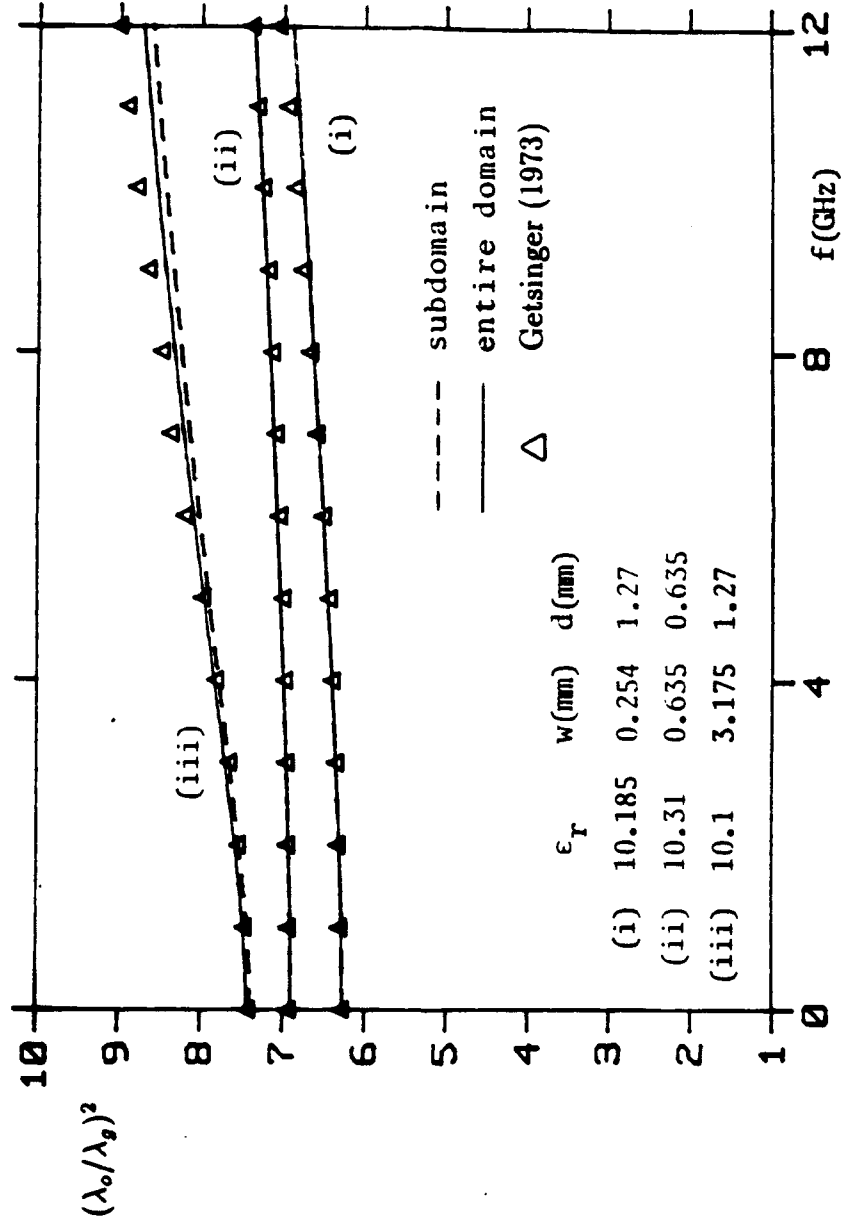


Fig. 13 Dispersion characteristics of the fundamental mode, where λ_0 and λ_g are the free space and guide wavelengths, respectively.

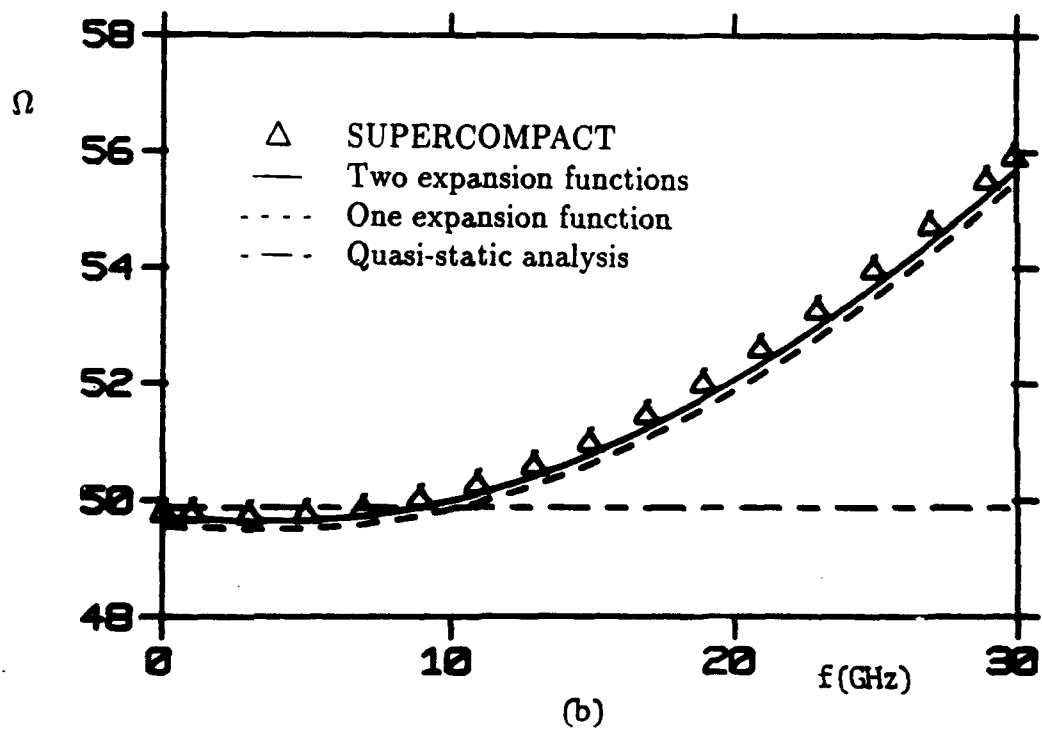
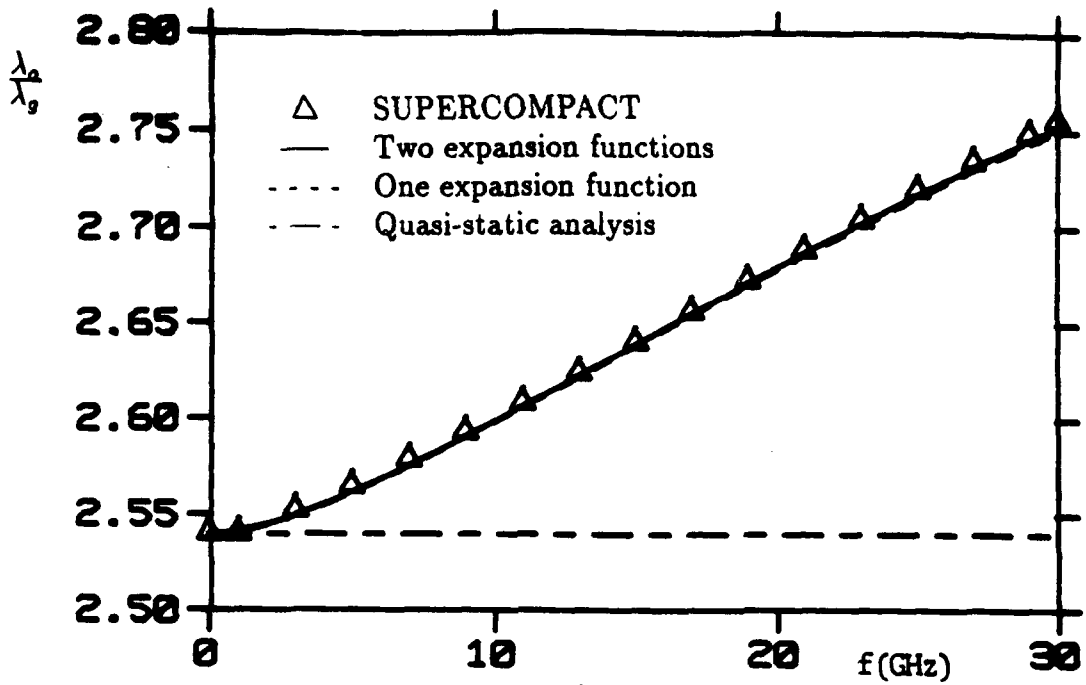


Fig. 14 (a) Normalized propagation constant and (b) characteristic impedance for a microstrip line with $\epsilon_r = 9.6$, $w = 0.6\text{mm}$, $d = 0.6\text{mm}$.

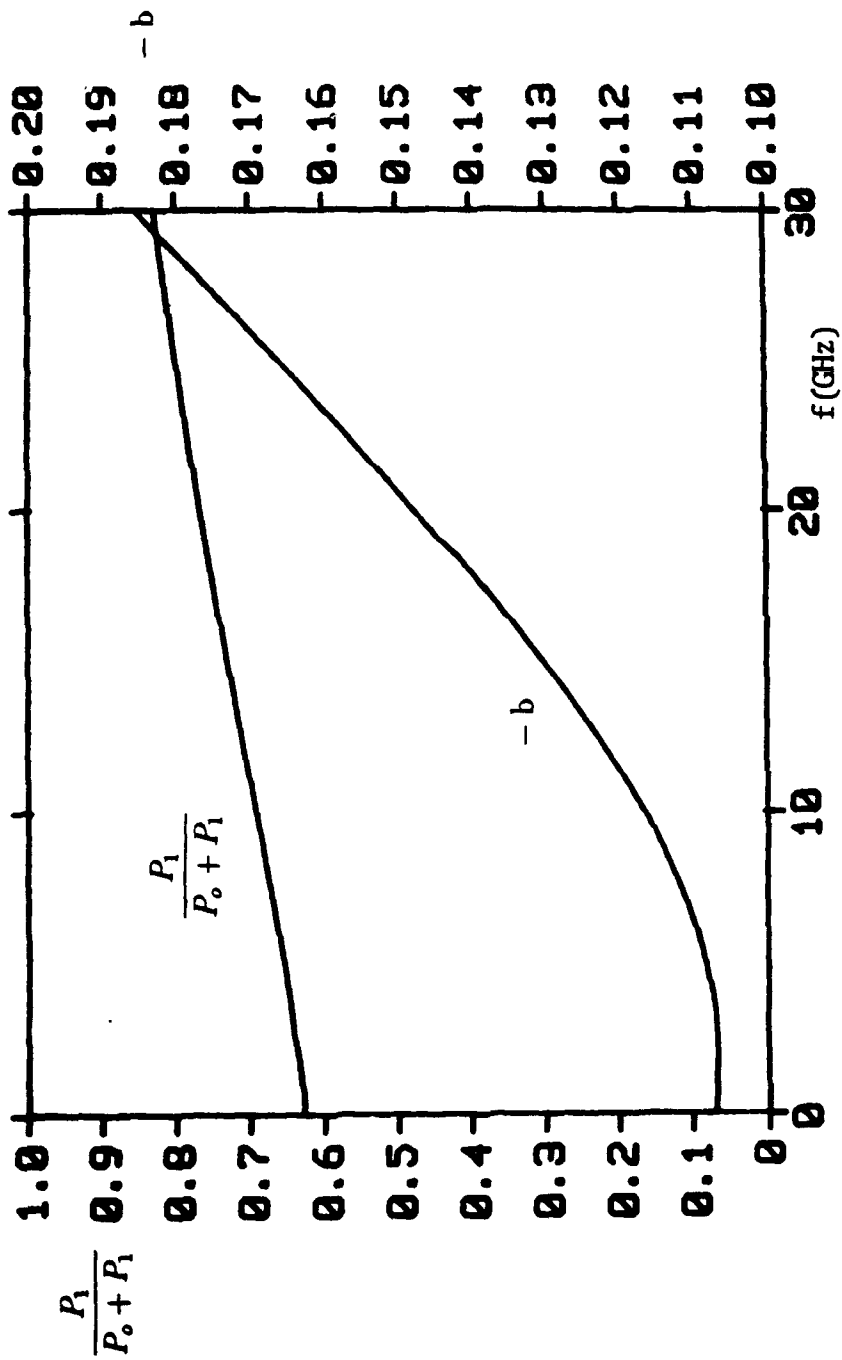
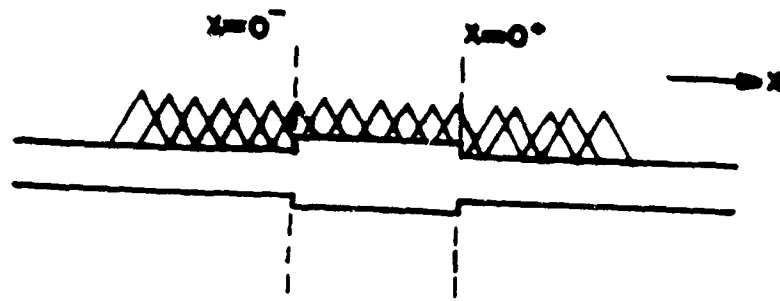
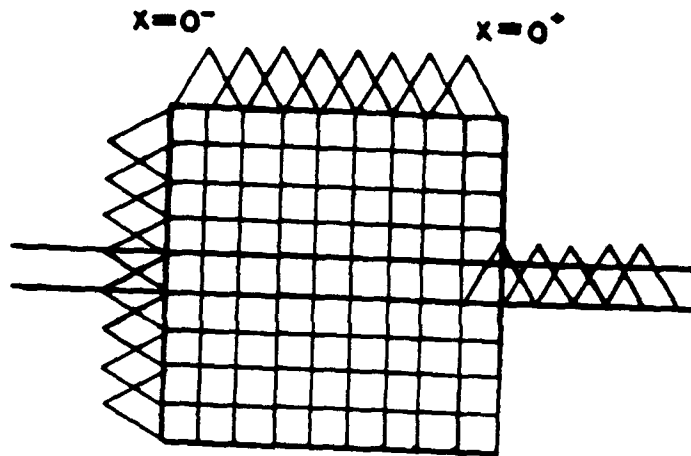


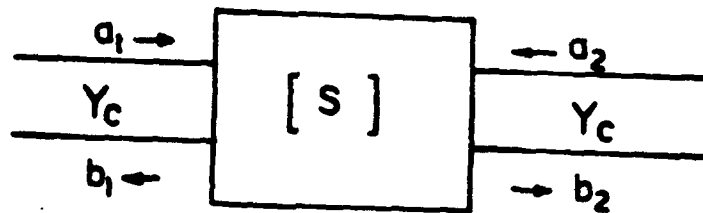
Fig. 15 The power ratio ($\frac{P_1}{P_0 + P_1}$) and the coefficient b versus frequency for a microstrip line with $\epsilon_r = 9.6$, $w = 0.6$ mm, $d = 0.6$ mm. The transverse variation of the axial current is proportional to $T_0(2y/w) + b T_2(2y/w)$.



(a) subdomain basis function for small double step discontinuity

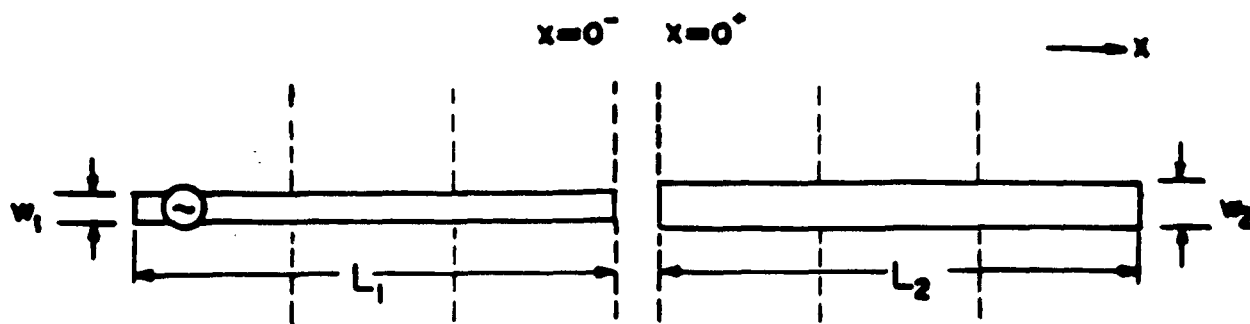


(b) subdomain basis function for large double step discontinuity

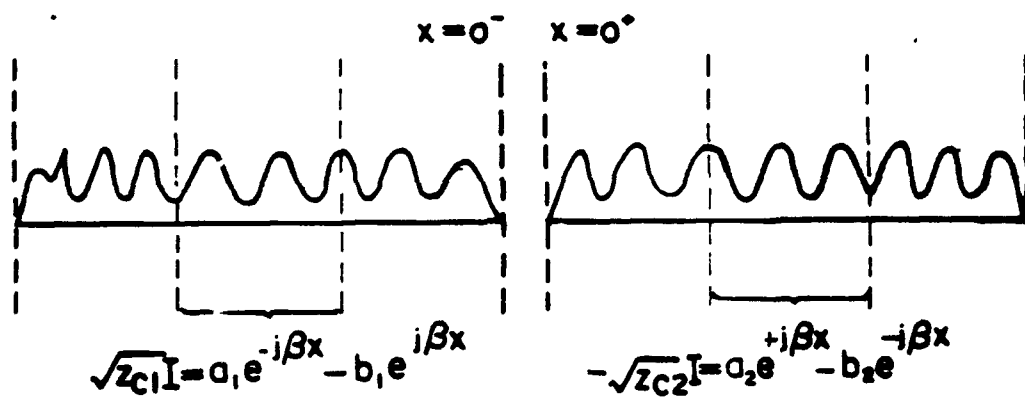


(c) equivalent network represented by its scattering matrix

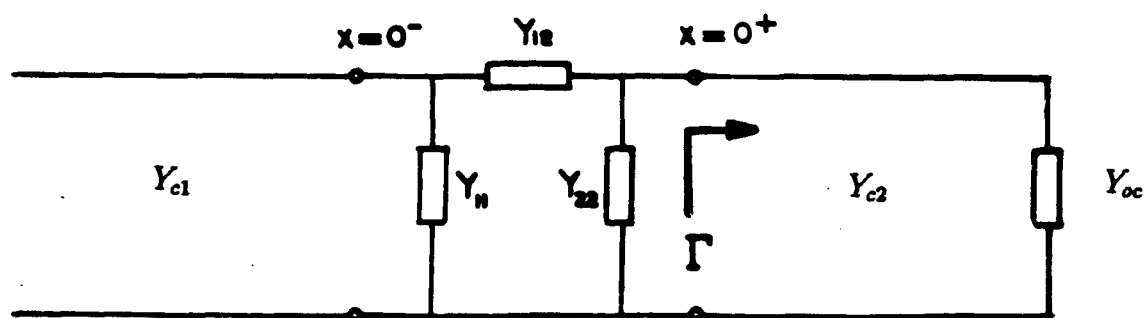
Fig. 16 Modeling of microstrip double step discontinuity.



(a) microstrip gap discontinuity



(b) current distribution



(c) equivalent circuit of the discontinuity

Fig. 17 Modeling of microstrip gap discontinuity.

References

- [1] K. C. Gupta, R. Garg, and I. J. Bahl, *Microstrip Lines and Slotlines*. Dedham, MA: Artech House, 1979.
- [2] T. C. Edwards, *Foundations for Microstrip Circuit Design*. New York: Wiley, 1981.
- [3] R. K. Hoffmann, *Handbook of Microwave Integrated Circuits*. Dedham, MA: Artech House, 1987.
- [4] F. E. Gardiol, "Design and layout of microstrip structures," *IEE proceedings*, vol. 135, Pt. H, pp. 145–157, June 1988.
- [5] A. Farrar and A. T. Adams, "Computation of lumped microstrip capacitances by matrix methods—Rectangular sections and end effect," *IEEE Trans. Microwave Theory Tech.*, vol. MTT-19, pp. 495–497, 1971.
- [6] P. Benedek and P. Silvester, "Equivalent capacitances for microstrip gaps and steps," *IEEE Trans. Microwave Theory Tech.*, vol. MTT-20, pp. 729–733, 1972.
- [7] T. Itoh (editor), *Numerical Techniques for Microwave and Millimeter-wave Passive Structures*. New York: Wiley, 1989.
- [8] P. B. Katehi and N. G. Alexopoulos, "Frequency-dependent characteristics of microstrip discontinuities in millimeter-wave integrated circuits," *IEEE Trans. Microwave Theory Tech.*, vol. MTT-33, pp. 1029–1035, Oct. 1985.
- [9] R. F. Harrington, *Field Computation by Moment Methods*. New York: Macmillan, 1968. Reprinted by Krieger Publishing Co., Melbourne, FL, 1982.

- [10] J. R. Mosig and F. E. Gardiol, "A dynamical radiation model for microstrip structures," in *Advances in Electronics and Electron Physics*, vol. 59, pp. 139-237. New York: Academic Press, 1982.
- [11] K. A. Michalski and D. Zheng, "Modeling antennas and scatterers of arbitrary shape embedded in layered dielectric media," Technical Report, Dept. Elec. Eng., Texas A&M University, Nov. 1989.
- [12] R. E. Collin, *Field Theory of Guided Waves*. New York: McGraw-Hill, 1960.
- [13] S. Barkeshli, "Efficient approaches for evaluating the planar microstrip Green's function and its applications to the analysis of microstrip antennas," Ph.D. dissertation, Dept. Elec. Eng., Ohio State Univ., 1988.
- [14] P. B. Katehi and N. G. Alexopoulos, "Real axis integration of Sommerfeld integrals with applications to printed circuit antenna," *J. Math. Phys.*, vol. 24(3), pp. 527-533, Mar. 1983.
- [15] C.-I. G. Hsu, R. F. Harrington, J. R. Mautz, and T. K. Sarkar, "On the location of leaky wave poles for a grounded dielectric slab," submitted to *IEEE Trans. Microwave Theory Tech.*, 1990.
- [16] J. R. Mosig and F. E. Gardiol, "Analytic and numerical techniques in the Green's function treatment of microstrip antennas and scatterers," *IEE Proc.*, vol. 130, Pt. H., pp. 175-182, Mar., 1983.
- [17] I. E. Rana and N. G. Alexopoulos, "Current distribution and input impedance of printed dipoles," *IEEE Trans. Antennas Propagat.*, vol. AP-29, pp. 99-105, Jan. 1981.

- N. G. Alexopoulos and I. E. Rana, "Mutual impedance computation between printed dipoles," *IEEE Trans. Antennas Propagat.*, vol. AP-29, pp. 106-111, Jan. 1981.
- [19] W. J. Getsinger, "Microstrip dispersion model," *IEEE Trans. Microwave Theory Tech.*, vol. MTT-21, pp. 34-39, Jan., 1973.
- [20] A. Farrar, "Fourier integral methods for static and dynamic problems in microstrip," Ph.D. Dissertation, Syracuse University, 1975.
- [21] N. Faché and D. De Zutter, "Rigorous full-wave space-domain solution for dispersive microstrip lines," *IEEE Trans. Microwave Theory Tech.*, vol. 36, pp. 731-737, Apr. 1988.
- [22] J. B. Knorr and A. Tufekcioglu, "Spectral domain calculation of microstrip characteristic impedance," *IEEE Trans. Microwave Theory Tech.*, vol. MTT-23, pp. 725-728, Sep. 1975.